AFRL-SN-WP-TR-1999-1133

ELECTROOPTIC MODULATION RESEARCH

ELECTROOPTIC MODULATORS

H. JOHN CAULFIELD
ZHENLI ZHANG

ALABAMA A&M UNIVERSITY
DEPARTMENT OF PHYSICS
P.O. BOX 1268
NORMAL, AL 35762

APRIL 1997

FINAL REPORT FOR OCT 1993 – APR 1997

SENSORS DIRECTORATE
AIR FORCE RESEARCH LABORATORY
AIR FORCE MATERIEL COMMAND
WRIGHT-PATTERSON AIR FORCE BASE OH 45433-7318

NOTICE

USING GOVERNMENT DRAWINGS, SPECIFICATIONS, OR OTHER DATA INCLUDED IN THIS DOCUMENT FOR ANY PURPOSE OTHER THAN GOVERNMENT PROCUREMENT DOES NOT IN ANY WAY OBLIGATE THE US GOVERNMENT. THE FACT THAT THE GOVERNMENT FORMULATED OR SUPPLIED THE DRAWINGS, SPECIFICATIONS, OR OTHER DATA DOES NOT LICENSE THE HOLDER OR ANY OTHER PERSON OR CORPORATION; OR CONVEY ANY RIGHTS OR PERMISSION TO MANUFACTURE, USE, OR SELL ANY PATENTED INVENTION THAT MAY RELATE TO THEM.

THIS REPORT IS RELEASABLE TO THE NATIONAL TECHNICAL INFORMATION SERVICE (NTIS). AT NTIS, IT WILL BE AVAILABLE TO THE GENERAL PUBLIC, INCLUDING FOREIGN NATIONS.

THIS TECHNICAL REPORT HAS BEEN REVIEWED AND IS APPROVED FOR PUBLICATION.

LOUIS A. TAMBURINO, PH.D.
Target Recognition Branch
Project Engineer

DALE E. NELSON, CHIEF
Target Recognition Branch

JERRY L. COVERT
Sensor ATR Technology Division

REPORT DOCUMENTATION PAGE	Form Approved OMB No. 0704-0188

1. AGENCY USE ONLY *(Leave blank)*	2. REPORT DATE	3. REPORT TYPE AND DATES COVERED
	APRIL 1997	FINAL REPORT FOR OCT 1993 - APR 1997

4. TITLE AND SUBTITLE
ELECTROOPTIC MODULATION RESEARCH
ELECTROOPTIC MODULATORS

5. FUNDING NUMBERS
C F33615-93-1-1351
PE 62204
PR 2003
TA 12
WU 22

6. AUTHOR(S)
H. JOHN CAULFIELD
ZHENLI ZHANG

7. PERFORMING ORGANIZATION NAME(S) AND ADDRESS(ES)
ALABAMA A&M UNIVERSITY
DEPARTMENT OF PHYSICS
P.O. BOX 1268
NORMAL, AL 35762

8. PERFORMING ORGANIZATION REPORT NUMBER

9. SPONSORING/MONITORING AGENCY NAME(S) AND ADDRESS(ES)
SENSORS DIRECTORATE
AIR FORCE RESEARCH LABORATORY
AIR FORCE MATERIEL COMMAND
WRIGHT-PATTERSON AFB, OH 45433-7318
POC: LOUIS A. TAMBURINO, AFRL/SNAT, 937-255-1115 EXT. 4389

10. SPONSORING/MONITORING AGENCY REPORT NUMBER
AFRL-SN-WP-TR-1999-1133

11. SUPPLEMENTARY NOTES

12a. DISTRIBUTION AVAILABILITY STATEMENT
APPROVED FOR PUBLIC RELEASE, DISTRIBUTION UNLIMITED.

12b. DISTRIBUTION CODE

13. ABSTRACT *(Maximum 200 words)*

The work is aimed mainly at improving the overall performance of Pockels electrooptic modulators. Current Pockels cells have very limited field of view, high driving voltages, and low speed. This severely limits Pockels cells for many practical applications. It would be very important to have a large field of view, low driving voltage, and high speed Pockels cell. A Pockels cell can be explained using polarization theory and the electrooptic effect. Based on these theories, the propagation of polarized light at various angles through Pockels cells can be traced by computer, but that method offers little insight. This work recasts the problem in a new way which is both accurate and straightforward. It develops a simplified computer model by extending a model developed at NIST (National Institutes of Standards and Technology). To improve the field of view two material-independent approaches are derived. The first this work proves (for the first time) the thinner-is-better hypothesis. Second, it derives a system configuration which both allows an arbitrary field of view and improved performance. It then shows how this analysis can be used to improve Spatial Light Modulators.

14. SUBJECT TERMS	15. NUMBER OF PAGES
Modulator, Polarization, Pockels Cell	191
	16. PRICE CODE

17. SECURITY CLASSIFICATION OF REPORT	18. SECURITY CLASSIFICATION OF THIS PAGE	19. SECURITY CLASSIFICATION OF ABSTRACT	20. LIMITATION OF ABSTRACT
UNCLASSIFIED	UNCLASSIFIED	UNCLASSIFIED	SAR

PAGE iii

PAGE iv

THESE PAGES HAVE BEEN INTENTIONALLY LEFT BLANK

ELECTROOPTIC MODULATORS

This work is aimed mainly at improving the overall performance of Pockels electrooptic modulators. Current Pockels cells have very limited field of view, high driving voltage, and low speed. This severely limits Pockels cells for many practical applications. It would be very important to have a large field of view, low driving voltage, and high speed Pockels cell.

A Pockels cell can be explained using polarization theory and the electro-optic effect. Based on these theories, the propagation of polarized light at various angles through Pockels cells can be traced by computer, but that method offers little insight. I have recast this problem in a new way which is both accurate and straightforward. We developed a simplified computer model by extending a model developed at NIST(National Institutes of Standards and Technology).

To improve the field of view we derived two material-independent approaches. First, we proved (for the first time) the thinner-is-better hypothesis. Second, we deviced a system configuration which both allowed arbitrary field of

view and improved performance. We then showed how this analysis can be used, as well as, to improve Spatial Light Modulators (SLMs).

KEY WORDS: modulator, polarization, Pockels cell

TABLE OF CONTENTS

LIST OF TABLES

LIST OF FIGURES

LIST OF ABBREVIATIONS / ACRONYMS

EO	Electro-optic
FOV	Field of view
IO	Integrated optics
LCD	Liquid crystal display
MQW	Multiple quantum well
SLM	Spatial light modulator

CHAPTER I

INTRODUCTION

1.1 Objectives

Modulator users are often frustrated by the limited field of view, high driving-voltage and monochromatic operation requirement of Pockels cell modulators. This research work is aimed mainly at improving the overall performance of Pockels electrooptic modulators. In order to reach this overall objective, the following tasks were accomplished: a) the invention of a new method for calculating cascades of birefrigent cells; b) the invention of a new simplified model to simulate Pockels cells; c) the creation of an approach to achieve a high FOV, low voltage and great bandwidth modulator; d) the analysis of FOV in Pockels cell; e) the investigation of fundamental constraints on SLMs supporting NxN FANIN/FANOUT.

1.2 Approach and Accomplishments

This work uses available materials and seek improved configurations of Pockels cell. An overall improvement of the Pockels cell and several new accomplishments are achieved.

1. A new method for calculating cascades of birefrigent cells

This new method allows us to determine the directions and amplitudes of rays propagating through an arbitrary system of homogenous and/or uniaxial materials.

2. A modified NIST model for Pockels cell

This model is a modification of a NIST model for electrooptic modulator. Angular effects of an elctrooptic modulator are introduced so that simulation of electrooptic modulator becomes more effective and acurate in predicting fields of view.

3. General solution for an electrooptic modulator with arbitrary FOV, voltage, and bandwidth

Field of view, sensitivity to voltage, and bandwidth are increased by any factor through longitudinal, lateral, and multichannal expansions. This gives the designer of electrooptic modulators full freedom to pick the voltage, FOV, and the bandwidth of his system.

4. FOV and voltage effects in Pockels cell

FOV and driving voltage are important in Pockels modulators. For fully understanding of them, the effects of varying thickness on FOV and voltage in Pockels modulators are studied.

5. Fundamental constraints on SLMs supporting NxN FANIN/FANOUT

This work severely constrains optical computer design and is, therefore, potentially, very valuable.

1.4 Dissertation Outline

This dissertation is divided into six chapters. It starts with the objectives and accomplishments of this research work in Chapter I to claim improving over-all performance of Pockels cell as the main goal and to suggest how much can be done to achieve this goal. Chapter II provides the background for fully understanding electrooptic modulators. The basis of light polarization is discussed along with key polarization components: polarizer and analyzer. Polarization based EO modulators, such as Kerr cell, Pockels cell and integrated waveguide modulator are introduced here also. This chapter is concluded with a brief survey of some applications of polarization like Q-switch, SLM, and LCD. Chapter III includes most of my theoretical analyses of light propagation through EO modulators. Basically, there are three categories of analytical theories: ray tracing algorithm, matrix algorithm and NIST model. The extension of current analytical theory and modified NIST model are fully discussed in this chapter. Two major characteristics of EO modulator: FOV and speed, are explored in Chapter IV. Chapter V discusses thickness effects, extended FOV, fundamental constraints on SLM, and RC limited - Ω tradeoff. Finally, This dissertation are concluded with a summary of our important results and some suggestions for future research.

CHAPTER II

BACKGROUND

2.1 Polarization Effects in Crystals

Here we assume that optical media are homogeneous and transparent and can be characterized by a real dielectric constant ε (which is not really constant but varies with wavelength (frequency)). Alternately, we could consider the refractive index $n = \sqrt{\varepsilon}$. The solutions of Maxwell's equations are then monochromatic plane waves which propagate with a phase velocity c/n without a change in amplitude or polarization, regardless of the direction of propagation and initial polarization. Consequently, these media are called singly refracting, a term that will be understood shortly.

In optical media the velocity of the light transmission is determined by the direction of oscillation or vibration and not by direction of transmission. If we have three orthogonal axes each characterized by its own refractive index, then the velocity of propagation depends on the refractive indices of the axes which are *transverse* to the direction of propagation. If this fact is clearly remembered, then much of the behavior of optical propagation in crystals can be readily understood.

When light propagates through many types of crystals , a surprising phenomenon is observed. If a single beam of light enters the crystal, then two beams displaced from each other emerge. This phenomenon is called double refraction[1]. It is best known in the crystal calcite. Further investigations show that all transparent media can divided into the class of singly refracting or doubly refracting media . Mathematically, these media (crystals) are characterized by isotropic *or* anisotropic dielectric constants. Furthermore, anisotropic crystal are divided into uniaxial or biaxial crystals. Finally, it is found that some crystals have the additional property of being optically active; crystals of this type rotate the polarization ellipse. Quartz is one of the best representatives of an optically active and birefringent crystals.

With respect to polarization, it is found that in doubly refracting media monochromatic waves can be supported for any given frequency and in any direction. However, there are two polarizations for which there is a definite refractive index; the refractive indices associated with each of the two polarizations are different. The two polarizations are, in general, elliptical. Their polarization ellipses have the same eccentricities, their major axes are perpendicular to each other, and their ellipticities are opposite to each other.

In Maxwell's theory a dielectric medium is characterized by the relation between $\vec{D}(\bar{r},t)$ and $\vec{E}(\bar{r},t)$. For a transparent, singly refracting medium the specific relation between these two quantities is

$$\vec{D}(\vec{r},t) = \varepsilon\, \vec{E}(\vec{r},t) \qquad (2\text{-}1\text{-}1)$$

In order to describe double refraction (anisotropic media) it is natural to try the most general linear relation between $\vec{D}$ and $\vec{E}$, namely

$$D_x = \varepsilon_{xx}E_x + \varepsilon_{xy}E_y + \varepsilon_{xz}E_z \qquad (2\text{-}1\text{-}2a)$$

$$D_y = \varepsilon_{yx}E_x + \varepsilon_{yy}E_y + \varepsilon_{yz}E_z \qquad (2\text{-}1\text{-}2b)$$

$$D_z = \varepsilon_{zx}E_x + \varepsilon_{zy}E_y + \varepsilon_{zz}E_z \qquad (2\text{-}1\text{-}2c)$$

For nonactive media all the ε_{ij} coefficients are real, while for active media some are complex. We are only interested in nonactive media. For this case one can show that

$$\varepsilon_{ij} = \varepsilon_{ji} \qquad (2\text{-}1\text{-}3)$$

where ij represents any pair of letter x, y, and z. Equation (2) can be written in matrix form:

$$\begin{pmatrix} D_x \\ D_y \\ D_z \end{pmatrix} = \begin{pmatrix} \varepsilon_{xx} & \varepsilon_{xy} & \varepsilon_{xz} \\ \varepsilon_{yx} & \varepsilon_{yy} & \varepsilon_{yz} \\ \varepsilon_{zx} & \varepsilon_{zy} & \varepsilon_{zz} \end{pmatrix} \begin{pmatrix} E_z \\ E_z \\ E_z \end{pmatrix} \qquad (2\text{-}1\text{-}4)$$

If all the ε_{ij}'s are real and are related to each other by (2-1-3), then the 3×3 matrix (2-1-4) is *symmetric*. This fact is very important, because if a crystal can be represented by symmetric matrix A then it is always possible to reduce (2-1-4) to a diagonal form S by using an orthogonal transformation matrix C; that is,

$$S = C^{-1}AC \qquad (2\text{-}1\text{-}5a)$$

and

$$C^{-1} = C^{T} \tag{2-1-5b}$$

Equation (2-1-5b) is the orthogonality condition for the matrix C, and C^{-1} and C^{T} are the inverse matrix and transposed matrix, respectively.

The transformation described by (2-1-5) for a real symmetric matrix A allows us to write (2-1-2) in a diagonalized form as

$$D_x = \varepsilon_x E_x \tag{2-1-6a}$$

$$D_y = \varepsilon_y E_y \tag{2-1-6b}$$

$$D_z = \varepsilon_z E_z \tag{2-1-6c}$$

The new set of axes are called the principal axes of the crystal, and $\varepsilon_x, \varepsilon_y$, and ε_z are the principal dielectric constants. The principal indices of refraction are defined by

$$n_x = \sqrt{\varepsilon_x} \tag{2-1-7a}$$

$$n_y = \sqrt{\varepsilon_y} \tag{2-1-7b}$$

$$n_z = \sqrt{\varepsilon_z} \tag{2-1-7c}$$

The great value of the principal axes form (2-1-7) is that Maxwell's equations, as we shall soon see, are then particularly easy to solve in terms of plane-wave solutions.

We can represent (2-1-6) as a diagonal matrix and write

$$\begin{pmatrix} D_x \\ D_y \\ D_z \end{pmatrix} = \begin{pmatrix} \varepsilon_x & 0 & 0 \\ 0 & \varepsilon_y & 0 \\ 0 & 0 & \varepsilon_z \end{pmatrix} \begin{pmatrix} E_z \\ E_z \\ E_z \end{pmatrix} \qquad (2\text{-}1\text{-}8)$$

Uniaxial crystals are characterized by the equality of two the principal indices (axes). We arbitrarily take these axes to be

$$n_x = n_y = n_0 \qquad (2\text{-}1\text{-}9a)$$

$$n_z = n_e \neq n_0 \qquad (2\text{-}1\text{-}9b)$$

Equation (2-1-9) is invariant under a rotation about the z axes. The subscripts o and e stand for *ordinary* and *extraordinary*, for reasons we shall soon understand. The z axis turns out to have a peculiar property: along this axis the anisotropic crystal behaves as thought it were an isotropic crystal (medium). This axis is along a special direction in the crystal, which we call the *optic axis*; the significance of the optic axis will appear shortly. When (2-1-9)is true, the real parts of $\vec{D}$ and $\vec{E}$ are collinear if and only if the real part of $\vec{E}$ is along or perpendicular to the z axis. This also holds for the imaginary parts.

For a biaxial crystal all three principal indices are different, so (without loss of generality)

$$n_x > n_y > n_z \qquad (2\text{-}1\text{-}10)$$

We then find that there are two optic axes in the xz plane with the angles between them being bisected by the x and y axes. Fortunately, the two most

important polarizing crystals, calcite and quartz, are uniaxial. In practice, biaxial crystals are not so widely used as these two uniaxial crystals.

In an optically active crystal or medium the relation between $\vec{D}$ and $\vec{E}$ referred to suitable cartesian axes is described by

$$D_x = \varepsilon_x E_x + i\left(\delta \times \vec{E}\right)_x \qquad (2\text{-}1\text{-}11a)$$

$$D_y = \varepsilon_y E_y + i\left(\delta \times \vec{E}\right)_y \qquad (2\text{-}1\text{-}11b)$$

$$D_z = \varepsilon_z E_z + i\left(\delta \times \vec{E}\right)_z \qquad (2\text{-}1\text{-}11c)$$

where

$$\delta \times \vec{E} = \begin{pmatrix} \hat{x} & \hat{y} & \hat{z} \\ \delta_x & \delta_y & \delta_z \\ E_x & E_y & E_z \end{pmatrix} \qquad (21\text{-}11d)$$

and $i = \sqrt{-1}$. In (2-1-11) the dielectric constants are real, and δ is a real vector. From (2-1-11c) and (2-1-11d), we have

$$\varepsilon_{xx} = \varepsilon_x \qquad \varepsilon_{xy} = -i\delta_z \qquad \varepsilon_{xz} = i\delta_y \quad \text{etc.} \qquad (2\text{-}1\text{-}12)$$

the dielectric constants are determined by the medium and weakly dependent on frequency. However, δ is a complicated parameter and depends on the medium, the direction of propagation of the plane wave, and, strongly, on the wavelength.

We now solve Maxwell's equations for anisotropic media. We recall Maxwell's equations are

$$\nabla \times \vec{H} = \frac{4\pi}{c}\vec{j} + \frac{1}{c}\frac{\partial D}{\partial t} \qquad \text{(2-1-13a)}$$

$$\nabla \times \vec{E} = -\frac{1}{c}\frac{\partial \vec{B}}{\partial t} \qquad \text{(2-1-13b)}$$

$$\nabla \cdot \vec{D} = 4\pi\rho \qquad \text{(2-1-13c)}$$

$$\nabla \cdot \vec{B} = 0 \qquad \text{(2-1-13d)}$$

In a crystal there are no currents or free charges. Furthermore, we assume the permeability μ is constant and $\vec{B} = \mu\vec{H}$. Equations (2-1-13) then reduce to

$$\nabla \times \vec{H} = \frac{1}{c}\frac{\partial D}{\partial t} \qquad \text{(2-1-14a)}$$

$$\nabla \times \vec{E} = -\frac{\mu}{c}\frac{\partial \vec{H}}{\partial t} \qquad \text{(2-1-14b)}$$

$$\nabla \cdot \vec{D} = 0 \qquad \text{(2-1-14c)}$$

$$\nabla \cdot \vec{H} = 0 \qquad \text{(2-1-14d)}$$

We now assume plane-wave solutions of the form

$$\vec{D}(\vec{r},t) = \vec{D}_0 \exp\{i[\vec{k} \cdot \vec{r} - \omega t]\} \qquad \text{(2-1-15a)}$$

$$\vec{E}(\vec{r},t) = \vec{E}_0$$

$$\vec{H}(\vec{r},t) = \vec{H}_0$$

If we have plane-wave solutions, we can replace the ∇ and the $\partial/\partial t$ operators by

$$\nabla \rightarrow i\vec{k} \qquad \text{(2-1-16a)}$$

$$\frac{\partial}{\partial t} \rightarrow -i\omega \qquad (2\text{-}1\text{-}16b)$$

so (2-1-13) becomes

$$\vec{k} \times \vec{H} = -(\frac{\omega}{c})\vec{D} \qquad (2\text{-}1\text{-}17a)$$

$$\vec{k} \times \vec{E} = (\frac{\mu\omega}{c})\vec{H} \qquad (2\text{-}1\text{-}17b)$$

$$\vec{k} \cdot \vec{D} = 0 \qquad (2\text{-}1\text{-}17c)$$

$$\vec{k} \cdot \vec{H} = 0 \qquad (2\text{-}1\text{-}17d)$$

We now operate on (2-1-17b) with $\vec{k}\times$ and use (2-1-17a). We then find

$$\vec{k} \times (\vec{k} \times \vec{E}) = -k_0^2 \vec{D} \qquad (2\text{-}1\text{-}18)$$

where $k_0 = \omega/c$ and we have set $\mu = 1$.

Using the well-known vector identity

$$\vec{a} \times (\vec{b} \times \vec{c}) = \vec{b}(\vec{a} \cdot \vec{c}) - \vec{c}(\vec{a} \cdot \vec{b}) \qquad (2\text{-}1\text{-}19)$$

we rewrite (2-1-18) as

$$k^2 \vec{E} - \vec{k}(\vec{k} \cdot \vec{E}) = k_0^2 \vec{D} \qquad (2\text{-}1\text{-}20)$$

From (2-1-17c), $\vec{k} \cdot \vec{D} = 0$. thus $\vec{k}$ and $\vec{D}$ continue to be perpendicular to each other even in an anisotropic medium. Expanding (2-1-17c) in Cartesian components, we obtain

$$k_x D_x + k_y D_y + k_z D_z = 0 \qquad (2\text{-}1\text{-}21)$$

We now subsititude the relations between D_x and E_x, etc., given by (2-1-6) into (2-1-21) and find

$$k_x\varepsilon_x E_x + k_y\varepsilon_y E_y + k_z\varepsilon_y E_z = 0 \qquad (2\text{-}1\text{-}22)$$

Equation (2-1-22) shows that in an anisotropic (crystal) medium $\vec{k}$ and $\vec{E}$ are not perpendicular to one another. Expanding (2-1-20) in terms of its components yields

$$k^2E_x - k_x(\vec{k}\cdot\vec{E}) = k_0^2 D_x \qquad (2\text{-}1\text{-}23a)$$

$$k^2E_y - k_y(\vec{k}\cdot\vec{E}) = k_0^2 D_y \qquad (2\text{-}1\text{-}23b)$$

$$k^2E_z - k_z(\vec{k}\cdot\vec{E}) = k_0^2 D_z \qquad (2\text{-}1\text{-}23c)$$

We now solve (2-1-23) for a nonactive uniaxial crystal. A uniaxial crystal is characterized by (2-1-9). These relations are invariant under the rotation of the coordinate axes about the z axes through any angle. therefore, it is sufficient to consider only directions of $\vec{k}$ lying in a plane through this axis. This plane can be conveniently chosen to be the xz plane, so

$$k_y = 0 \qquad (2\text{-}1\text{-}24a)$$

$$k^2 = k_x^2 + k_z^2 \qquad (2\text{-}1\text{-}24b)$$

This allows us to write immediately

$$\vec{k}\cdot\vec{r} = k_x x + k_y y + k_z z = k_x x + k_z z \qquad (2\text{-}1\text{-}25)$$

Substituting (2-1-24) into (2-1-23) leads to the following set of equations:

$$(k_z^2 - n_0^2 k_0^2)E_x - k_x k_z E_z = 0 \qquad (2\text{-}1\text{-}26a)$$

$$(k^2 - n_0^2 k_0^2)E_y = 0 \qquad (2\text{-}1\text{-}26b)$$

$$-k_x k_z E_x + (k_x^2 - n_e^2 k_0^2)E_z = 0 \qquad (2\text{-}1\text{-}26c)$$

Equation (2-1-26) has two solutions. In (2-1-26b) we see that we have zero if either factor is zero. We assume that first factor is zero. Then

$$E_x' = E_z' = 0 \,, \qquad E_y' \neq 0 \tag{2-1-27a}$$

$$k' = n_0 k_0 \tag{2-1-27b}$$

where the prime represents the first solution. The corresponding wave vector is denoted by $\vec{k}'$; we note that its magnitude is independent of the direction of propagation. Thus (2-1-24b) and (2-1-27b) show that the propagation of the wave is described by

$$k'^2 = k_x'^2 + k_z'^2 = (n_0 k_0)^2 \tag{2-1-28}$$

Equation (2-1-28) is the equation of a circle. In three-dimensional K-space the wave associated with n_0 is called the ordinary wave. It always propagates as a spherical wave. The plane wave associated with this solution appears to behave in the same way as a plane wave in an isotropic, single refracting medium. Consequently, the plane wave associated with this solution, (2-1-27), is called the ordinary wave and the pricipal index n_0 is called the ordinary index. The solution D' can then be written as

$$D' = D_y = \varepsilon_y E_y = \sqrt{n_0} E_{0y} e^{i(k_x' x + k_z' z)} \tag{2-1-29}$$

or, simply,

$$D_y' = D_0' e^{i(k_x' x + k_z' z)} \tag{2-1-30}$$

We see that (2-1-30) describes a linearly polarized wave propagation in the direction $\vec{k}'$ with a magnitude $k_0 n_0$. The ordinary wave is always linearly polarized with $\vec{D}'(\vec{E}')$ perpendicular to the axis of symmetry.

We can obtain the second solution by assuming that E_y in (2-1-26b) is zero. The condition for a solution is that the determinant of the coefficients of E_x and E_z in (2-1-26a) and (2-1-26b) vanish. Then we find

$$\frac{k_x''^2}{n_e^2} + \frac{k_z''^2}{n_o^2} = k_0^2 \qquad (2\text{-}1\text{-}31)$$

and

$$\frac{E_z''}{E_x''} = -\frac{n_0^2 k_x''^2}{n_e^2 k_z''^2} \qquad (2\text{-}1\text{-}32)$$

Equation (2-1-32) shows that the field is constrained to the xz plane, so the field is linearly polarized, with $\vec{E}''$ and $\vec{D}''$ in the plane defined by $\vec{k}''$ and the axis of symmetry. Unlike the first solution, however, (2-1-31) shows that the wave field does not propagate as a sphere but an ellipsoid. Consequently, this wave field is now called extraordinary, and the principal index n_e is called the extraordinary index. We can now write this second solution simply as

$$D'' = D_0'' \, e^{i(k_x'' x + k_z'' z)} \qquad (2\text{-}1\text{-}33)$$

In Figure (2.1.1) we show the wave vector surfaces for (2-1-28) and (2-1-30). The vectors $\vec{k}'$ and $\vec{k}''$ radiate from a fixed point. Their end points describe two surfaces of revolution about the symmetry axis of the crystal. These surfaces are called wave vector surfaces; they are not to be confused

with the wave velocity surfaces and the ray velocity surfaces used in other texts to describe double refraction. From (2-1-28) $\bar{k}'$ is a sphere of radius n_0k_0 and $\bar{k}''$,(2-1-31), describes an ellipsoid whose section through the axis is an ellipse. The pricipal radius of the ellipsoid along the axis of symmetry is n_ek_0, and perpendicular to this axis it is n_0k_0. If $n_e < n_0$ the uniaxial crystal is called negative. On the other hand, if $n_e > n_0$ the uniaxial crystal is called

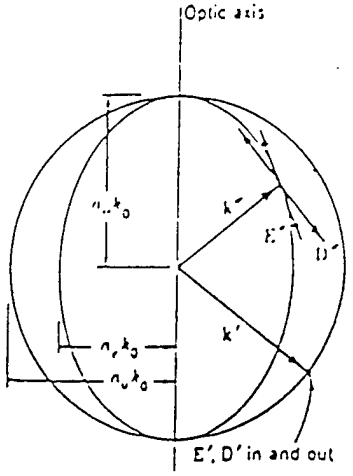

Figure 2.1.1 Wave vector surfaces for a negative uniaxial crystal.

positive. The primary example of a negative uniaxial crystal is calcite, whose refractive indices at the Na D line (5893 A^0) are

$$n_e = 1.486 \qquad n_0 = 1.658 \tag{2-1-34}$$

On the other hand, quartz is a positive crystal, and its indices are

$$n_e = 1.553 \qquad n_0 = 1.544 \tag{2-1-35}$$

Let us examine the consequences of these results. First, consider the propagation along the axis of symmetry. For this case we see that $k_x = 0$. Hence (2-1-28) and (2-1-31) reduce to

$$k_z^{\cdot} = n_o k_0 \qquad \text{(2-1-36a)}$$

$$k_z^{\cdot\cdot} = n_o k_0 \qquad \text{(2-1-36b)}$$

Thus, the propagators are identical. The corresponding fields, (2-1-30a) and (2-1-30b), are seen to be

$$D^{\cdot} = D_0^{\cdot} e^{in_o k_0 z} \qquad \text{(2-1-37a)}$$

$$D^{\cdot\cdot} = D_0^{\cdot\cdot} e^{in_o k_0 z} \qquad \text{(2-1-37b)}$$

Specifically, from (2-1-28a) and (2-1-32) we see that (2-1-37a) and (2-1-37b) can be written in terms of Cartesian coordinates as

$$D_y = D_{0y} e^{in_o k_0 z} \qquad \text{(21-38a)}$$

$$D_x = D_{0x} e^{in_o k_0 z} \qquad \text{(2-1-38b)}$$

The phase factors in (2-1-38a) and (2-1-38b) are identical, so the field components propagate with the same velocity in the z direction, that is along the axis of symmetry n_e. Because the velocities are equal as the field propagates along this axis, it is called the optic axis. In optical crystallography it is also called the crystallgraphic or c axis. We emphasize that the optic axis corresponds to a direction in the crystal. When the optical field propagates in the direction of the optic axis, the crystal behaves as

though it were an isotropic medium; the phenomenon of double refraction does not appear.

We now consider that the propagation is perpendicular to the axis of symmetry. In this case $k_z = 0$, so we have from (2-1-28) and (2-1-31) that

$$k_x^{\cdot} = n_o k_0 \qquad \text{(2-1-39a)}$$

$$k_x^{\cdot} = n_e k_0 \qquad \text{(2-1-39b)}$$

The fields are now described by

$$D_y = D_{0y}\, e^{i n_o k_0 x} \qquad \text{(2-1-40a)}$$

$$D_z = D_{0z}\, e^{i n_e k_0 x} \qquad \text{(2-1-40b)}$$

Thus we see that phases of the two components in (2-1-40) are different. This phase difference is called birefringence. We now restore the time factor in (2-1-40), so we can write

$$D_y = D_{0y} \cos(\omega t - n_o k_0 x) \qquad \text{(2-1-41a)}$$

$$D_z = D_{0z} \cos(\omega t - n_e k_0 x) \qquad \text{(2-1-41b)}$$

If we eliminate ωt between these equations, we arrive at the familiar polarization ellipse.

Since one wave propagates faster then the other, a phase difference δ develops between them. After a distance l has been traveled , the phase difference is

$$\delta = k_0(n_e - n_o)l \qquad \text{(2-1-42)}$$

Thus , if we allow an electric field to propagate perpendicular to the optic axis, we can obtain any desired shift by varying the propagation length x. This fact is the basis for optical wave plates. For a quarter-wave plate x must be varied so that $\delta = \pi/2$, and, similarly, for a half-wave plate x must be varied so that $\delta = \pi$.

If an optical beam is allowed to propagate through a crystal, its polarization state can be changed to any desired ellipticity by varying its phase. This can be done by means of a device which can introduce a variable phase shift in the optical path. The most obvious way to do this is to take two wedges

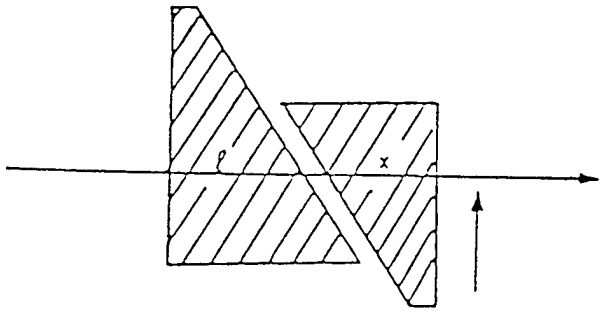

Figure 2.1.2 Construction of a variable phase-shifting device. The first wedge is stationary, and the second wedge is movable. In both wedge the optic axis are perpendicular to the direction of propagation and parallel to each other. The solid lines in the wedges indicate that the transverse ordinary and extraordinary axes are parallel to each other.

with their ordinary and extraordinary axes parallel to each other as shown in Figure 2.1.2.

The phase shift through the first wedge is

$$\delta_1 = k_0(n_e - n_o)l \qquad (2\text{-}1\text{-}43a)$$

where l is the fixed thickness of the wedge at the center. Similarly the phase shift through the second (movable) wedge along the same optical path is

$$\delta_2 = k_0(n_e - n_o)x \qquad (2\text{-}1\text{-}43b)$$

The total phase shift δ is then

$$\delta = \delta_1 + \delta_2 = k_0(n_e - n_o)(l + x) \qquad (2\text{-}1\text{-}44)$$

Thus, the phase shift increases with increasing x. Equation (2-1-44) is perfectly satisfactory from a theoretical point of view. However, in optical measurements it is usually preferable to calibrate polarizing instruments at a null intensity. Ideally, it would be preferable to make two wedges and mount them so that when the thickness of the moving wedge is equal to the thickness of the stationary wedge a null intensity is obtained; a null intensity can be observed when the two wedges are placed between crossed polarizers. To obtain a null intensity when l = x, we must express l and x by a difference rather than a sum. In this form the phase-shifting devices is called a Babinet compensator. A difference in l and x can be obtained, as we shall now show, by reversing the directions of the optic axis in each wedge. In Figure 2.1.3 we show the basic construction of the Babinet compensator.

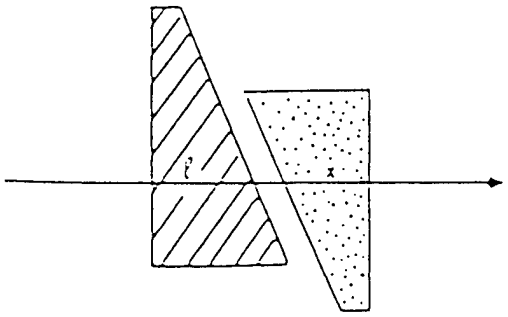

Figure 2.1.3 Construction of the Babinet compensator. The solid lines in the first quartz wedge and the dots in the second quartz wedge indicate that the ordinary and extraor dinary axes are reversed.

The phase variation is again obtained by fixing the first wedge and moving the second wedge over the first wedge, as indicated in the figure. Moving the second quartz wedge again changes the path length, so the total path length and phase vary. We can determine the total phase shift as follows. In the first wedge the phase shift δ_1 is

$$\delta_1 = k_0(n_e - n_o)l \qquad (2\text{-}1\text{-}45a)$$

where l is the fixed path length through the first quartz wedge. In the second quartz wedge the ordinary and extraordinary axes are rotated 90° , that is, reversed. The phase shift is now

$$\delta_2 = k_0(n_o - n_e)x \qquad (2\text{-}1\text{-}45b)$$

The total phase shift is then

$$\delta = \delta_1 + \delta_2 = k_0(n_e - n_o)(l - x) \qquad (2\text{-}1\text{-}46)$$

Thus, the phase δ varies linearly with x. By changing x, the thickness or total path length that beam travels in both quartz wedge, any desired phase can be obtained. We also see from(2-1-44) that when l = x the phase shift is zero. Thus, for this position the Babinet compensator is effectively removed from the optical path.

We can summarize these results as follows:

1. If there is propagation along the direction of the optic axis, there is no birefringence and no double refraction.

2. If the propagation is perpendicular to the optic axis, there is birefringence but no double refraction.

3. If there is propagation in any direction other than along the principal indices of refraction, there is both birefringence and double refraction.

Not surprisingly, the detailed description of wave propagation through crystals is quite complicated.

We have seen that the velocity of light transmission determined by the direction of oscillation or vibration and not by the direction of transmission. Thus, if we have propagation along the optic axis (the z axis) where the refractive index is n_e the orthogonal components are along the x and y axes where the refractive indices are both n_o. The propagation factor for each

oscillation is identical, and so there is no birefringence. On the other hand, If the propagation is along the x axis (n_o) and we have an oscillation along the optic axis (n_e) and the y axis (n_o), the birefringence is proportional to $|n_e - n_o|$.

Uniaxial crystals have two principal indices of refraction. Light traveling in any direction except the direction of the optic axis consists of two sets of waves with different velocities and the same frequency. The change of two sets of waves with different velocities and the same frequency. The change of refractive index with the direction of light propagation may be visualized by the use of uniaxial indicatrix, a three-dimensional geometric figure showing the variation of the indices of refraction of a crystal for monochromatic light waves in their direction of vibration. Each radius vector represents a vibration direction whose length measures the index of refraction of the crystal for waves vibrating parallel to the direction.

Figure 2.1.4 shows indicatrices for positive and negative uniaxial crystals. Figure 2.1.4a is a prolate ellipsoid of revolution constructed so that its semimajor and semiminor axes are proportional, respectively, to the maximum and minimum refractive indices of a uniaxial crystal. Figure 2.1.4b shows a negative uniaxial indicatrix which is an oblate ellipsoid of revolution. Any section passing through and including the optic axis of either indicatrix is an ellipse and is called a principal section. Equatorial sections at right angles to the optic axis are circles.

If unpolarized light is normally incident on a crystal plate cut perpendicular to the optic axis, the light entering the crystal is not refracted and passes through without becoming polarized. However, in any other direction the light is doubly refracted. We now calculate the rays and the wave normals for light propagating in a uniaxial crystal in the pricipal section of a uniaxial positive indicatrix for which $n_o = 1.5$ and $n_e = 2.0$.

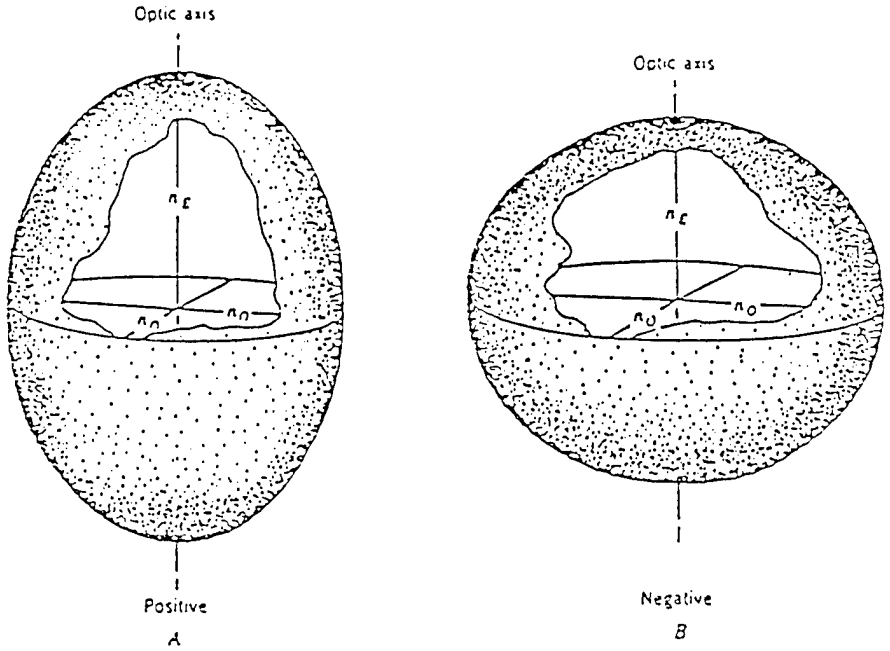

Figure 2.1.4 Positive and negative uniaxial indicatrices.

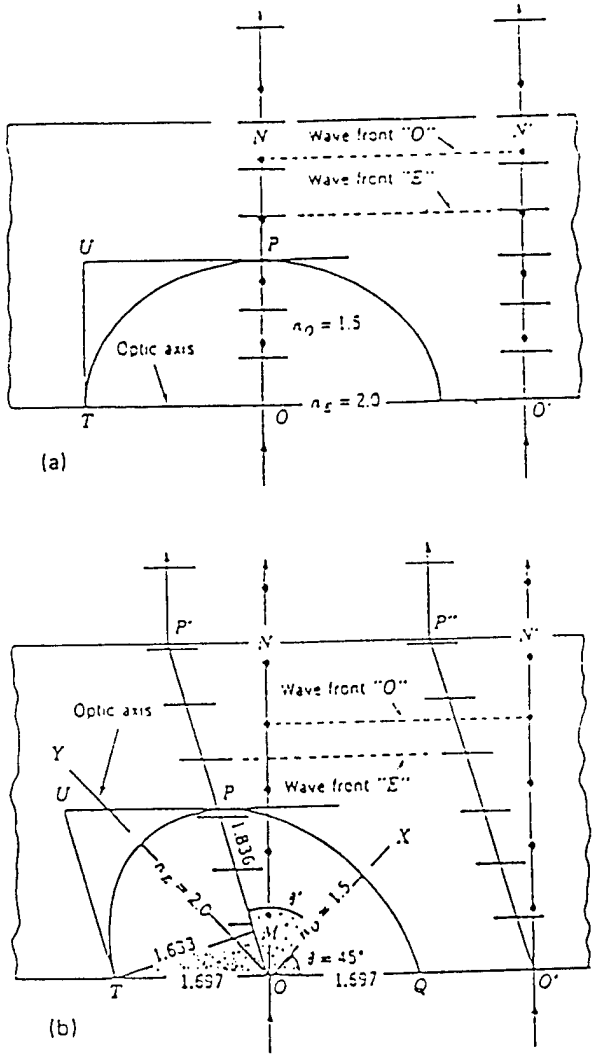

Figure 2.1.5 Principal section of a uniaxial positive indicatrix showing relationships between rays and wave normals (from Wahlstrom). (a) Unpolarized light normally incident on a section of uniaxial positive crystal. Section cut parallel to the optic axis. (b) Unpolarized light normally incident on a section of a uniaxial crystal. Section inclined to optic axis.

In Figure 2.1.5a, unpolarized light is normally incident at O and O' on a crystal plate cut parallel to the optic axis (c axis). The light wave in one

component (the extraordinary component) vibrates in the principal section (the plane of the drawing) and travels through the crystal in the direction of the wave normal, ON. For this component, the crystal has a refractive index n_e, and the waves and the wave fronts travel through the crystal with velocity c/n_e. In Figure 2.1.5a the relative velocities and directions of arrows along the rays. Certain wave fronts for both components also are indicated. ON and ON' are the directions of both the rays and the wave normals, and we can say that the rays and the wave normals coincide.

The amplitude of the light vector shown for the e component, vibrating in the principal section and parallel to the optic axis, is indicated arbitrarily by the lengths of the arrows in Figure 2.1.5. The dimension of indicatrix parallel to the vibration direction bears no direct relationship to the amplitudes of the light vectors. Instead, the amplitudes depend on the amplitude of the incident light and the manner in which the light is resolved and absorbed by the crystal.

Several relationships for the ellipse, developed in the note following ,are now used. The equation for the uniaxial indicatrix is

$$\frac{x^2 + y^2}{n_o^2} + \frac{z^2}{n_e^2} = 1 \qquad (2\text{-}1\text{-}47)$$

and the equation for the ellipse in principal section is

$$\frac{x^2}{n_o^2} + \frac{z^2}{n_e^2} = 1 \qquad (2\text{-}1\text{-}48)$$

where x and z are the coordinates for any point on the ellipse; by convention x is measure in a direction normal to the optic axis, and z is parallel to the optic axis.

The equation for the ellipse in the principal section of the indicatrix also can be expressed in polar coordinates as

$$r^2 = \frac{(n_o n_e)^2}{n_o^2 \sin^2\theta + n_e^2 \cos^2\theta} \qquad (2\text{-}1\text{-}49)$$

where r is a radius vector measured from the center of the ellipse to some point on the ellipse and θ is the angle between the radius vector and a reference axis, the x axis of the coordinates. In the following discussions, we use the polar coordinate equation for the indicatrix in the principal section to analyze certain conditions in which light waves do not pass through the crystal in the direction of the optic axis or in a direction normal to the optic axis.

We can now determine the direction of propagation and the refraction of the ordinary ray in crystals. The ordinary ray is found to follow Snell's law of refraction. However, the law of refraction for the extraordinary ray is somewhat more complicated. For the special case in which the optic axis is at right angles to the plane of incidence, the extraordinary ray follows Snell's law also, except the refractive index is n_e rather than n_o. For other case the normal to the wave front and the ray direction, that is, the direction of propagation of the wave as given by the Poynting vector, no longer coincide.

If the principal plane of the e ray and the principal section coincide, the wave normal (but not the e ray) obeys Snell's law. Then we can see from (2-1-49) that the refractive index is given by

$$\frac{1}{n_\theta^2} = \frac{\sin^2\theta}{n_e^2} + \frac{\cos^2\theta}{n_o^2} \qquad \text{(2-1-50a)}$$

or,

$$n_\theta = \frac{n_o n_e}{\sqrt{n_o^2 \sin^2\theta + n_e^2 \cos^2\theta}} \qquad \text{(2-1-50b)}$$

In (2-1-50), θ Is the angle between the direction of the wave normal and the optic axis ($\theta \le 90°$). When $\theta = 0°$, $n_\theta = n_e$, and when $\theta = 90°$, $n_\theta = n_e$. The angle of refraction is $\theta - \beta$, where β is the angle the normal to the surface makes with the optic axis. Snell's law of refraction for the extraordinary ray then becomes

$$n \cdot \sin i = n_\theta \cdot \sin(\theta - \beta) \qquad \text{(2-1-51)}$$

where I is the angle incidence of light in a medium of refractive index n. Substituting n_θ from (2-1-50b) into (2-1-51), we then have

$$n \cdot \sin i = \frac{n_o n_e}{\sqrt{n_o^2 \sin^2\theta + n_e^2 \cos^2\theta}} \cdot \sin(\theta - \beta) \qquad \text{(2-1-52)}$$

Since all other equations in (2-1-52) are known, θ can be determined; very often this must be done by iteration. The angle of refraction r for the extraordinary ray can be determined as follows. If θ' is the angle the ray makes with the optic axis, then $r = \theta' - \beta$ and we have

$$\tan\theta' = \frac{n_0^2}{n_e^2}\cot\theta \qquad (2\text{-}1\text{-}53)$$

Solving for θ' and knowing β, we then find r.

We now turn to the problem of determining the behavior of the ray within a crystal. In Figure 2.1.5b the unpolarized light is normally incident on a crystal plate which, in the pricipal section, makes an angle θ. The angle θ is arbitrarily set to 45°. The incident light is resolved into two components vibrating in mutually perpendicular planes and, as in Figure 2.1.5a, the o wave are not refracted and pass through the crystal in the direction of the normal to the wave front with a velocity proportional to $1/n_o$. The e wave vibrating in the principal section follows the ray OP' and O'P'' and upon leaving the crystal plate is refracted so as to move in a direction parallel to that of the incident light. OP' is obtained by drawing a line from O through P, the point of tangency with ellipse of line drawn parallel to TQ.

The velocity of a wave as it moves along OP' is proportional to 1/TM, where TM is obtained by dropping a perpendicular from T to OP'. Calculation of the velocity of the wave front in the direction of the wave normal is made using (2-1-41). For n_e = 1.5, n_o = 2.0, and θ = 45° yield a refractive index of 1.697 for the wave vibrating in the pricipal section and in the wave front. The velocity of wave front in the direction of its normal, ON, is proportional to 1/1.697, that is , to 1/OT. The tangent UP is parallel to the wave front for the wave vibrating in the pricipal section. Another radius of the ellipse OP is

conjugate to a second radius if the first radius is parallel to the tangent to the ellipse at the end of the second radius. From the geometry of the ellipse, it is known that area enclosed by conjugate radii and their associated tangents is constant. Figure 2-1-5 shows that n_e and n_o are conjugate radii and the enclosed area is $n_o n_e = 3.0$. In Figure 2-1-5, the parallelogram UTOP encloses the same area. The radius OP has a dimension which can be obtained from

$$r_2^2 = n_o^2 + n_e^2 - r_1^2 \qquad (2\text{-}1\text{-}54)$$

where r_2 is the length of a radius that is conjugate to the reference radius r_1. Computation yields a value of 1.836 for OP. Because the area of a parallelogram is the product of its base and altitude, dividing the area of the parallelogram (3.0) by 1.836 yields a value of 1.633 for TM. By construction TM is normal to OP' along which the light wave vibrating in the principal section is propagated. The velocity of the light wave moving along OP' is proportional to 1/TM = 1/1.633, and in Figure 2.1.5b the arrows in the wave front are spaced accordingly.

The angle θ' between OP' and the same reference axis that was used to measure off θ in Figure 2.1.5b (the x axis) can be calculated from (2-1-53)

$$\tan\theta' = \left(\frac{n_o}{n_e}\right)^2 \cot\theta \qquad (2\text{-}1\text{-}53)$$

from which we find that $\theta' = 60.632°$. The total angle measured from the x axis is then 105.63°. From Figure 2.1.5b we see that if we subtract 90° then the angle measured from the direction ON is 15.632°.

Finally, we illustrate the phenomenon of double refraction with the following example of the construction of a Nicol polarizing prism. We have seen that calcite has a large difference in refractive indices. If the propagation is not perpendicular to the direction of the optic axis, the ordinary and extraordinary rays separate. Each of these rays is linearly polarized. A Nicol prism is a polarizing prism constructed so that one of the linear polarized beams is rejected and the other is transmitted through the prism unaltered.

In a Nicole prism a flawless piece of calcite is split so as to produce an elongated cleavage rhomb about three times as long as it is broad. The end faces, which naturally meet the edges at angles of 70°53',are ground so that that angles become 68° (this allows the field-of-view angle to be increased); apparently, this practice of "trimming" was started by Nicole himself. In Figure 2.1.6 the construction of the Nicol prism is shown. The calcite is sawed diagonally at right angles to ground and polished end faces. The halves are cemented together with balsam, and the sides of the prism are covered with an opaque, light absorbing coating. The refractive index of the Canada balsam is 1.54, a value intermediate to the refractive indices of the calcite. Its purpose is to deflect the ordinary easy (by total internal reflection)

out of the prism and to allow the extraordinary ray to be transmitted through the prism.

We now compute the angles as follows. The limiting angle for the ordinary ray (ray A) can be determined simply from Snell's law. The refractive index of the Canada balsam is approximately 1.54 and n_o is 1.6584 . at 5893 $\mathring{A}$ the critical angle I_2 for total internal reflection is

$$1.6583 \cdot \sin i_2 = 1.54 \cdot \sin(90°) \qquad (2\text{-}1\text{-}55)$$

so $i_2 = 68.28°$ (2-1-56)

The cut is made to the entrance face of the prism, so that the angle of refraction r_1 at the entrance face is 90° - 68.28° = 21.72°. Then from Snell's law the angle of incidence i_1 is

$$\sin i_1 = 1.6583 \cdot \sin 21.72° \qquad (2\text{-}1\text{-}57a)$$

so

$$i_1 = 37.88° \qquad (2\text{-}1\text{-}57b)$$

Since the entrance face makes an angle of 68° with the longitudinal axis of the prism, the normal to the entrance face is 90° - 68° = 22° to the longitudinal axis. The limiting angle at which the extraordinary ray is not totally reflected at the cut is computed in a similar manner except that now the refractive index of the extraordinary ray is a function of the angle θ and the optic axis. Ray B in Figure 2-1-6 indicates the path of the wave normal for the e ray in

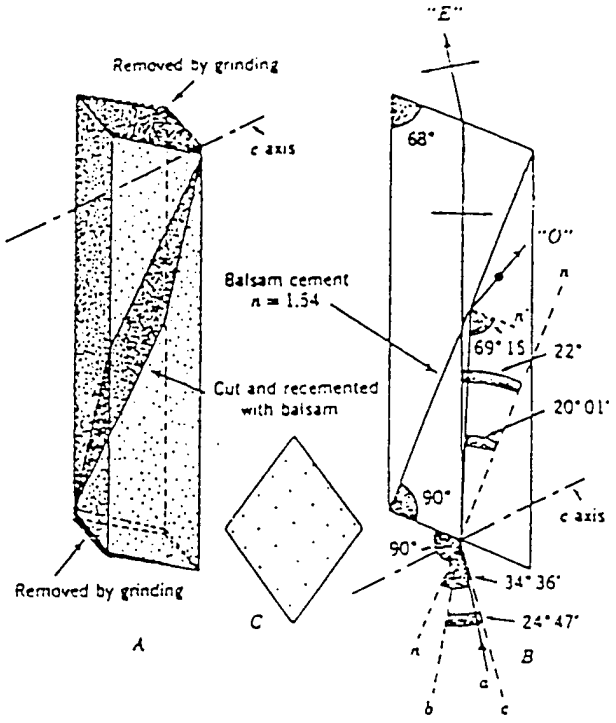

Figure 2.1.6 Construction of a Nicol prism: (a) construction of the prism; (b) passage of light through the prism, longitudinal section; (c) cross section (From Wahlstrom)

the prism for which Snell's law applies. As before, $i_2' = 90° - r_1'$, so that at the critical angle at the cut

$$\sin(90° - r_1') = \cos r_1' = \frac{1.54}{n_0} \qquad (2\text{-}1\text{-}58)$$

The quantity n_0 is given by (2-1-51) for which $\theta = r_1' + 41°44'$, so that one obtains the transcedental equation

$$\frac{\cos^2 r_1'}{1.54^2} = \frac{\sin^2\left(r_1' + 41.73°\right)}{1.4864^2} + \frac{\cos^2\left(r_1' + 41.73°\right)}{1.6583^2} \qquad (2\text{-}1\text{-}59)$$

This equation is easily solved on a computer for r_1', which is found to be 7.44° and $i_1' = 11.61°$. The half-angle θ_1 is then 22° - 11.61° = 10.39°. Since θ_1' is smaller than θ_1, the semifield angle is 2 × 10.39° = 20.78°.

The design of other, more modern, prisms takes place along the same lines. A through discussion of these designs is given in the review article by Beneath and Beneath.

Finally, with respect to optically active anisotropic crystals, represented most prominently by quartz, the optical activity shows up most markedly along the optic axis. Thus, the double refraction due to anisotropy is zero, and only the phenomenon of optical rotation is observed. However, for propagation of waves in directions perpendicular to the optic axis all uniaxial crystals exhibit double refraction, and quartz behaves like a positive crystal with pricipal refractive indices of (at 5893 Å) of

$$n_o = 1.5444 \qquad n_e = 1.553 \qquad (2\text{-}1\text{-}60)$$

Measurement of the specific rotation θ at 5893 Å is

$$\theta = \pm 3.79 \text{ rad cm}^{-1} \qquad (2\text{-}1\text{-}61)$$

2.2 Polarizers and Analyzers

Conventional polarizing prisms fall into two general categories(Bennett 1978): Glan types and Nicol types, which are illustrated in Fig 2.2.1. Glan types have the optic axis in the plane of the entrance face. If the principal section is parallel to the plane of the cut, the prism is a Glan-Thompson design; if perpendicular, a Lippich design; and if 45°, a Frank-Ritter design. In Nicol type prisms, the principal section is perpendicular to the entrance face, but the optic axis is neither parallel nor perpendicular to the face.

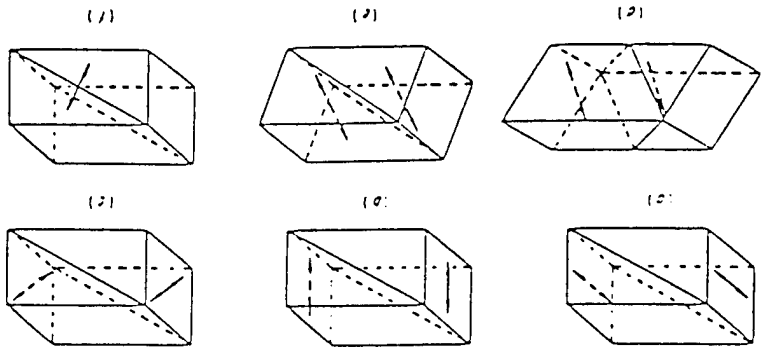

Fig 2.2.1 Types of conventional polarizing prisms. Glan types: (a) Glan-Thompson, (b) Lippich, and (c) Frank-Ritter; Nicol types: (d) conventional Nicol, (e) Nicol-Halle form, and (f) Hartnack-Prazmowsky. The optic axis are indicated by the double-pointed arrows.

Air-spaced prisms can be used at shorter wavelengths than cemented prisms, and special names have been given to some of them. An air-spaced Glan-Thompson prism is called a Glan-Foueault, and an air-spaced Lippich prism, a Glan-Taylor. In common practice, either of these may be called a Glan prism. An air-spaced Nicol prism is called a Foueaut prism. Double prisms can also be made, thus increasing the prism aperture without a corresponding increase in length. Most double prisms are preferred to as Frank-Ritter, ect., but a double Glan-Thompson is called an Anrens prism.

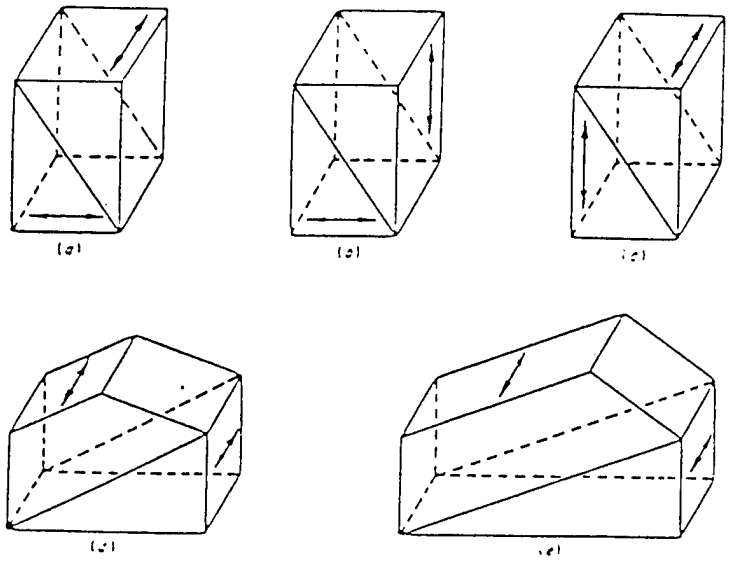

Fig 2.2.2 Types of polarizing beam-splitter prisms: (a) Rochon, (b) Sénarmont, (c) Wollaston, (d) Foster (shaded face is silvered), and (e) beam-splitter Glan-Thompson. In each case, the light is incident on the left face.

In polarizing beam-splitter prisms, two beams, which are polarized at right angles to each other, emerge but separated spatially. The prisms have usually been used in applications for which both beams are needed, e.g., in interference experiments, but they can also be used when only one beam is desired. These prisms are also of two general types, illustrated in Figure 2.2.2, those having the optic axis in the two sections of the prism perpendicular and those having them parallel.

2.3 Polarization Based Electro-Optic Modulators

2.3.1 Kerr Cell and Pockels Cell

We have seen throughout this text that Maxwell's electromagnetic theory is capable of explaining the main features of the propagation and polarization of light as it propagates through free space and matter, e.g., anisotropic crystals. In addition, there is another group of phenomena which can be explained and described by Maxwell's equations: the magneto-optical effect and the electro-optical effect. The primary examples of the former are the Zeeman effect and the Faraday effect. In this section we discuss only electro-optical effect and electro-optical crystals(Collette 1993 and Heriter 1990). Among the most important applications of the electro-optical effect are electro-optical modulation, the electro-optical shutter, and Q switching. After discussing the phenomenological behavior of the electro-optical effect, we consider these three applications.

In 1875, Kerr discovered that when a plate of glass is subjected to a strong electric field it becomes doubly refracting. That effect is due not to the strains but to the applied electric field on the glass is shown by the fact that the phenomenon also appears in many liquids; it has ever been observed in gases. When a liquid is placed in an electric field, it behaves optically like a uniaxial crystal with the optic axis parallel to the field direction. Kerr

observed a quadratic electro-optical effect in carbon disulfide. A linear effect was investigated by Pockels in crystals of quartz, tourmaline, potassium, chorate, and Rochelle salt; he also demonstrated that the effect was independent of a piezoelectrically induced strain.

It is common to refer to these two phenomena simply as the Kerr effect and the Pockels effect. The former is proportional to the square of the electric field, and the latter is linearly proportional to the electric field. In both phenomena the electro-optical effect causes a phase shift between the orthogonal field components of an optical beam propagating through the medium. In Kerr effect the field is applied perpendicular to the incident light. This is shown in Figure 2.3.1, where the medium a liquid.

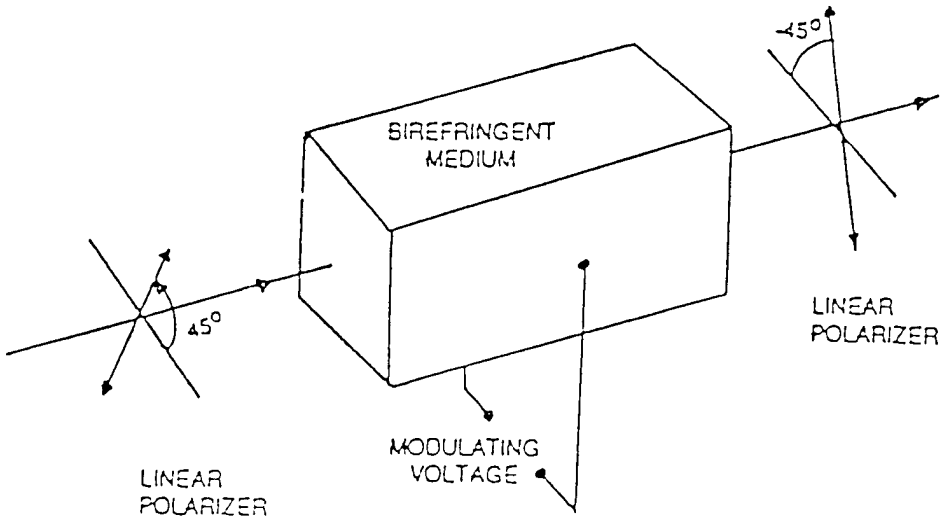

Figure 2.3.1 Propagation of a polarized beam of light through a Kerr cell.

In the Pockels effect the field is applied parallel to the crystal optic axis in the same direction as the incident light. This is shown in Figure 2.3.2. We see, therefore, that for Kerr quadratic effect the field is applied transversely to the incident beam, and for the Pockels linear effect the field is applied longitudinally to the direction of the incident beam.

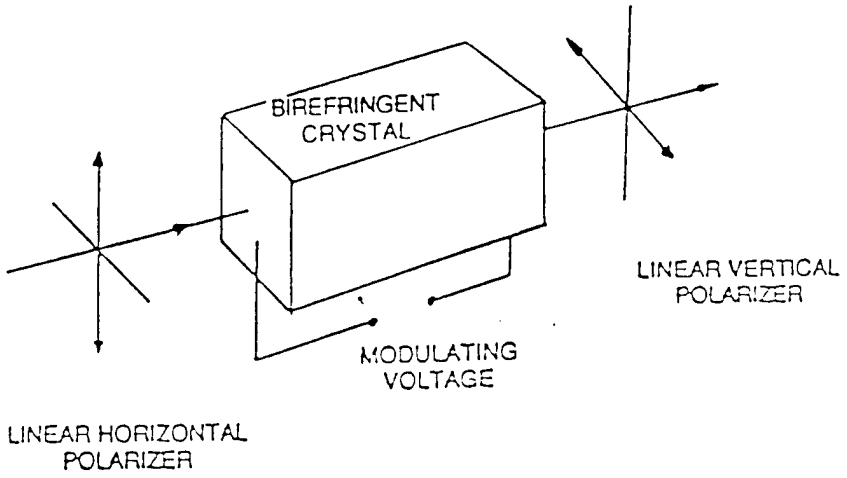

Figure 2.3.2 Propagation of a polarized beam of light through a longitudinal Pockels cell.

In Figure 2.3.1 and Figure 2.3.2, the electric field is shown as an applied voltage. Kerr showed that when an isotropic liquid is placed in the

electric field it behaves like a uniaxial crystal with the optic axis in the direction of propagation. If n is the index of refraction of the substance in the absence of a field and n_p and n_s are the refractive indices for directions of $\vec{D}$ parallel and perpendicular to the field, then the following equation can be considered to be a statement of Kerr's law:

$$n_p - n_s = \lambda B \varepsilon^2 \qquad (2\text{-}3\text{-}1)$$

where ε is the applied field, λ is the wavelength of the incident light, and B is Kerr's constant.

With respect to the origins and theory of the Kerr effect, it is explained by the Lorentz-Lorenz theory of dispersion. It is assumed that electric action on a given electron due to a light wave may be calculated by imagining that the electron is placed at the center of a small spherical cavity, the net effect of the matter removed from the cavity being zero. Havelock assumed that an external electric field makes this cavity elliptical, and from this assumption he deduced the relations

$$n_p - n = \left[\frac{K(n^2 - 1)^2}{n}\right]\varepsilon^2 \qquad (2\text{-}3\text{-}2a)$$

and

$$n - n_s = \left[\frac{K(n^2 - 1)^2}{n}\right]\varepsilon^2 \qquad (2\text{-}3\text{-}2b)$$

where K is a constant. Subtracting (2-3-2b) from (2-3-2a) leads to (2-1-2). A detailed theory of the effect is given by Born and Langevin. They consider the effect to be due to (1) orientation of polar molecules and (2) creation of electric moments in nonpolar molecules and the alteration of existing moments in polar molecules. The orientation effect is naturally important in polar liquids and gases. It takes an appreciable time, of course, to alter the orientation of molecules in highly viscous liquids, and this accounts for the relaxation effects.

Kerr cells have been replaced largely with Pockels cells, that is cells in which the phase shift varies linearly with the applied field. While there are many crystals which show the effect , in practice only three have commercial and practical significance: ammonium dihydrogen phosphate (ADP), potassium dihydrogen phosphate (KDP), and potassium dideuterium phosphate (KD*P). ADP has been largely replaced by KDP, which has a lower half-wave voltage (this term will be understood shortly). If the lowest possible range of operating voltages is also a requirement, then KD*P, a "deuterated" from of KDP, is the best choice.

We now turn to the problem of characterizing the electro-optical effect in terms of the Mueller matrix. In the previous section we saw that an anisotropic medium, that is, a crystal, could be described by the index ellipsoid

$$\frac{x^2}{n_x^2} + \frac{y^2}{n_y^2} + \frac{z^2}{n_z^2} = 1 \qquad (2\text{-}3\text{-}3)$$

where x,y, and z are the pricipal dielectric axes, that is, the directions in the crystal along which $\vec{D}$ and $\vec{E}$ are parallel. Analysis shows that the electro-optical effect exists only in crystals that do not possess inversion symmetry. Following convention, we take the equation of the ellipsoid in the presence of an electric field to be

$$\left(\frac{1}{n^2}\right)_1 x^2 + \left(\frac{1}{n^2}\right)_2 y^2 + \left(\frac{1}{n^2}\right)_3 z^2 + 2\left(\frac{1}{n^2}\right)_4 yz + 2\left(\frac{1}{n^2}\right)_5 xz + 2\left(\frac{1}{n^2}\right)_6 xy = 1$$

(2-3-4)

The change in the linear coefficients

$$\left(\frac{1}{n^2}\right)i \qquad I = 1,\ldots,6 \qquad (2\text{-}3\text{-}5)$$

due to an arbitrary electric field $\vec{E}$ (E_x,E_y,E_z) is defined by

$$\Delta\left(\frac{1}{n^2}\right)i = \sum_{j=1}^{3} r_{ij}E_j \qquad (2\text{-}3\text{-}6)$$

where in the summation over j the convention 1 = x, 2 = y, 3 = z is used. Yariv has shown that (2-1-6) can be written in matrix form in which we have a 6×3 matrix with elements r_{ij} called the electro-optic tensor:

$$r_{ij} = \begin{pmatrix} r_{11} & r_{12} & r_{13} \\ r_{21} & r_{22} & r_{23} \\ r_{31} & r_{32} & r_{33} \\ r_{41} & r_{42} & r_{43} \\ r_{51} & r_{52} & r_{53} \\ r_{61} & r_{62} & r_{63} \end{pmatrix} \qquad (2\text{-}3\text{-}7)$$

He has further shown for a crystal with a fourfold axis of symmetry, e.g., KDP, that the specific electro-optic tensor is

$$r_{ij} = \begin{pmatrix} 0 & 0 & 0 \\ 0 & 0 & 0 \\ 0 & 0 & 0 \\ r_{41} & 0 & 0 \\ 0 & r_{41} & 0 \\ 0 & 0 & r_{63} \end{pmatrix} \qquad (2\text{-}3\text{-}8)$$

If the applied field is parallel to the z axis, then the index ellipsoid (2-3-4), using (2-3-1),(2-3-6), and (2-3-8), reduces to

$$\frac{x^2 + y^2}{n_o^2} + \frac{z^2}{n_e^2} + 2r_{63}E_z xy = 1 \qquad (2\text{-}3\text{-}9)$$

where $n_x = n_y = n_o$ and $n_z = n_e$. It now becomes necessary to find the directions and magnitudes of a new set of axes in the presence of $\bar{E}$ so that we may determine the effect of the field on the propagation. That is, a new coordinate system (x',y',z') in which the index ellipsoid (2-3-9) contains no mixed terms. Then x', y', and z' determine the directions of the major axes of

the ellipsoid in the presence of an external field applied parallel to z. The lengths of major axes of the ellipsoid are then $2n_{x'}$, $2n_y$, and $2n_z$, and these will, in general, depend on the applied field.

Inspecting (2-3-9), we see that the xy term can be removed by a rotation around the z axis. The variable n_o is common to both the x and y terms, so we can transform (2-3-9) by a 45° rotation; that is,

$$x = x' \cos 45° + y' \sin 45° \qquad \text{(2-3-10a)}$$

$$y = -x' \sin 45° + y' \cos 45° \qquad \text{(2-3-10b)}$$

Substituting (2-3-10) into (2-3-9) gives

$$\left(\frac{1}{n_o^2} + r_{63}E_z\right)x'^2 + \left(\frac{1}{n_o^2} - e_{63}E_z\right)y'^2 + \frac{z'^2}{n_e^2} = 1 \qquad \text{(2-3-11)}$$

Equation (2-3-11) shows that x', y', and z' are the pricipal axes of the ellipsoid when a field is applied along the z direction. According to (2-3-11), the length of the x' axis of the ellipsoid is $2n_{x'}$, where

$$\frac{1}{n_{x'}^2} = \frac{1}{n_o^2} + r_{63}E_z \qquad \text{(2-3-12)}$$

We can solve for $n_{x'}$, so (2-3-12) becomes

$$n_{x'} = n_o\left(1 + n_o^2 r_{63} E_z\right)^{1/2} \qquad (2\text{-}3\text{-}13)$$

Assuming $n_o^2 r_{63} E_z << 1$, (2-3-13) can be approximated as

$$n_{x'} = n_o - \frac{n_o^3 r_{63} E_z}{2} \qquad (2\text{-}3\text{-}14a)$$

Similarly, we find that

$$n_{y'} = n_o + \frac{n_o^3 r_{63} E_z}{2} \qquad (2\text{-}3\text{-}14b)$$

$$n_z = n_o \qquad (2\text{-}3\text{-}14c)$$

We now drop the primes for convenience and write x and y. The refractive indices (2-3-14a) and (2-3-14b) gives rise to phase shifts for the optical field components oscillating along the x and y axes as they propagate through the KDP crystal. The corresponding phase shifts ϕ_x and ϕ_y for the field as it propagates along the z axes are

$$\phi_x = kn_x z = kn_o z - \frac{kn_o^3 r_{63} E_z z}{2} \qquad (2\text{-}3\text{-}15a)$$

$$\phi_y = kn_y z = kn_o z + \frac{kn_o^3 r_{63} E_z z}{2} \qquad (2\text{-}3\text{-}15b)$$

We can now determine the Mueller matrix for KDP crystal. If the incident field components are E_x and E_y, the emerging components are

$$E_{x'} = E_x \exp(i\phi_x) \tag{2-3-16a}$$

$$E_{y'} = E_x \exp(i\phi_y) \tag{2-3-16b}$$

where ϕ_x and ϕ_y are given by (2-3-15). We now form the Stokes polarization parameters in the usual manner and find that the Mueller matrix for an electro-optical crystal is

$$M = \begin{pmatrix} 1 & 0 & 0 & 0 \\ 0 & 1 & 0 & 0 \\ 0 & 0 & \cos\phi & -\sin\phi \\ 0 & 0 & \sin\phi & \cos\phi \end{pmatrix} \tag{2-3-17a}$$

where

$$\phi = \phi_y - \phi_x = k n_o^3 r_{63} E_z z \tag{2-3-17b}$$

or

$$\phi = \frac{\omega n_o^3 r_{63} V}{c} \tag{2-3-17c}$$

and $k = \omega/c$, $V = Ez$ is the applied voltage. The phase ϕ is very often simply called the retardation. The constants within (2-3-17c) can be eliminated and the phase expressed only in terms of "a half-wave" voltage V_π, that is the value of the applied voltage required to cause a phase shift of π. For this condition (2-3-17c) becomes

$$\pi = \frac{\omega n_o^3 r_{63} V_\pi}{c} \qquad (2\text{-}3\text{-}18)$$

Dividing (2-3-17c) by (2-3-18), the phase retardation is now expressed as

$$\phi = \pi\left(\frac{V}{V_\pi}\right) \qquad (2\text{-}3\text{-}19)$$

The foregoing analysis is applicable to the entire class of "dihydrogen phosphate" crystals. Table 2.3.1 lists the characteristic constants for a number of crystals in this class. For a typical electro-optical crystal (e.g., ADP) we see from the table that the half-wave voltage $V_{1/2}$ is 9040 V.

TABLE 1 Electro-optical Characteristics of :Phosphate" Crystals

Crystal	$r_{63}(\mu/V \times 10^{-6})$	$V_{1/2}$(KV) at 5461A°	n_0
ADP(ammonium dihydrogen phosphate)	8.5	9.2	1.526
KDP(potassium dihydrogen phosphate)	10.5	7.5	1.51
KD*P(potassium dideuterium phosphate)	26.4	2.9-3.4	1.52
KDA(potassium dihydrogen phosphate)	10.9	6.4	1.57
RDP(rubidium dihydrogen phosphate)	11.0	7.3	1.64

Electro-optical crystals have wide scientific, engineering, and commercial applications. We now examine several of these application.

The first example we consider is electro-optical amplitude modulation. In order to understand this process we consider Figure 2.3.3. We can immediately express the electro-optical modulation components in terms of their Mueller matrices. We see from Figure 2.3.3 that

$$M_{EOM} = M(+45^\circ)M_\phi M(-45^\circ) \tag{2-3-20}$$

where M_ϕ is given by (2-3-17a), and M(+45°) and M(-45°) are the Mueller matrices for a linear +45° and a linear -45° polarizer, respectively. We note that linear 45° polarizers are used rather than linear horizontal and linear vertical polarizers. This orientation, as the reader can readily prove, allows the phase terms in (2-3-17a) to appear in the final intensity; it also corresponds to the axes of the electro-optical crystal. Carrying out the matrix multiplication, we find that

$$M_{EOM} = \left(\frac{1-\cos\phi}{4}\right)\begin{pmatrix} 1 & 0 & 1 & 0 \\ 0 & 0 & 0 & 0 \\ -1 & 0 & -1 & 0 \\ 0 & 0 & 0 & 0 \end{pmatrix} \tag{2-3-21}$$

The negative signs in (2-3-21) show that an electro-optical modulator behaves as a pseudolinear -45° polarizer. The Stokes vector of the incident beam is

$$S = \begin{pmatrix} S_0 \\ S_1 \\ S_2 \\ S_3 \end{pmatrix} \qquad (2\text{-}3\text{-}22)$$

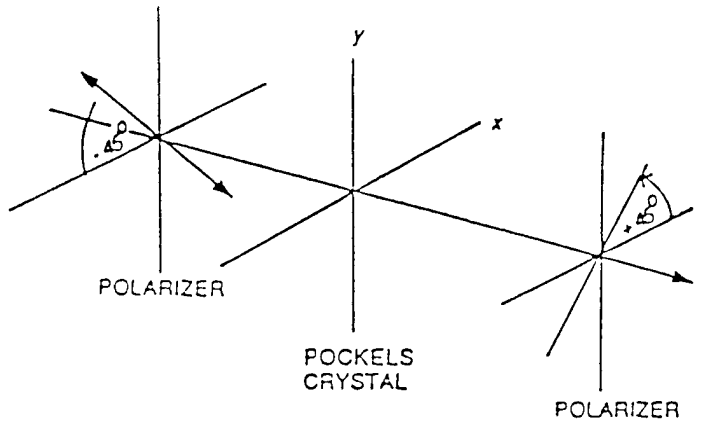

Figure 2.3.3 Configuration for electro-optical amplitude modulation.

The intensity $I(\phi)$ of the beam out of the electro-optical modulator assembly is found by multiplying (2-3-21) by (2-3-22), so

$$I(\phi) = I_0\left(\frac{1-\cos\phi}{4}\right) \qquad (2\text{-}3\text{-}23a)$$

$$= \frac{I_0}{2}\sin^2\left(\frac{\phi}{2}\right) \qquad (2\text{-}3\text{-}23b)$$

or, using (2-3-19),

$$I(V) = \frac{I_0}{2}\sin^2\left[\frac{\pi V}{2V_\pi}\right] \qquad (2\text{-}3\text{-}24)$$

To describe amplitude modulation, the applied voltage V varies according to

$$V = \frac{V_\pi}{2} + V_m \sin(\omega_m t) \qquad (2\text{-}3\text{-}25)$$

where V_m is the maximum modulation voltage and ω_m is the angular modulation frequency. Substituting (2-3-25) into (2-3-24) yields

$$\frac{I(V)}{I_0} = \sin^2\left[\frac{\pi}{4} + \frac{\pi V_m}{2V_\pi}\sin(\omega_m t)\right] \qquad (2\text{-}3\text{-}26a)$$

$$= \frac{1}{2}\left[1 + \sin\frac{\pi V_m}{V_\pi}\sin(\omega_m t)\right] \qquad (2\text{-}3\text{-}26b)$$

For small arguments , $\sin\theta$ can be replaced by θ, so (2-3-16b) becomes

$$\frac{I(V)}{I_0} = \frac{1}{2}\left[1 + \frac{\pi V_m}{V_\pi}\sin(\omega_m t)\right] \qquad (2\text{-}3\text{-}27)$$

Equation (2-3-27) is the well-known representation of amplitude modulation. Thus, by applying a modulation voltage of the form given by (2-3-25) to the

electro-optical modulator, the intensity modulation is a linear replica of the modulating voltage $V_m \sin(\omega_m t)$. If the condition $V_m << V_\pi$ is not fulfilled, then the intensity variation is distorted and will contain an appreciable amount of the higher (odd) harmonic terms.

Another important application of electro-optical crystals is that of optical shutters. An optical shutter (OS) has the same configuration as an optical modulator, so its Mueller matrix is

$$M_{OS} = \left(\frac{1-\cos\phi}{4}\right)\begin{pmatrix} 1 & 0 & 1 & 0 \\ 0 & 0 & 0 & 0 \\ -1 & 0 & -1 & 0 \\ 0 & 0 & 0 & 0 \end{pmatrix} \qquad (2\text{-}3\text{-}28)$$

The output intensity is again

$$I(\phi) = I_0\left(\frac{1-\cos\phi}{4}\right) \qquad (2\text{-}3\text{-}29)$$

We see that if the phase ϕ is zero, then the output intensity is zero. In this state the Mueller matrix (2-3-17a) is unity and resultant Mueller matrix is the product of the two crossed 45° polarizers. If the phase is now changed to 180°, the intensity (2-3-13a) becomes $I(180°) = I_0/2$ and the output intensity is a maximum. Thus, by changing the phase with a step voltage the electro-optical/crossed polarizer configuration can be changed rapidly from a maximum value to a minimum value in an extremely short time can be used

as an optical chopper. Another application is to block laser radiation (e.g., protective laser goggles).

2.3.2 Integrated Waveguide Modulator

Integrated-optic (I-O) modulators(Bossi 1992, Giguers 1990, Robert 1990, Burton 1991, Walker 1991, Gomatam 1992,Ishikawa 1992, Solgaard 1991, Chorey 1988, Railton 1989, Tan 1990, Jungerman 1990, Jiang 1992, Huang 1993, Chung 1991, Neyer 1990, Burton 1991, and Dolfi 1988) operating on the linear electro-optic (E-O) effect are crucial components of many high-performance lightwave systems. Although a variety of commercially available lithium niobate($LiNbO_3$) I-O components are implemented in real-world systems, research and development of $LiNbO_3$, semiconductor, and polymer devices continue to advance the performance limits of electro-optics technology. Small size and weight, high band-width, low power consumption, and compatibility with fiber optic systems are features of I-O modulators that make them attractive for fiber optics applications.

The continuous-wave output from either a semiconductor or solid-state laser is coupled into an I-O modulator to form an externally modulated optical source. External modulation has important advantage compared to direct modulation of laser-diode injection current, including increased bandwidth, enhanced linearity and dynamic range, and elimination of wavelength chirp.

As a result, I-O modulators are well suited for use in high-bit-rate digital-telecommunications and analog fiberoptic-link applications such as cable-TV distribution, microwave antenna remoting, and optical control of phased-array radar. Integrated-optic modulators are also key components in optical sensor systems such as fiberoptic gyroscopes.

Most commercial I-O modulators are based on the linear E-O (Pockels) effect, in which an applied electric field is used to linearly change the refractive index(n) of a material through which light is propagating. For a given light polarization and direction of applied electric field(E), the refractive-index change is related to the magnitude of the applied field via the E-O coefficient (r), expressed as

$$\Delta\left(\frac{1}{n^2}\right) = rE \qquad (2\text{-}3\text{-}30)$$

In an I-O modulator, the optical beam propagates within a waveguide whose transverse dimensions measure only a few microns. Applying a modulating voltage between two closely spaced electrodes surrounding the waveguide creates a strong electric field that overlaps the optical mode. The electric-field-induced refractive-index change modifies the velocity of light in the waveguide, thereby changing the phase of the optical wave at the output of the device(see Figure 2.3.4, top). The magnitude of the phase shift is linearly proportional to the E-O coefficient, the applied voltage(V), and the interaction length(L).

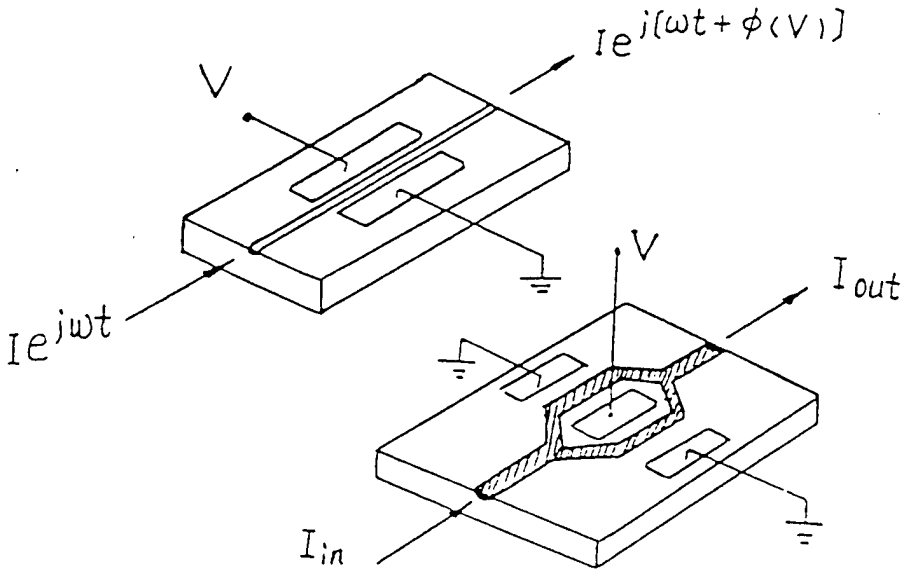

Figure 2.3.4 Voltage applied to electrodes in phase (top) and intensity (bottom)modulators produces a refractive-index change that causes a phase shift or sinusoidal intensity variation, respectively, in output light.

An I-O intensity modulator may be produced by combining two E-O phase modulators in parallel to form an interferometric Mach-Zehnder device (see Figure 2.3.4, bottom). Light is coupled into one single-mode optical waveguide, split evenly between two phase-modulator sections, and then recombined into a single-mode output waveguide. Depending on the relative phase delay between the two modulator sections, the recombined output results in maximum or minimum optical transmission. The Mach-Zehnder

modulator has an output optical intensity that varies sinusoidally with the applied voltage.

2.4 Applications of Polarization

2.4.1 Switches

An important application of electro-optical crystals is their use as voltage-controlled gate inside the optical resonator of laser. Its purpose is to allow the lasing medium to reach a high population state after it has been excited, say, by a flash lamp. To understand the operation, we consider Figure 2.4.1. The laser operates by a technique known as Q-switching, a method which leads to the emission of intense, short bursts of laser radiation. The Q refers to the quality

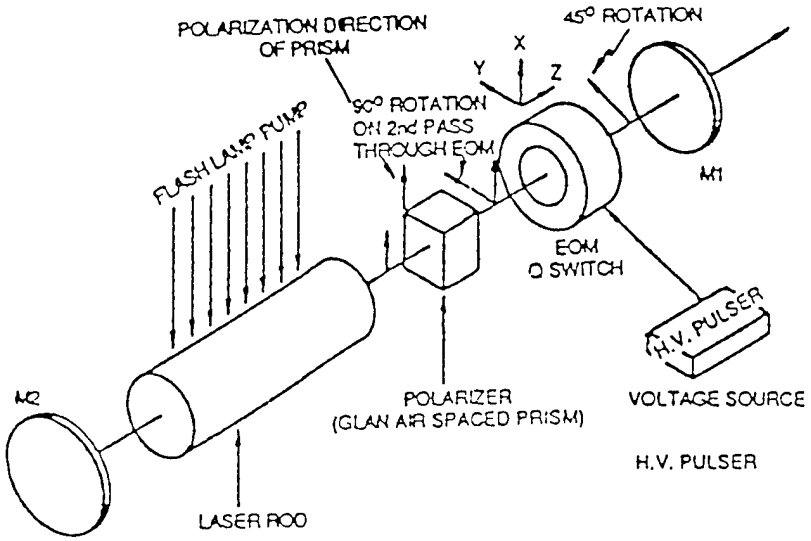

Figure 2.4.1 Electro-optical crystal used as a voltage-controlled gate in Q-switching a laser.

factor Q, a widely used term in electrical engineering. The Q factor is a measure of the energy which can be stored in a medium or a microwave cavity (or optical resonator). One definition of the Q factor is

$$Q = 2\pi \frac{\text{peak density of optical energy}}{\text{optical energy dissipated in one cycle}} \qquad (2\text{-}4\text{-}1)$$

The objective of Q-switching is to "spoil" the Q of the optical cavity (or resonator). The laser medium then cannot oscillate and is forced to store as much energy as possible until all the atoms or molecules are in their uppermost energy state. This is done by "dumping" any optical radiation out of the optical resonator during the buildup so that it cannot create unwanted oscillations. That is, as much of the optical radiation is dissipated as possible. Under this condition the denominator of (119) is extremely large and Q is, ideally, zero. When all the atoms and molecules are in their uppermost energy state, the laser medium/optical cavity (or resonator) is returned to its most efficient oscillatory configuration. The quality factor Q of the optical resonator (the mirror pair shown in the figure acts as an optical resonator cavity) is degraded (lowered) during the pumping so that the gain (the inversion $N_1 \rightarrow N_2$) can build up to a very high value without oscillation; the spoiling of the Q raises the threshold inversion to a value higher than that obtained by pumping. When the inversion reaches its peak, the Q is restored abruptly to its (ordinary) high value. The gain (per pass) in the laser medium is now well above threshold. This causes an extremely rapid buildup

of the oscillations and a simultaneous exhaustion of the inversion by stimulated 2 → 1 transitions. This process converts most of the energy that was stored by atoms pumped into the upper laser level into photons, which are now inside the optical resonator. These proceed to bounce back and forth between the reflectors, with a fraction of photons "escaping" from the resonator each time.

The process of spoiling the Q can be analyzed with Mueller matrices. The laser is pumped by the light from a flashlamp and a voltage is simultaneously applied to the electro-optical crystal, so the phase is $\pi/2$. When the lasing medium has been completely excited, the voltage is removed from the electro-optical crystal. Inspecting Figure 2.4.1 we see the Mueller matrix M, starting with the beam entering the linear polarized and returning through the linear polarizer, is

$$M = M(-45°)\cdot M(\phi)\cdot M(2)\cdot M(\phi)\cdot M(+45°) \qquad (2\text{-}4\text{-}2)$$

The Mueller matrix M(45°) of the linear polarizer is

$$M(+45°) = \frac{1}{2}\begin{pmatrix} 1 & 0 & 1 & 0 \\ 0 & 0 & 0 & 0 \\ 1 & 0 & 1 & 0 \\ 0 & 0 & 0 & 0 \end{pmatrix} \qquad (2\text{-}4\text{-}3)$$

Similarly, the Mueller matrices of the electro-optical crystal and the reflecting mirror are $M(\phi)$ and M(2), respectively; that is,

$$M(\phi) = \begin{pmatrix} 1 & 0 & 0 & 0 \\ 0 & 1 & 0 & 0 \\ 0 & 0 & \cos\phi & -\sin\phi \\ 0 & 0 & \sin\phi & \cos\phi \end{pmatrix} \qquad (2\text{-}4\text{-}4)$$

$$M(2) = \begin{pmatrix} 1 & 0 & 0 & 0 \\ 0 & 1 & 0 & 0 \\ 0 & 0 & -1 & 0 \\ 0 & 0 & 0 & -1 \end{pmatrix} \qquad (2\text{-}4\text{-}5)$$

Finally, the Mueller matrix of the linear polarizer on the return path back to the laser crystal now has the form (the transmission axis appears to be at -45° for the returning beam)

$$M(-45^\circ) = \frac{1}{2}\begin{pmatrix} 1 & 0 & -1 & 0 \\ 0 & 0 & 0 & 0 \\ -1 & 0 & 1 & 0 \\ 0 & 0 & 0 & 0 \end{pmatrix} \qquad (2\text{-}4\text{-}6)$$

We carry out the multiplication of the inner matrices in (2-4-2) first:

$$M(2\phi) = M(\phi)\cdot M(2)\cdot M(\phi) \qquad (2\text{-}4\text{-}7a)$$

$$= \begin{pmatrix} 1 & 0 & 0 & 0 \\ 0 & 1 & 0 & 0 \\ 0 & 0 & -\cos 2\phi & \sin 2\phi \\ 0 & 0 & -\sin 2\phi & -\cos 2\phi \end{pmatrix} \qquad (2\text{-}4\text{-}7b)$$

We now multiply the outer matrices (2-4-3) and (2-4-6) with (2-4-7b):

$$M = \frac{1}{4}\begin{pmatrix} 1 & 0 & -1 & 0 \\ 0 & 0 & 0 & 0 \\ -1 & 0 & 1 & 0 \\ 0 & 0 & 0 & 0 \end{pmatrix} \cdot \begin{pmatrix} 1 & 0 & 0 & 0 \\ 0 & 1 & 0 & 0 \\ 0 & 0 & -\cos 2\phi & \sin 2\phi \\ 0 & 0 & -\sin 2\phi & -\cos 2\phi \end{pmatrix} \cdot \begin{pmatrix} 1 & 0 & 1 & 0 \\ 0 & 0 & 0 & 0 \\ 1 & 0 & 1 & 0 \\ 0 & 0 & 0 & 0 \end{pmatrix}$$

(2-4-8a)

to get

$$M = \left(\frac{1+\cos 2\phi}{4}\right)\begin{pmatrix} 1 & 0 & 1 & 0 \\ 0 & 0 & 0 & 0 \\ -1 & 0 & -1 & 0 \\ 0 & 0 & 0 & 0 \end{pmatrix} \tag{2-4-8b}$$

We see immediately from (2-4-7b) that if a voltage is applied to the electro-optical crystal so $\phi = \pi/2$, then (2-4-7b) reduces to a null Mueller matrix,

$$M = \begin{pmatrix} 0 & 0 & 0 & 0 \\ 0 & 0 & 0 & 0 \\ 0 & 0 & 0 & 0 \\ 0 & 0 & 0 & 0 \end{pmatrix} \tag{2-4-9}$$

Thus, no light can reenter the laser crystal and cause unwanted oscillations and interference with the buildup of energy. On the other hand, when the energy has been built up to a maximum value, the voltage on the electro-optical crystal is abruptly removed, so $\phi = 0$ and the Mueller matrix becomes

$$M = \frac{1}{4}\begin{pmatrix} 1 & 0 & 1 & 0 \\ 0 & 1 & 0 & 0 \\ -1 & 0 & -1 & 0 \\ 0 & 0 & 0 & 0 \end{pmatrix} \tag{2-4-10}$$

which is the Mueller matrix of a pseudolinear -45° polarizer, that is, a nonzero Mueller matrix. Thus, the light can now reenter the crystal and contribute to the stimulation of laser radiation.

It follows that the voltages on the losses are high so that oscillation is prevented. The Q-switching is timed to coincide with the point at which the inversion reaches its peak, and is achieved by the removal of the voltage applied to the electro-optical crystal. This reduces the retardation to zero, so state of polarization of the wave passing through the crystal is unaffected and the Q regains its high value associated with ordinary losses to the system.

2.4.2 SLM

A light beam carries information with very high throughput because of the inherently massive parallelism of light in free space. Processing light beams is therefore particularly effective for inherently two-dimensional data, including optical images and matrix data arrays. For instance, holographic filtering can give the spatial multiplication of Fourier transforms in parallel by utilizing the spatial coherence of light. Also, introducing a parallel algorithm makes optical digital operations more effective, by using unique pattern logics such as symbolic substitution and optical array logic. Spatial light modulators (SLMs)(Neff 1990 and Kurokawa 1992) are expected to evolve as key devices for optical parallel processing in free space because they can

spatially, as well as temporally, modulate a two-dimensional optical wavefront.

Some SLMs are controlled electrically, but for the direct processing of light signals it is important to develop optically addressed SLMs that are one kind of optically controlled switching device. The control of light by light can be achieved either by hybrid and monolithic integrated optoelectronic structures or by nonlinear optical effects that occur without external electricity. Liquid-crystal spatial light modulators (LC-SLMs), multiple quantum well (MQW) devices and nonlinear optical effect devices are positioned along three axes representing parallelism, sensitivity and response time. The LC-SLMs have very high resolution and a high sensitivity and response of < 1 nWpixel^{-1}, so large parallelism of $> 10^6$ bits can be achieves for a device despite the slow response time. In contrast, the parallelism of MQW devices is limited by their low sensitivities, but their response speed is much faster; they are more than three orders of magnitude faster than SLMs. Finally, nonlinear optical effect materials have extremely high speed potential up to the femtosecond range, but they require large switching power.

Most important function in these various optically controlled switching devices should be realized in the context of system applications, since different system require different device attributes. A consideration of these device attributes suggests that SLMs have advantages for image processing

and that MQW devices are well suited for high speed digital logic processing and switching.

Since the first liquid-crystal light valve was developed about 20 years ago , many optically addressed spatial light modulators with hybrid structures have been developed applying various combinations of photodetector and materials. For example, photoconductive, photovoltaic and photo-emissive materials have used as photodetectors, and electro-optic and magneto-optic materials have been used as modulators. These hybrid structure SLMs are generally employed to deal with optical images to exploit their large parallelism and high sensitivity compared with other monolithic structure MQW devices and nonlinear optical effect devices. Of course, ordinary photographic film can be read out after exposure and development, but an optically addressed SLMs is capable of capturing, storing and reading out images in real time, as shown in Fig 2.4.2. In other words, an optically addressed SLM is a kind of real-time, development-free photographic film. The most important functions imposed on SLMs are those of image acceptance and transducers, because SLMs are expected to accept optical image of external objects and transduce them to other forms; For example, wavelength conversion, incoherent-to-coherent conversion and intensity amplification.

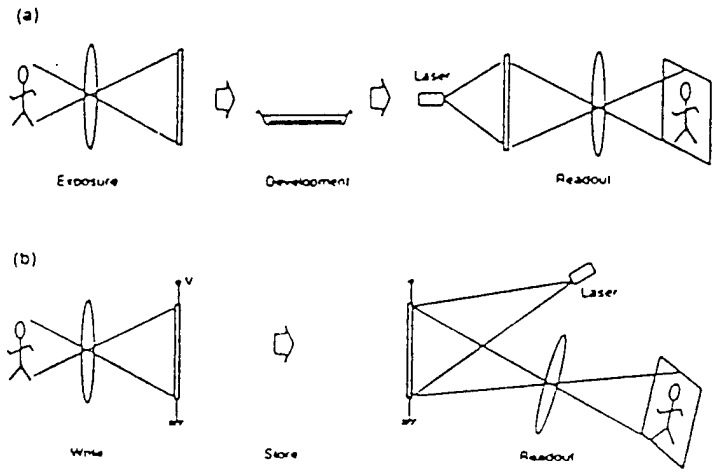

Figure 2.4.2 Basic function of (a) photographic film and (b) spatial light modulator.

A typical SLM operation is described as follows. Two beams are incident on the SLM, one is a write beam and other a read beam. By the illumination of the write beam from the objects, the photodetector in the SLM changes the intensity distribution of the write beam into a voltage distribution across the electro-optic materials. The read-out beam, which is the reflected or transmitted light of the read-in beam, is modulated corresponding to the voltage distribution electro-optic materials. Signal conversion results from

the lightwave difference between the write and read beams. An incoherent optical image from the object can be read out as a coherent image by a laser beam. Furthermore, if the photodetector has high sensitivity, and if the modulator losses can be minimized, then a small amount of optical input power could effect modulation of a stronger read beam. It can thus function as a ream-time image transducer, including incoherent-to-coherent image conversion, image intensity amplification, etc. When an SLM was developed for a projection display in the 1970s, all requirements were centered around image amplification. The wavelength and coherent conversions have often been used in the parallel processing of Fourier optics. In contrast, recent optical digital processing and neural processing requires nonlinear functions between input and output intensities, such as threshholding or contrast inversion.

In any case, SLMs also satisfy essential requirements for high levels of resolution, sensitivity and response speed. For dealing with optical images, 10^5 pixels in a chip and sensitivities of $100\mu Wcm^{-2}$ will be necessary. Also, a response speed at least 10 ms faster than TV framing rates will be required. In addition to these three important factors of parallelism, speed and sensitivity, other factors may be important, depending on the system requirements. For example, a continuous pixel structure becomes important when spatial coherence is utilized in the processing. The

acceptance of different types of signals (gray scale, binary and visible, or infrared) depends on what signals are handled in the systems.

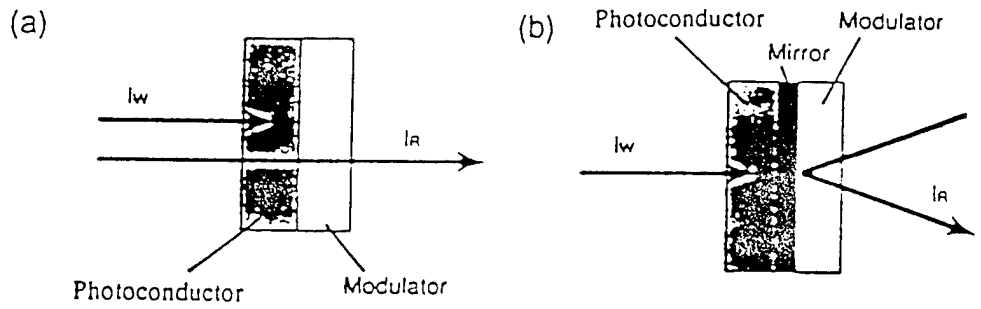

Figure 2.4.3 Schematic diagrams of two kinds of optically addressed spatial light modulator: (a) transmission type and (b) reflection type.

Optical processing often requires that the input and output wavelength be the same so that devices can be cascaded. There are two types of optically addressed SLMs: transmission and reflection types, as shown in Figure 2.4.3. In the transmission type SLM the read wavelength must generally be longer than the write wavelength so that it is not absorbed by

the photodetector. On the other hand, the reflection type SLM with a mirror between the photoconductor and modulator can isolate the read and write beams, so operation at the same wavelength is easily achieved.

2.4.3 LCD

Not all E-O modulators use the Pockels or Kerr effect in their design. Another important class of E-O modulators controls light by exploiting the anisotropic medium of liquid crystals(LCs)(Higgins 1994).

As the name implies, LCs consist of an orderly arrangement of molecules of in a liquid state. This interesting phase of matter occurs in organic liquids made up of long or flat molecules usually organize themselves into one of three states classified as nematic, smectic, or cholesteric.

In nematic LCs, the long axes of all the molecules point in the same direction but their centers are randomly distributed. In smectic LCs, not only do the long axes align, so do their centers. In cholesteric LCs, the molecules contained in a single layer all point in the same direction, like the nematic variety, but in each successive layer the direction of alignment rotates through a constant angle. Therefore, when a cholesteric LC is viewed through all the molecular layers, each column of molecules resembles a spiral staircase.

The oblong molecules in a nematic LC can be made to twist like the choleteric variety by placing the liquid between two glass plates whose surfaces have been specially prepared so that all the molecules touching the glass point in the same predetermined direction. If, for example, the

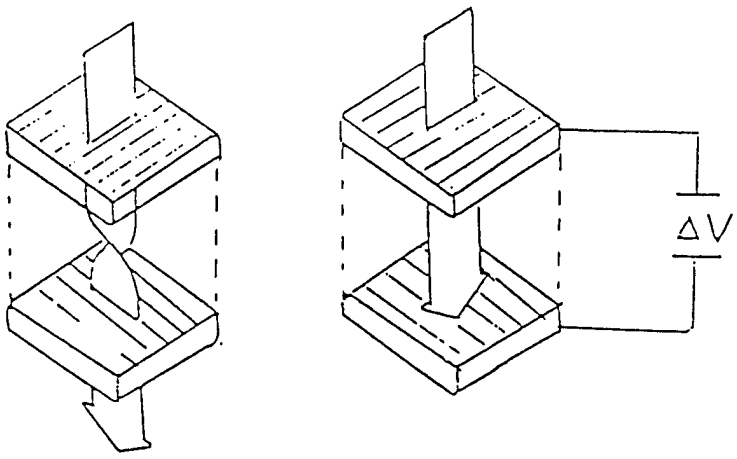

Figure 2.4.4 Twisted-nematic liquid crystal correctly oriented between crossed polariers will transmit a linearly polarized light beam by rotating its polarization plane 90° (left). In the presence of a longitudinal electric field, however, no rotation occurs and the beam is blocked (right).

molecules in contact with the front plate all point in the x direction and those contacting the back plate point in the y direction, the molecules of the molecules in contact with the front plate all point in the x direction and those contacting the back plate point in the y direction, the molecules of the intervening layers will rotate incrementally about the z axis, like the bristles of a bottle brush (see Fig 2.4.4,left). The result is called a twisted-nematic LC. And if the 90° molecular rotation is gradual enough, the device will function as a 90° polarization rotator for linearly polarized light.

When placed between crossed polarizers, a twisted-nematic LC will therefore rotate the linearly polarized light from the first polarizer, allowing it to pass through the second polarizer. If, however, a voltage differential is applied across the LC in the longitudinal direction (z axis), most of the molecules will align themselves with electric field. In this condition, the LC no longer acts like a rotator and the light is blocked by the second polarizer (see Fig 2.4.4, right). Modulating the voltage on and off therefore switches the transmitted light off and on, respectively.

Like other E-O modulators, LC modulators can modify the polarization, phase, and intensity of light, but perhaps their best-known application is the liquid-crystal display (LCD). LCDs consist of many individually addressable LC intensity modulators arranged in a pattern or array, which is generically referred to as a spatial light modulator.

When placed in the path of a broad, uniform light beam, spatial light modulators generate spatial changing intensity patterns in the light. For example, a typical clock or calculator LCD uses a fixed pattern of seven bar

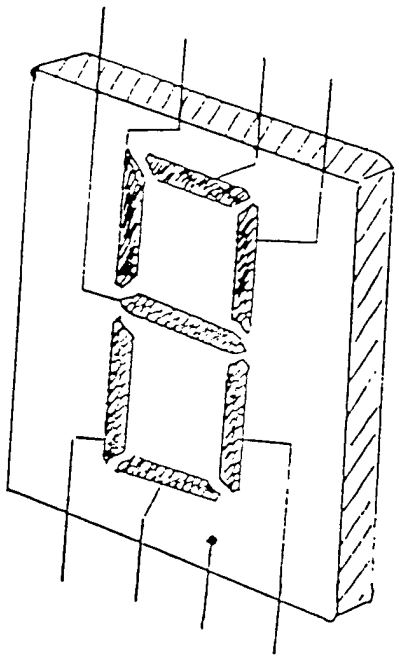

Figure 2.4.5 To display the number 0 through 9, a typical LCD uses seven bar-shaped intensity modulators arranged in a squared-off figure-eight pattern defined by the electrodes.

shaped intensity modulators-defined by the position and contour of the electrodes-to display the numbers 0 through 9 (see Fig. 2.4.5). When voltage is applied to all seven electrodes, the modulators block light and the number 8 is displayed. But if voltage to the two vertical electrodes on the left is turned off, the number 3 appears.

CHAPTER III

ANALYTICAL DESCRIPTIONS OF PROPAGATION THROUGH EO MODULATORS

3.1 Current Analytical Theories

3.1.1 Mueller and Jones Calculi

A. Mueller Calculus

The Mueller calculus(Shurcliff 1966) is a matrix algebraic method of specifying a beam of light and the optical devices encountered by the beam, and computing the output through the optical devices.

The Mueller calculus condenses all the necessary parameters for describing a beam of light and a given polarizer, retarder, or scatterer into a single package. Thus any given polarizer, retarder, or scatterer in a given beam can be determined merely by multiplying the appropriate packages together in standard manner. The output of any pertinent experiment can be determined by one fixed procedure: selecting the appropriate package from a table and multiplying them together.

The package describing the light beam is simply the four-parameters, called Stokes vector. Stokes vector describes the intensity and polarization

of a beam of light. The beam may be polarized completely, partially, or not at all; it may be monochromatic or polychromatic. Thus the description, though very concise, is broadly applicable.

The four parameters have the dimensions of intensity; each corresponds not to an instantaneous intensity but to a time-averaged intensity, the average being taken over a period long enough to permit practical measurement. The vector, though consisting of four physically real parameters, is a mathematical vector; it exists in four-dimensional mathematical space, not in a three-dimensional physical space.

The four quantities of Stokes vector comprise a column vector:

$$\begin{bmatrix} I \\ M \\ C \\ S \end{bmatrix}.$$

The first parameter , I, is called the intensity. The parameters M, C, and S are regarded as the "horizontal preference," "plus 45° preference," and "right circular preference" respectively. When a parameter has a negative value, the preference is for the orthogonal polarization form; thus if the parameter S has value -0.5 the polarization form is more alike to left-circular polarization than to right-circular polarization.

These four parameters can be defined as :

$$I = < a_x^2 + a_y^2 >,$$

$$M = < a_x^2 - a_y^2 >,$$

$$C = < 2a_x a_y \cos\gamma >,$$

$$S = < 2a_x a_y \sin\gamma >,$$

where a_x and a_y are two scalar components of the electric field, γ is the phase angle between the two components, and the angular brackets are employed to indicate that time averages are meant.

The package describing the polarizer, retarder, scatterer, or other optical device is called Mueller matrix. It is a 4 x 4 matrix, and thus contains 16 elements. But, most of the elements are zero for various ideal devices (referring to Appendix A). The individual matrix is indicative not only of the composition of the device but also of its orientation; thus the matrix of a linear polarizer whose transmission axis is horizontal is different from the matrix of a similar polarizer that has been turned so that its axis is at.

The main rules used in performing the multiplications are the standard rules of matrix algebra. One must also observe the following convention: the vector representing the incident beam must be written at the right, and the successive matrices representing the successively encountered devices must be arranged in order, the matrix of the last-to-be-encountered device being written at the left.

B. Jones Calculus

The Jones calculus is another treatment in which the incident light is described by a vector, the optical device is described by a matrix, and the output is computed by multiplying the vector by the matrix. However, the Jones calculus has the advantage over the Mueller calculus of employing a small matrix (2 x 2, instead of 4 x 4), and is applicable even to problems in which information as to phase must be preserved. on the other hand, many of its matrix elements are complex. Also, it is entirely inapplicable to optical devices that have depolarizing tendencies. Thus in several respects the Jones calculus complements, rather than competes with, the Mueller calculus.

In using the Jones calculus, one specifies the incident beam in terms of its Jones vector, specifies the various polarizers and retarders encountered by means of the appropriate Jones matrices, multiplies these expressions to obtain the Jones vector of the emerging beam.

The Jones vector is a two-element column vector which describes a beam's polarization form and amplitude components at some given position along the beam. If the beam is traveling along the Z-axis, the vector has the general form:

$$\begin{bmatrix} E_x \\ E_y \end{bmatrix} \text{ or } \begin{bmatrix} A_x e^{i(\phi_x + 2\pi\nu t)} \\ A_y e^{i(\phi_y + 2\pi\nu t)} \end{bmatrix},$$

where E_x and E_y are the scalar components (of the instantaneous electric vector) along the X-and Y-axis; A_x is the maximum value of E_x, and A_y is the maximum value of E_y. The quantity ϕ_x is the phase of the component E_x at time t = 0 and at the given location; ϕ_y is the phase of the component E_y. In general, each element of the column vector is a complex quantity.

We may convert the vector to the following equivalent form:

$$e^{i2\pi\nu t}\begin{bmatrix} A_x e^{i\phi_x} \\ A_y e^{i\phi_y} \end{bmatrix}.$$

Since the magnitude of any quantity of the form e^{iM} is unity, the magnitude of $e^{i2\pi\nu t}$ is unity. Thus this latter quantity may be dropped entirely in those problems in which details of variation with time are not of interest. Most problems are of this type, and accordingly the Jones vector is often written in the following form, called the full Jones vector:

$$\begin{bmatrix} A_x e^{i\phi_x} \\ A_y e^{i\phi_y} \end{bmatrix}.$$

In certain cases the full vector can simplified further. Consider horizontally polarized light: here $A_y = 0$, so the vector reduces to

$$\begin{bmatrix} A_x e^{i\phi_x} \\ 0 \end{bmatrix}.$$

For light that is linearly polarized at 45°, the two quantities A_x and A_y are equal, the quantities ϕ_x and ϕ_y are equal, and the vector reduces to

$$\begin{bmatrix} A_x e^{i\phi_x} \\ A_y e^{i\phi_x} \end{bmatrix} \text{ or } A_x e^{i\phi_x} \begin{bmatrix} 1 \\ 1 \end{bmatrix}.$$

For right-circularly polarized light, $A_x = A_y$ and $\gamma \equiv \phi_x - \phi_y = 1/2\ \pi$. Thus the vector is

$$\begin{bmatrix} A_x e^{i\phi_x} \\ A_y e^{i(\phi_x + \frac{1}{2}\pi)} \end{bmatrix}.$$

The intensity of the beam is proportional to the sum of the squares of the magnitudes of the individual elements. If the units of intensity or amplitude are chosen so that the proportionality constant is unity, the relation becomes

$$I = A_x^2 + A_y^2 .$$

The Jones matrices of the most important polarizers and retarders are listed in Appendix B. Each matrix describes a given device in a given orientation, and assumes that a given face serves as entrance face. The matrices are derived from the usual mathematical expression for a monochromatic (polarized) wave train and from mathematical analysis of the changes produced by interposing a given polarizer or retarder.

The matrices presented in Appendix B are in the simplest form and are called standard matrices. They are ideally designed for use by an investigator interested in the intensity and polarization form of an emerging beam. However, they contain no information as to the change produced in the absolute phase.

3.1.2 Ray tracing Algorithm

The method presented here(Trollinger 1991, Simon 1983, Simon 1986, Zhang 1992, Simon 1987, Simon 1978, McClain 1992, Simon 1988, Robb 1990, Waluschka 1988 and Swindell 1975) described by J.D.Trolinger, Jr., R.A.Chipman, and D.K.Wilson contains a single algorithm for tracing rays in isotropic media and tracing both ordinary rays and extraordinary rays in uniaxial media.

Many optical systems contain uniaxial optical elements such as polarizers, retarders, birefringent filters, and electro-optical modulator. Such systems are often configured so that collimated light is transmitted through these uniaxial elements. These elements are usually plane parallel plates so that they introduce no wavefront aberrations in collimated beams. During optical design, systems containing uniaxial elements with parallel faces in collimated beams can be safely ray traced by ignoring the birefrigent nature of the uniaxial elements. A detailed polarization analysis is usually not required and conventional ray-tracing techniques can be used to balance wavefront aberration.

Anisotropic optical media are characterized by treating the permittivity of the medium, ε, as a tensor. This tensor describes the variation of the electrical response of the medium with respect to electric field direction. If the medium is nonabsorbing and not optically active, the permttivity tensor is

symmetric and a coordinate system exists for which only the diagonal elements are nonzero. The axes of this coordinate system are called the "principal axes" and the diagonal elements of the permittivity tensor correspond to the permittivity in the direction of each of these principal axes. These diagonal tensor elements are called the "principal values" of the permittivity. A further simplification occurs in uniaxial media, where two of the principal values of the permittivity are equivalent. In such media, a coordinate system is usually chosen based on the principal axes such that the x and y directed principal values of permittity are the same and the z directed principal value is different. The z axis then corresponds to the crystal axis, which is the axis of symmetry of the crystal. The permittivity of a uniaxial medium in its principal coordinate system is

$$\varepsilon_{ij} = \begin{pmatrix} \varepsilon_x & 0 & 0 \\ 0 & \varepsilon_y & 0 \\ 0 & 0 & \varepsilon_z \end{pmatrix} = \varepsilon_0 \begin{pmatrix} n_0^2 & 0 & 0 \\ 0 & n_0^2 & 0 \\ 0 & 0 & n_e^2 \end{pmatrix}, \qquad (3\text{-}1\text{-}1)$$

where n_0 is the ordinary refractive index for the medium and n_e is the extraordinary refractive index for the medium. For such a medium, the relationship between $\vec{D}$ and $\vec{E}$ is

$$D_i = \varepsilon_{ij} E_j . \qquad (3\text{-}1\text{-}2)$$

This equation implies that the optical properties of the medium are invariant with rotation about the crystal axis. Consider plane wave solution to Maxwell's equations of the form:

$$\vec{E} = \vec{E}_0 \exp[-j(\omega t - \vec{k} \cdot \vec{r})] . \qquad (3\text{-}1\text{-}3)$$

The vector $\vec{k}$ is the wave vector and has a magnitude given by

$$|k| = \frac{\omega}{c} n , \qquad (3\text{-}1\text{-}4)$$

where ω is the angular frequency of the wave, c is the speed of light, and n is the refractive index in a given medium. For a given wave both c and ω are constant for all medium, but n varies as the wave passes through different medium. For such plane wave solutions, Maxwell's equations become:

$$i\vec{k} \cdot \vec{D} = 0 , \qquad (3\text{-}1\text{-}5)$$

$$i\vec{k} \cdot \vec{B} = 0 , \qquad (3\text{-}1\text{-}6)$$

$$\vec{k} \times \vec{E} = \mu_0 \omega \vec{H} , \qquad (3\text{-}1\text{-}7)$$

$$\vec{k} \times \vec{H} = \omega \vec{D} . \qquad (3\text{-}1\text{-}8)$$

These equations imply that $\vec{D}$, $\vec{E}$, and $\vec{k}$ are all perpendicular to $\vec{H}$ and thus coplanar. Since $\vec{D}$, $\vec{E}$, and $\vec{k}$ are coplanar, and the relationship between that $\vec{D}$ and $\vec{E}$ is invariant with respect to rotation about the crystal axis, $\vec{k}$ can be limited to the x-z plane without loss of generality. This plan, which contains both the crystal axis and $\vec{k}$, is called the "principal section." Manipulation of the two Maxwell curl equations for the assumed plane wave solutions leads to a wave equation for uniaxial media. Taking the curl of Eq.(3-1-7) yields

$$\frac{1}{\mu_0 \omega} \vec{k} \times \vec{k} \times \vec{E} = \vec{k} \times \vec{H} \ . \qquad (3\text{-}1\text{-}9)$$

Substitution of Eq. (3-1-2) gives

$$-\frac{1}{\mu_0 \omega^2} (\vec{k} \times \vec{k} \times \vec{E})_i = \varepsilon_{ij} E_j \ . \qquad (3\text{-}1\text{-}10)$$

This expression, which relates $\vec{E}$ and $\vec{k}$, is in the form of a wave equation. Because $\vec{k}$ can be limited to the principal section of the medium, its direction can specified in this plane by the angle θ it makes with the crystal axis. The components of $\vec{k}$ in terms of θ are then

$$k_x = \frac{\omega}{c} n \sin\theta, \ k_y = 0, \ k_z = \frac{\omega}{c} n \cos\theta \ . \qquad (3\text{-}1\text{-}11)$$

Performing the cross multiplication in Eq. (3-1-10) and substituting the components of $\vec{k}$ in terms of θ yields the following three equations:

$$n^2 \cos\theta (E_x \cos\theta - E_z \sin\theta) = n_0^2 E_x \ , \qquad (3\text{-}1\text{-}12)$$

$$n^2 E_y = n_0^2 E_y \ , \qquad (3\text{-}1\text{-}13)$$

$$-n^2 \sin\theta (E_x \cos\theta - E_z \sin\theta) = n_e^2 E_z \ . \qquad (3\text{-}1\text{-}14)$$

This system of equations has two solutions. The first solution occurs when

$$E_x = 0 \ , \ E_y \neq 0 \ , \ E_z = 0 \ , \ n = n_0 \ . \qquad (3\text{-}1\text{-}15)$$

This solution corresponds to the ordinary wave because the refractive index for this wave is constant for all directions within a given medium and equal to the ordinary refractive index of the medium. This wave is similar to a wave

propagating in an isotropic medium because $\vec{D}$ and $\vec{E}$ are in the same direction. The eigenstate for this wave is linearly polarized light whose $\vec{E}$ is orthogonal to the principal section of the crystal.

The second solution, which corresponds to the extraordinary wave, occurs when

$$E_x \neq 0, \; E_y = 0, \; E_z \neq 0 \; . \tag{3-1-16}$$

Completing this solution requires

$$(n^2\cos^2\theta - n_0^2)E_x - n^2 \cos\theta \sin\theta \, E_z = 0 \tag{3-1-17}$$

$$-n^2\cos\theta \sin\theta \, E_x + (n^2 \sin^2\theta - n_e^2) \, E_z = 0 \; . \tag{3-1-18}$$

Solving this system of two equations leads to the expression for the refractive index in the uniaxial medium

$$\frac{1}{n^2} = \frac{\sin^2\theta}{n_e^{\,2}} + \frac{\cos^2\theta}{n_0^{\,2}} \; , \tag{3-1-19}$$

which is the equation of the index ellipsoid for extraordinary wave in uniaxial media. The index ellipsoid equation describes the dependence of the refractive index for an extraordinary wave on the direction of $\vec{k}$ given in term of θ. The eigenstate for the extraordinary wave is linearly polarized light whose $\vec{E}$ is in the plane of the principal section as expected for extraordinary wave.

An optical ray is defined as a path along which optical energy is transported. In electromagnetic field theory, the Poynting vector is defined

as the vector representing the energy flux of the field. Thus, an optical ray travels in the direction of the Poynting vector for a given set of fields. The direction of the Poynting vector in a uniaxial medium is needed to trace optical rays through such a medium. The Poynting vector is given by:

$$\vec{S} = \vec{E} \times \vec{H} \ . \qquad (3\text{-}1\text{-}20)$$

This implies that the Poynting vector is perpendicular to $\vec{H}$ and $\vec{E}$. To be perpendicular with $\vec{H}$, the Poynting vector must be coplanar with $\vec{D}$, $\vec{E}$ and $\vec{k}$. Maxwell's equations require that $\vec{D}$ and $\vec{k}$ be perpendicular and the Poynting vector is defined such that $\vec{S}$ and $\vec{E}$ are perpendicular. With the ordinary wave solution, $\vec{D}$ and $\vec{E}$ are in the same direction and thus $\vec{k}$ and $\vec{S}$ must also be in the same direction. This further indicates that propagation of the ordinary wave is the same as propagation in isotropic media because the energy flux is in the direction of the wave normal. For the extraordinary wave solution, $\vec{D}$, $\vec{E}$ and $\vec{k}$ all lie in this plane. Figure 3.1.1 shows the $\vec{D}$, $\vec{E}$, $\vec{S}$ and $\vec{k}$ vectors for an extraordinary wave and their direction with respect to one another and the crystal axis. The direction of $\vec{k}$ in the principal section for some arbitrary extraordinary wave in a uniaxial medium is given by the angle θ defined previously. Because $\vec{S}$ also lies in the principal section, its direction can also be defined in terms of an angle θ'

between the $\bar{S}$ and the crystal axis. The angles θ and θ' can be related to $\bar{D}$ and $\bar{E}$ as follows:

$$\frac{D_z}{D_x} = \cot(\theta - 90°) = -\tan\theta \quad , \tag{3-1-21}$$

$$\frac{E_z}{E_x} = \cot(\theta' - 90°) = -\tan\theta' \quad . \tag{3-1-22}$$

From the relation between $\bar{D}$ and $\bar{E}$ given by Eq. (3-1-2),

$$\frac{D_z}{D_x} = \frac{n_e^2 E_z}{n_o^2 E_x} \quad . \tag{3-1-23}$$

Thus,

$$\tan\theta' = \frac{n_o^2}{n_e^2}\tan\theta \quad . \tag{3-1-24}$$

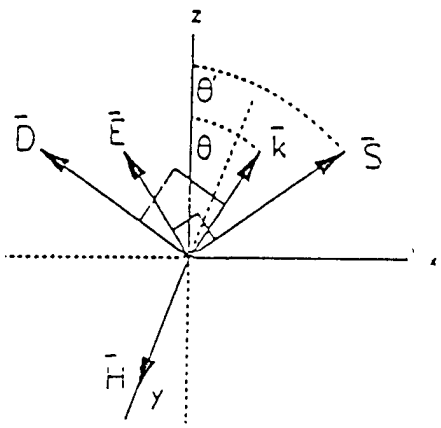

Figure 3.1.1 Wave and field vectors associated with extraordinary wave.

This expression for θ' in terms of θ provides a relationship between the direction of a Poynting vector $\vec{S}$ and the direction of the corresponding wave vector $\vec{k}$. This relationship is needed so that the ray direction for extraordinary waves can be determined, since this direction is not the same as the wave vector direction.

Ray tracing is performed by iterative loops of refraction or reflection calculations at each surface of an optical system followed by calculations to transfer the ray to the next surface. The differences in wave propagation in anisotropic media and wave propagation on isotropic media require that each of these operations be modified to include extraordinary rays.

When a ray is incident on an optical boundary, both a refracted and a reflected ray are produced. The formulas for tracing the new rays result from the condition that the phases of the fields on both sides of the boundary must match. The plane of incidence is defined as the plane containing both the surface normal and the incident wave vector $\vec{k}_i$. The angle between $\vec{k}_i$ and the surface normal is defined as ϕ_i. The refracted wave vector $\vec{k}_t$ and the reflected wave vector $\vec{k}_r$ also lie in the plane of incidence and their directions are defined by the angles ϕ_t and ϕ_r, respectively, measured from the surface normal. Applying the phase matching condition to these waves yields

$$|\vec{k}_i| \sin\phi_i = |\vec{k}_t| \sin\phi_t \qquad (3\text{-}1\text{-}25)$$

$$|\vec{k}_i| \sin\phi_i = |\vec{k}_r| \sin\phi_r \qquad (3\text{-}1\text{-}26)$$

Equation (3-1-25) is known as Snell's law and Eq. (3-1-26) is a general form of the law of reflection for anisotropic incident media. For an isotropic incident medium, $|\bar{k}_i| = |\bar{k}_r|$ so that Eq.(3-1-26) can be simplified to $\phi_i = \phi_r$, the common form of the law of reflection.

Snell's law is easily applied when refracting rays into an isotropic medium because the only unkown is the refracted wave vector direction given by ϕ_t. The magnitude of the refracted wave vector $|\bar{k}_t|$ depends on the refractive index of the refracting medium. This is a known constant quantity because it is a design parameter. Since ordinary rays in a uniaxial refracting medium behave as if the medium were isotropic, Snell's law may be applied to these rays as if the medium were isotropic. In the case of extraordinary rays in a uniaxial refracting medium, Snell's law is not as easily applied because the refractive index of the medium is not constant. The refractive index of the refracting medium depends on the direction of the refracted wave vector with respect to the crystal axis. The refracted wave direction and the refractive index of the uniaxial medium are mutual dependent. The application of Snell's law on extraordinary refracted waves requires solving a system of two independent equations, each depending the refractive index in the medium of refraction and the direction of the refracted wave vector.

When reflecting rays in an isotropic incident medium, the simplified form of the law of reflection, $\phi_r = \phi_i$, can be applied because $|\bar{k}_r| = |\bar{k}_i|$. The same is true for reflected ordinary rays in a uniaxial incident medium. Reflected extraordinary rays in a uniaxial incident medium require the same treatment as refracted extraordinary rays in a uniaxial refracting medium. The $|\bar{k}_r|$ depends on the refractive index in the direction of $\bar{k}_r$. This refractive index depends on the direction of $\bar{k}_r$ with respect to the crystal axis. In general, $\bar{k}_i$ and $\bar{k}_i$ are not in the same direction with respect to the crystal axis so that it can no longer be assumed that $|\bar{k}_r| = |\bar{k}_i|$ and Eq.(3-1-26), the general form of the law of reflection, is required. As with refraction of extraordinary rays, there are two unknowns in Eq.(3-1-26). The reflected wave vector's direction and magnitude are mutually dependent and a system of two independent equations relating them is required.

The conventional ray tracing method in isotropic media uses a vector form of the law of reflection and Snell's law to perform reflection or refraction of rays. This method uses a normalized wave vector $\bar{N}$, which is parallel to $\bar{k}$ with magnitude equal to the refractive index n of the medium. The normalized wave vector $\bar{N}$ is related to the wave vector $\bar{k}$ by

$$\bar{N} = \frac{c}{\omega}\bar{k} \qquad (3\text{-}1\text{-}27)$$

and has a magnitude given by

$$|\bar{N}| = \frac{c}{\omega}|\bar{k}| = n \ . \qquad (3\text{-}1\text{-}28)$$

where $\bar{N}$ contains all the useful information needed to represent $\bar{k}$ in a given medium since the angular frequency ω and the speed of light c are constant in all media for a given wave. In the vector form of Snell's law, $\bar{N}_i$ represents the incident wave vector and $\bar{N}_{r,t}$ is used to represent either the reflected or refracted wave vector. The unit vector normal to the surface is defined as $\hat{\eta}$. All of these vectors lie in the plane of incidence as shown in Figure 3.1.2. Without loss of generality, a coordinate system can be chosen such that the plane of incidence is

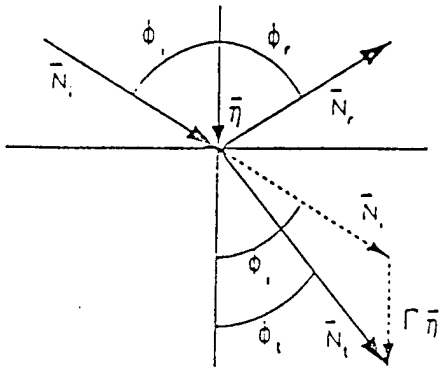

Figure 3.1.2 Vector refraction.

the x-z plane and the reflecting or refracting surface is tangent to the y-z plane. The vector form of the law of reflection and Snell's law is

$$\vec{N}_{r,t} = \vec{N}_i + \Gamma \hat{\eta}, \tag{3-1-29}$$

where Γ is a scaling constant and is determined by talking the dot product of Eq. (3-1-29) with itself to get

$$\vec{N}_{r,t} \cdot \vec{N}_{r,t} = \vec{N}_i \cdot \vec{N}_i + 2\Gamma(\vec{N}_i \cdot \hat{\eta}) + \Gamma^2(\hat{\eta} \cdot \hat{\eta}) \tag{3-1-30}$$

or

$$\Gamma^2 + 2\Gamma(\vec{N}_i \cdot \hat{\eta}) + (|\vec{N}_i|^2 - |\vec{N}_{r,t}|^2) = 0 . \tag{3-1-31}$$

Solving Eq.(3-1-31) for Γ yields

$$\Gamma = \pm\sqrt{(\vec{N}_i \cdot \hat{\eta})^2 - (|\vec{N}_i|^2 - |\vec{N}_{r,t}|^2)} - \vec{N}_i \cdot \hat{\eta} . \tag{3-1-32}$$

If the direction of $\hat{\eta}$ is chosen such that

$$\vec{N}_i \cdot \hat{\eta} \geq 0 . \tag{3-1-33}$$

the negative square root of Eq.(3-1-32) gives the scaling factor for reflection and the positive square root gives the scaling factor for refraction.

In Eq. (3-1-32), Γ depends on $|\vec{N}_{r,t}|^2$, the square of the refractive index in the medium of either reflection or refraction. For extraordinary rays, this is not a known quantity prior to performing the reflection or refraction calculations. An expression for Γ in terms of quantities known prior to the reflection or refraction calculations is required. If a unit vector $\hat{\alpha}$ in the

direction of the crystal axis is defined, then Eq.(3-1-19), the index ellipsoid equation, can be written as

$$|N_{r,t}|^2 = n_e^2 - \frac{n_e^2 - n_0^2}{n_0^2} |N_{r,t} \bullet \hat{\alpha}|^2 . \qquad (3\text{-}1\text{-}34)$$

Substitution of Eq. (3-1-29) for $N_{r,t}$ on the right side yields

$$|N_{r,t}|^2 = n_e^2 - q(N_{r,t} \bullet \hat{\alpha} + \Gamma \hat{\eta} \bullet \hat{\alpha})^2 , \qquad (3\text{-}1\text{-}35)$$

where

$$q = \frac{n_e^2 - n_0^2}{n_0^2} . \qquad (3\text{-}1\text{-}36)$$

Equation (3-1-35) can be substituted into Eq.(3-1-31) to provide the quadratic equation for Γ in terms of prior known quantities

$$\Gamma^2 [1 + q(\hat{\eta} \bullet \hat{\alpha})^2] + 2\Gamma[(N_i \bullet \hat{\alpha} + q(N_i \bullet \hat{\alpha})(\hat{\eta} \bullet \hat{\alpha})] + |N_i| - n_e^2 + q(N_i \bullet \hat{\alpha})^2 = 0 . \qquad (3\text{-}1\text{-}37)$$

Solving this equation for Γ with the negative square root of the quadratic formula yields the scaling factor for reflection. The solution resulting from the positive square root in the quadratic formula corresponds to the scaling factor for refraction. Both solutions express Γ in terms of prior known quantities. The expressions resulting from solving this quadratic equation are complicated, but are easily evaluated by computer. If rays in isotropic media or ordinary rays are specified with $n_e = n_o$. then $q = 0$ and Eq.(3-1-37) for Γ reduces to Eq.(3-1-31), the quadratic formula for Γ in the isotropic case.

Thus, using Eq.(3-1-37) o find the value of Γ required in Eq.(3-1-29) makes the reflection and refraction calculations completely general for all types of rays.

The ray transfer operation between surfaces also requires modification for uniaxial media. Recall that an optical ray travels in the direction of the Poynting vector, not the wave vector. A vector in the same direction as the Poynting vector is defined as a ray vector. For rays in isotropic media and ordinary rays in uniaxial media, the wave vector and the Poynting vector are in the same direction and so the wave vector also serves as a ray vector. For extraordinary rays in uniaxial media, The Poynting vector is not generally in the same direction as the wave vector, thus, the wave vector can not longer serve as ray vector. Therefor, tracing an extraordinary ray requires two different vectors, the wave vector and an explicitly determined ray vector.

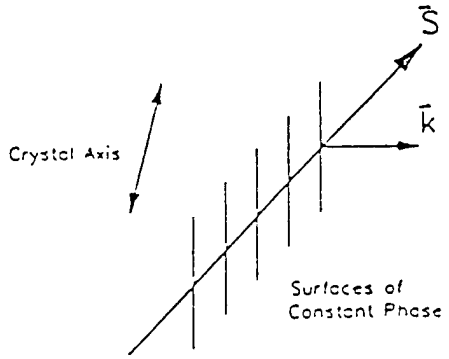

Figure 3.1.3 Propagation of extraordinary waves

Figure 3.1.3 shows these vectors and the surfaces of constant phase for a propagating extraordinary wave. These wavefronts appear to slip in the direction of the ray vector as they propagate in this direction.

After performing reflection or refraction calculation for a ray incident on a uniaxial medium, the reflected or refracted ray vector $\vec{\rho}_{r,t}$ can be determined from the reflected or refracted normalized wave vector $N_{r,t}$ and the crystal axis unit vector $\hat{\alpha}$, by using Eq.(3-1-24), the relationship between the wave vector direction in the principal section of a uniaxial medium and the corresponding Poynting vector direction. From Eq.(3-1-24), the components of $\vec{\rho}_{r,t}$ parallel and perpendicular to the crystal axis can be determined by scaling the components of $N_{r,t}$ parallel and perpendicular to the crystal axis. This leads to the equation

$$\vec{\rho}_{r,t} = n_e^2\left(\frac{\vec{N}_{r,t}\cdot\hat{\alpha}}{|\vec{N}_{r,t}|}\right)\hat{\alpha} + n_0^2\left[\frac{\vec{N}_{r,t} - (\vec{N}_{r,t}\cdot\hat{\alpha})\hat{\alpha}}{|\vec{N}_{r,t}|}\right] . \qquad (3\text{-}1\text{-}38)$$

The reflected or refracted ray vector determined in Eq.(3-1-38) is scaled until it intersect the next surface where the wave vector in the medium is then needed once again to perform reflection or refraction calculations at the new surface.

Note that, unlike reflected and refracted ordinary ray vectors, reflected and refracted extraordinary ray vectors do not in general lie in the plane of incidence. They lie in the principal section of the medium of reflection or

refraction, which is the plane containing the reflected or refracted wave vector and the crystal axis. Unless the crystal axis lies in the plane of incidence, the principal section of the medium of reflection or refraction and the plane of incidence are not parallel.

3.1.3 Matrix Algorithm

The Jones calculus is a powerful technique in which the state of polarization is presented by a two-component column vector and each optical element is presented by a 2 x 2 matrix. This method , however, is limited to normally incident and paraxial rays only. Following is a algorithm(Gu 1993, Yeh 1982, Fritsch 1991, Barkovskii 1991, Chen 1989, Cloude 1989, Lien 1990, Lawrence 1989, Wohler 1988, Smet 1993, Yeh 1980, Chakraborty 1989, and Bell 1989), proposed by C. Gu and P. Yeh, to extend the Jones matrix method to cover large incident angles and arbitrary crystal orientations.

Referring to Figure 3.1.4, we consider the reflection and the refraction of light at an interface between two media. The coordinates are chosen such that the (x,y) plane contains the interface and z direction is perpendicular to the interface. Given an incident condition, there are, in general, four eigenmodes of propagation

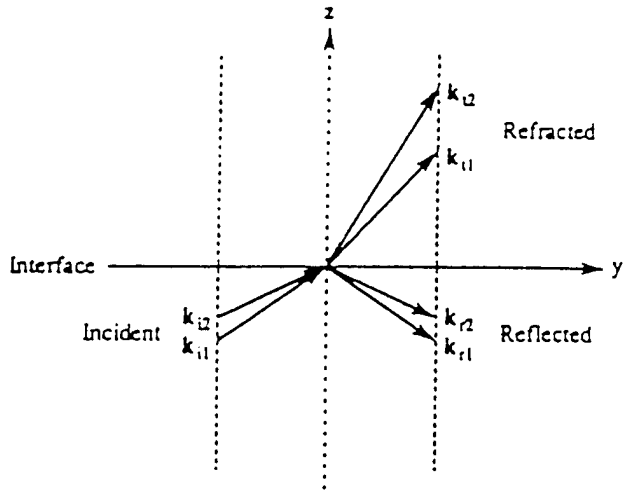

Figure 3.1.4 Reflection and refraction of light at an interface between two media. The coordinate are chosen such that the (x,y) plane contains the interface and z direction is perpendicular to the interface.

in each medium. Two of them propagation toward the +z direction, and the other two propagate toward the -z direction. Suppose that the incident and reflected wave propagated toward the +z direction and that reflected wave propagates toward the -z direction. The electric fields of the incident, reflected, and refracted wave are

Incident: $\vec{E} = [A_1 \hat{p}_{i1} \exp(-i k_{i1} \cdot \vec{r})$

$+ A_2 \hat{p}_{i2} \exp(-i k_{i2} \cdot \vec{r})] \exp(i\omega t)$,

Reflected: $\vec{E} = [B_1 \hat{p}_{r1} \exp(-i k_{r1} \cdot \vec{r})$

$+ B_2 \hat{p}_{r2} \exp(-i \vec{k}_{r2} \cdot \vec{r})] \exp(i\omega t)$,

Refracted: $\vec{E} = [C_1 \hat{p}_{t1} \exp(-i k_{t1} \cdot \vec{r})$

$$+ C_2 \hat{p}_{t2} \exp(-i k_{t2} \cdot \vec{r})]\exp(i\omega t), \qquad (3\text{-}1\text{-}39)$$

where A_1, A_2, B_1, B_2, C_1, and C_2 are amplitudes, k_{i1}, k_{i2}, k_{r1}, k_{r2}, k_{t1}, and k_{t2} are wave vectors, ω is the angular frequency, and $\hat{p}_{i1}$, $\hat{p}_{i2}$, $\hat{p}_{r1}$, $\hat{p}_{r2}$, $\hat{p}_{t1}$, and $\hat{p}_{t2}$ are unit vectors that represent the corresponding polarization states. The corresponding magnetic fields can be derived from Maxwell's equation

$$\vec{H} = (i/\omega\mu) \nabla \times \vec{E} \qquad (3\text{-}1\text{-}40)$$

and are written as

Incident: $\vec{H} = (1/\omega\mu) [A_1 k_{i1} \times \hat{p}_{i1} \exp(-i k_{i1} \cdot \vec{r})$

$$+ A_2 k_{i2} \times \hat{p}_{i2} \exp(-i k_{i2} \cdot \vec{r})]\exp(i\omega t),$$

Reflected: $\vec{H} = (1/\omega\mu) [B_1 \ k_{r1} \times \hat{p}_{r1} \exp(-i k_{r1} \cdot \vec{r})$

$$+ B_2 \ k_{r2} \times \hat{p}_{r2} \exp(-i k_{r2} \cdot \vec{r})]\exp(i\omega t),$$

Refracted: $\vec{H} = (1/\omega\mu) [C1 \ k_{t1} \times \hat{p}_{t1} \exp(-i k_{t1} \cdot \vec{r})$

$$+ C_2 \ k_{t2} \times \hat{p}_{t2} \exp(-i k_{t2} \cdot \vec{r})]\exp(i\omega t), \qquad (3\text{-}1\text{-}41)$$

where μ is the magnetic permeability. According to the boundary conditions at the interface, we have

$$(k_{i1} \cdot \hat{x}) = (k_{i2} \cdot \hat{x}) = (k_{r1} \cdot \hat{x}) = (k_{r2} \cdot \hat{x}) = (k_{t1} \cdot \hat{x}) = (k_{t2} \cdot \hat{x}) = \alpha,$$

$$(k_{i1} \cdot \hat{y}) = (k_{i2} \cdot \hat{y}) = (k_{r1} \cdot \hat{y}) = (k_{r2} \cdot \hat{y}) = (k_{t1} \cdot \hat{y}) = (k_{t2} \cdot \hat{y}) = \beta,$$

(3-1-42)

where $\hat{x}$, $\hat{y}$, and $\hat{z}$ are unit vectors along the x, y, and z directions, respectively, and α and β are the tangential components of the wave vectors.

If the electromagnetic wave is incident from an isotropic medium into a uniaxial medium, we can write $\hat{p}_{i1}=\hat{s}$, $\hat{p}_{i2}=\hat{p}$, $\hat{p}_{r1}=\hat{s}$, $\hat{p}_{r2}=\hat{p}'$, $\hat{p}_{t1}=\hat{o}$, and $\hat{p}_{t2}=\hat{e}$, where $\hat{s}$, $\hat{p}$, $\hat{p}'$, $\hat{o}$, and $\hat{e}$ are unit vectors that represent the polarization states of the TE wave, the TM wave for the incident beam, the TM wave for the reflected wave, the ordinary wave, and the extraordinary wave, respectively. In that special case, the relationships between the amplitudes of the incident and refracted waves are given by

$$C_o = A_s t_{so} + A_p t_{po}, \quad C_e = A_s t_{se} + A_p t_{pe}, \tag{3-1-43}$$

where C_o and C_e are the amplitudes of the refracted ordinary and extraordinary waves, respectively, A_s and A_p are the amplitudes of the incident TE and TM waves, respectively, and the transmission coefficients are given by

$$s_o = 2k_z D/(AD - BC), t_{po} = -2k_z B/(AD - BC),$$

$$t_{se} = -2k_z C/(AD - BC), \qquad t_{pe} = 2k_z A/(AD - BC), \tag{3-1-44}$$

with

$$A = \hat{o} \cdot (\hat{g} \times k) + \hat{o} \cdot (\hat{g} \times k_o),$$

$$B = \hat{e} \cdot (\hat{g} \times k) + \hat{e} \cdot (\hat{g} \times k_o),$$

$$C = k\hat{o} \cdot \hat{g} - [(\hat{g} \times k) \cdot (k_o \times \hat{o})/k],$$

$$D = k\hat{e} \cdot \hat{g} - [(\hat{g} \times k) \cdot (k_e \times \hat{e})/k],$$

$$k_z = [(n\omega/c)^2 - \alpha^2 - \beta^2]^{1/2}, \qquad (3\text{-}1\text{-}45)$$

Where k is the incident wave vector in the isotropic medium, k_z is the z component of the incident wave vector, k_o and k_e are the ordinary and extraordinary wave vectors in the uniaxial medium, $k=|k|$, n is the index of refraction of the isotropic medium, and $\hat{g}$ is the unit vector in the plane of

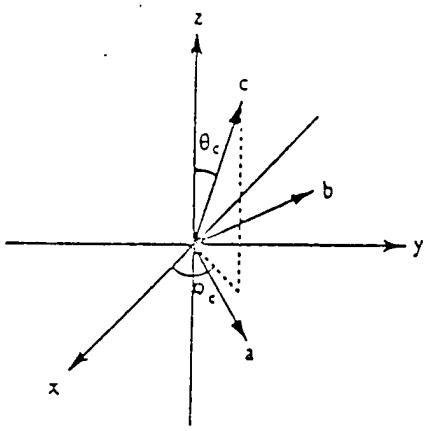

Figure 3.1.5 Orientation of the c axis. θ_c and ϕ_c are the angle between the c axis and the z direction and the angle between the projection of the axis on the (x, y) plane and the x direction, respectively.

incidence and is parallel to the interface between the two media (e.g., $\hat{g} = \hat{y}$ in Figure 3.1.4). Note that although Eqs. (3-1-43)-(3-1-45) were derived under the assumption that the c axis is parallel to the interface, those results are valid in the general case of an arbitrary c orientation. In the case of an arbitrary c-axis orientation, the z components of the ordinary and extraordinary waves, k_{oz} and k_{ez}, respectively, can be derived from the expression for the normal surface. Referring to Figure 3.1.5, we define θ_c and ϕ_c as the angle between the c axis and the z direction and the angle between the projection of the c axis on the (x, y) plane and the x direction, respectively. To calculate the z component of the extraordinary wave, k_{ez}, we use the principal coordinate system of the uniaxial medium. The unit vector $\hat{c}$ can be written as

$$\hat{c} = (\hat{x}\cos\phi_c + \hat{y}\sin\phi_c)\sin\theta_c + \hat{z}\cos\theta_c . \qquad (3\text{-}1\text{-}46)$$

In the princial coordinate system the wave-vector components of the extraordinary wave (see Figure 3.1.5) can be written as

$$k_{ea} = (\alpha\cos\phi_c + \beta\sin\phi_c)\cos\theta_c - k_{cz}\sin\theta_c$$

$$k_{eb} = -\alpha\sin\phi_c + \beta\cos\phi_c$$

$$k_{ec} = (\alpha\cos\phi_c + \beta\sin\phi_c)\sin\theta_c + k_{cz}\cos\theta_c \qquad (3\text{-}1\text{-}47)$$

where the $\hat{a}$ and $\hat{b}$ directions are chosen such that $\hat{b}$ is perpendicular to $\hat{z}$ while both $\hat{a}$ and $\hat{b}$ are perpendicular to $\hat{c}$. The normal surface for the extraordinary waves is given by

$$\frac{k_{ea}^2 + k_{eb}^2}{n_e^2} + \frac{k_{ec}^2}{n_0^2} = \left(\frac{\omega}{c}\right)^2 \qquad (3\text{-}1\text{-}47)$$

where n_o and n_e are the ordinary and the extraordinary indices of refraction, respectively. Substituting Eqs. (3-1-47) into Eq.(3-1-47), we obtain

$$uk_{ez}^2 - vk_{ez} + \omega = 0 \qquad (3\text{-}1\text{-}48)$$

where

$$u = \frac{\sin^2\theta_c}{n_e^2} + \frac{\cos^2\theta_c}{n_0^2},$$

$$v = k_d \sin(2\theta_c)\left(\frac{1}{n_e^2} - \frac{1}{n_0^2}\right),$$

$$\omega = \frac{k_d^2\cos^2\theta_c + k_{eb}^2}{n_e^2} + \frac{k_d^2\sin^2\theta_c}{n_o^2} - \left(\frac{\omega}{c}\right)^2 \quad , \qquad (3\text{-}1\text{-}49)$$

with

$$k_d = \alpha\cos\phi_c + \beta\sin\phi_c \quad . \qquad (3\text{-}1\text{-}50)$$

Solving Eq.(3-1-48), we obtain the z component of the extraordinary wave:

$$k_{ez} = \left[v + \left(v^2 - 4u\omega\right)^{1/2}\right]/2u \qquad (3\text{-}1\text{-}51)$$

where we have taken the positive sign for the square root, since the light is transmitting in the +z direction.

The z component of the ordinary wave, k_{oz}, does not depend on the orientation of the axis and is given by

$$k_{oz} = \left[\left(n_o\omega/c\right)^2 - \alpha^2 - \beta^2\right]^{1/2} \qquad (3\text{-}1\text{-}52)$$

The transmission of light through a birefringent network can be described by 2 x 2 matrices. For example, the refraction of light at an interface [Eqs.(3-1-43)]can be written in matrix form as

$$\begin{bmatrix} C_o \\ C_e \end{bmatrix} = \begin{bmatrix} t_{so} & t_{po} \\ t_{se} & t_{pe} \end{bmatrix} \begin{bmatrix} A_s \\ A_p \end{bmatrix} \tag{3-1-53}$$

where C_o, C_e, A_s, A_p, s_o, t_{po}, t_{se} and t_{pe} were defined following Eqs.(3-1-43). If the transmitted waves propagated in the uniaxial medium for a distance d and then exit through another interface from the uniaxial medium to an isotropic medium, the s and p components of the emerging electric field can be written as

$$\begin{bmatrix} A_s \\ A_p^1 \end{bmatrix} = \begin{bmatrix} t_{os} & t_{es} \\ t_{op} & t_{ep} \end{bmatrix} \begin{bmatrix} \exp^{(-ik_{oz}d)} & 0 \\ 0 & \exp^{(-ik_{ez}d)} \end{bmatrix} \begin{bmatrix} t_{so} & t_{po} \\ t_{se} & t_{pe} \end{bmatrix} \begin{bmatrix} A_s \\ A_p \end{bmatrix} \tag{3-1-54}$$

where t_{os}, t_{es}, t_{op}, and t_{ep} are another set of transmission coefficients that represent the transmission from ordinary (or extraordinary) wave to s (or p) wave, and k_{oz} and k_{ez} are the z components of the ordinary and extraordinary wave vectors, respectively. Note that Eq. (3-1-54) is valid provided that the multiple reflections between the two surfaces can be neglected.

Equation(3-1-54)can be written in a form similar to the Jones matrix formulation:

$$\begin{bmatrix} A_s^1 \\ A_p^1 \end{bmatrix} = D_0 P D_i \begin{bmatrix} A_s \\ A_p \end{bmatrix}, \tag{3-1-55}$$

where p is the propagation matrix and D_o and D_i are the output and input dynamical matrices, respectively. Those matrices are written explicitly as

$$P = \begin{bmatrix} \exp(-ik_{oz}d) & 0 \\ 0 & \exp(-ik_{ez}d) \end{bmatrix},$$

$$D_o = \begin{bmatrix} t_{os} & t_{es} \\ t_{op} & t_{ep} \end{bmatrix},$$

$$D_i = \begin{bmatrix} t_{so} & t_{po} \\ t_{se} & t_{pe} \end{bmatrix}. \qquad (3\text{-}1\text{-}56)$$

The matrix formalism developed above can be employed in the analysis of transmission properties of a series of birefringent elements(i.e., liquid crystals and polarizers)for an arbitrary angle of incidence. To do so, we writedown the 2 x 2 matrices for each birefringent element and multiply them in sequence to obtain the overall transfer matrix M. The relationship between the Jones vectors of the emerging and incident beams is given by

$$\begin{bmatrix} A_s^1 \\ A_p^1 \end{bmatrix} = \begin{bmatrix} M_{11} & M_{12} \\ M_{21} & M_{22} \end{bmatrix} \begin{bmatrix} A_s \\ A_p \end{bmatrix} \qquad (3\text{-}1\text{-}57)$$

The energy transmittance is

$$T = \left(|A_s^1|^2 + |A_p^1|^2\right) \Big/ \left(|A_s|^2 + |A_p|^2\right) \qquad (3\text{-}1\text{-}58)$$

For unpolarized incident light the transmittance is given by

$$T = \frac{1}{2}\left(|M_{11}|^2 + |M_{12}|^2 + |M_{21}|^2 + |M_{22}|^2\right) \qquad (3\text{-}1\text{-}59)$$

The 2 x 2 matrix method developed here, which is generally applicable to any birefringent network, can be significantly simplified under the small-

birefringence approximation. If we assume that $|n_e - n_0| \ll n_o, n_e$, which is valid for most of the practical birefringent materials including liquid crystals, the wave vectors for the ordinary and extraordinary modes will be approximately the same, i.e., $\bar{k}_e \approx \bar{k}_o$. although $|n_e - n_o| \approx 0.1 n_o$ in many liquid crystals ,the results obtained under this approximation are still to the exact solutions. The polarization vectors $\hat{o}$ and $\bar{c}$ can be written as

$$o = (\bar{c} \times \bar{k}_o) / |\bar{c} \times \bar{k}_o| , \tag{3-1-60}$$

$$\hat{e} \approx (\bar{k}_o \times \bar{c}) / |\bar{k}_o \times \bar{c}| . \tag{3-1-61}$$

Note that Eq. (3-1-60) is exact while relation (3-1-61) is an approximation. Consequently, the transmission coefficients can be written as

$$s_o \approx \hat{s} \cdot \hat{o}\, t_s, \qquad t_{po} \approx \hat{p}_o \cdot \hat{o}\, t_p, \; t_{se} \approx \hat{s} \cdot \hat{e}\, t_s$$

$$t_{pe} \approx \hat{p}_o \cdot \hat{e}\, t_p, \qquad t_{os} \approx \hat{o} \cdot \hat{s}\, t'_s, \quad t_{es} \approx \hat{e} \cdot \hat{s}\, t'_s$$

$$t_{op} \approx \hat{o} \cdot \hat{p}_o\, t'_p, \qquad t_{ep} \approx \hat{e} \cdot \hat{p}_o\, t'_p, \tag{3-1-62}$$

where we recall that $\hat{s}$ is a unit vector perpendicular to the plane of incidence, $\hat{p}_o$ is a unit vector perpendicular to both $\hat{s}$ and $\bar{k}_o$, i.e.,

$$\hat{p}_o = (\bar{k}_o \times \hat{s}) / |\bar{k}_o \times \hat{s}|, \tag{3-1-63}$$

and the Fresnel transmission coefficients are written as

$$t_s = \frac{2n\cos\theta}{n\cos\theta + n_o\cos\theta_o} , \qquad t_p = \frac{2n\cos\theta}{n\cos\theta_o + n_o\cos\theta} ,$$

$$t_s = \frac{2n\cos\theta_o}{n_o\cos\theta_o + n\cos\theta} \quad , \qquad t_p^1 = \frac{2n_o\cos\theta_o}{n_o\cos\theta + n\cos\theta_o} \quad , \quad (3\text{-}1\text{-}64)$$

where n is the index of refraction of the incident medium, $n_o \approx n_e$ is the index of refraction of the birefringent medium, θ is the incident angle, and θ_o is the refraction angle with $\theta_e \approx \theta_o$.

It is important to note that the transmission coefficients in relations (3-1-62) are determined by the Fresnel refraction and the scalar product between the polarization states in the incident medium and in the crystal plate. In other words, the transmission properties are mostly determined by the eigenmode projections and the Fresnel reflection and refraction.

The results obtained above can be further generalized to any media, including biaxial crystals and gyrotropic materials that exhibit optical rotation and Farady rotation. In the case of small anisotropy the 2×2 dynamical matrix at the boundary can be derived in the following way.

In general, when a homogeneous medium is specified by its dielectric tensor, the eigenmodes of propagation can be obtained from

$$\vec{k}\times\left(\vec{k}\times\vec{E}\right) + \omega^2\mu\varepsilon\vec{E} = 0 \qquad (3\text{-}1\text{-}65)$$

which leads to

$$\begin{bmatrix} \omega^2\mu\varepsilon_{xx} - k_y^2 - k_z^2 & \omega^2\mu\varepsilon_{xy} + k_xk_y & \omega^2\mu\varepsilon_{xz} + k_xk_z \\ \omega^2\mu\varepsilon_{yx} + k_yk_x & \omega^2\mu\varepsilon_{yy} - k_x^2 - k_z^2 & \omega^2\mu\varepsilon_{yz} + k_yk_z \\ \omega^2\mu\varepsilon_{zx} + k_zk_x & \omega^2\mu\varepsilon_{zy} + k_zk_y & \omega^2\mu\varepsilon_{zz} - k_x^2 - k_y^2 \end{bmatrix} \begin{bmatrix} E_x \\ E_y \\ E_z \end{bmatrix} = 0$$

(3-1-66)

where μ is the permeability, $\bar{k}$ is the wave vector, the ε_{ij}'s (i,j=x,y,z,)are elements of the dielectric tensor, and k_x, k_y, and k_z are components of the wave vector $\bar{k}$. Given k_x and k_y, which are specified by the incidence condition, we can obtain the z component of the eigenmode by solving the secular equation

$$\det\begin{bmatrix} \omega^2\mu\varepsilon_{xx}-k_y^2-k_z^2 & \omega^2\mu\varepsilon_{xy}+k_xk_y & \omega^2\mu\varepsilon_{xz}+k_xk_z \\ \omega^2\mu\varepsilon_{yx}+k_yk_x & \omega^2\mu\varepsilon_{yy}-k_x^2-k_z^2 & \omega^2\mu\varepsilon_{yz}+k_yk_z \\ \omega^2\mu\varepsilon_{zx}+k_zk_x & \omega^2\mu\varepsilon_{zy}+k_zk_y & \omega^2\mu\varepsilon_{zz}-k_x^2-k_y^2 \end{bmatrix}=0. \quad (3\text{-}1\text{-}67)$$

The above equation results in four solutions of k_z, two positive and two negative in the case of propagating mode. To discuss the transmission properties using the 2×2 matrix method, we need only the two positive eigenvalues k_{1z} and k_{2z}. The polarization states of the two eigenmodes can be obtained directly by solution of the eigenvale problem [Eq.(3-1-66)]. The propagation matrix within each medium of thickness d is given simply by

$$P=\begin{bmatrix} \exp(-ik_{1z}d) & 0 \\ 0 & \exp(-ik_{2z}d) \end{bmatrix} \quad (3\text{-}1\text{-}68)$$

Once the eigenmodes are obtained , the dynamical matrix at the boundary between two media can be derived. Suppose the electric fields inside the two media are given by Eqs. (3-1-39); then the dynamical matrix, which relates the refracted and waves, is written as

$$\begin{bmatrix} C_1 \\ C_2 \end{bmatrix} = D_{12}\begin{bmatrix} A_1 \\ A_2 \end{bmatrix} = \begin{bmatrix} t_{11} & t_{21} \\ t_{12} & t_{22} \end{bmatrix}\begin{bmatrix} A_1 \\ A_2 \end{bmatrix} \quad (3\text{-}1\text{-}69)$$

To determine D_{12}, we assume that the anisotropy is small for both media, so that the average indices of refraction can be written as two constants n_1 and n_2 for medium 1 and medium 2, respectively. For the purpose of obtaining D_{12}, we insert two imaginary isotropic layers of zero thickness between the two media. The layer on the side of medium 1 (2) has an index of refraction $n_1(n_2)$. Let the Fresnel transmission coefficients between the two imaginary layers be t_s and t_p, respectively, where

$$t_s = \frac{2n_1\cos\theta_1}{n_1\cos\theta_1 + n_2\cos\theta_2}, \qquad t_p = \frac{2n_1\cos\theta_1}{n_1\cos\theta_2 + n_2\cos\theta_1} \tag{3-1-70}$$

and θ_1 and θ_2 are incident and refraction angles (angles between the propagation direction and surface normal), respectively. From the above discussion the dynamical matrix between two media of the same refractive index of the eigenmodes. Therefore

$$D_{12} = \begin{bmatrix} \hat{s}\cdot\hat{p}_{t1} & \hat{p}_2\cdot\hat{p}_{t1} \\ \hat{s}\cdot\hat{p}_{t2} & \hat{p}_2\cdot\hat{p}_{t2} \end{bmatrix} \begin{bmatrix} t_s & 0 \\ 0 & t_p \end{bmatrix} \begin{bmatrix} \hat{p}_{i1}\cdot\hat{s} & \hat{p}_{i2}\cdot\hat{s} \\ \hat{p}_{i1}\cdot\hat{p}_1 & \hat{p}_{i2}\cdot\hat{p}_1 \end{bmatrix}$$

$$= \begin{bmatrix} t_s(\hat{p}_{i1}\cdot\hat{s})(\hat{s}\cdot\hat{p}_{t1}) + t_p(\hat{p}_{i1}\cdot\hat{p}_1)(\hat{p}_2\cdot\hat{p}_{t1}) & t_s(\hat{p}_{i2}\cdot\hat{s})(\hat{s}\cdot\hat{p}_{t1}) + t_p(\hat{p}_{i2}\cdot\hat{p}_1)(\hat{p}_2\cdot\hat{p}_{t1}) \\ t_s(\hat{p}_{i1}\cdot\hat{s})(\hat{s}\cdot\hat{p}_{t2}) + t_p(\hat{p}_{i1}\cdot\hat{p}_1)(\hat{p}_2\cdot\hat{p}_{t2}) & t_s(\hat{p}_{i2}\cdot\hat{s})(\hat{s}\cdot\hat{p}_{t2}) + t_p(\hat{p}_{i2}\cdot\hat{p}_1)(\hat{p}_2\cdot\hat{p}_{t2}) \end{bmatrix}$$

(3-1-71)

where $\hat{p}_{i1}, \hat{p}_{t1}, \hat{p}_{i2}, \hat{p}_1, \hat{p}_2, \hat{p}_{t2}$, and $\hat{s}$ are unit vectors that represent polarization states of the two incident eigenmodes, the two transmitted eigenmodes, TE waves in the imaginary layers, and TM waves in the imaginary layers 1 and

2, respectively. Note that when $n_1=n_2$, $t_s=t_p=1$ and $\hat{p}_1 = \hat{p}_2$, Eq.(3-1-71) reduces to

$$D_{12} = \begin{bmatrix} \hat{p}_{i1} \cdot \hat{p}_{t1} & \hat{p}_{i2} \cdot \hat{p}_{t1} \\ \hat{p}_{i1} \cdot \hat{p}_{t2} & \hat{p}_{i2} \cdot \hat{p}_{t2} \end{bmatrix} \qquad (3\text{-}1\text{-}72)$$

3.1.4 NIST Model

NIST (National Institute of Standards and Technology) has a model(Bennett 1995) to analyze the light transmission vs. angle in Kerr cell. This model is simple but probably good to first order.

Here is how a Kerr cell works, A transverse voltage V is applied and the light travels a distance L through the crystal as shown below.

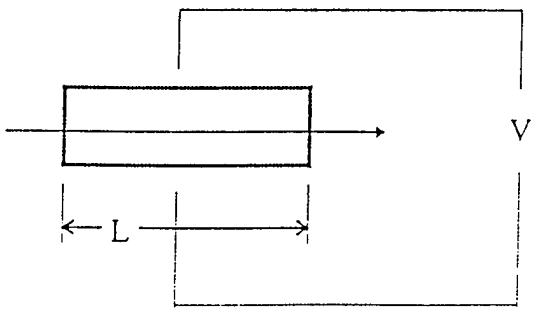

Figure 3.1.6 Kerr's cell with applied voltage V.

The birefringence induced is

$$\Delta n = \alpha E^2 = \alpha V^2 / L^2 ,$$

where α is a constant. The optical path difference is

$$OPD = \Delta nL = \alpha V^2 / L.$$

The half wave voltage occurs when

$$OPD = \alpha V^2 / L = \lambda / 2$$

or

$$V_{\frac{1}{2}} = (\lambda L / 2\alpha)^{\frac{1}{2}},$$

where $V_{\frac{1}{2}}$ is the half wave voltage.

Here is the NIST angular analysis. They distinguish between two planes (θ, in the plane of the drawing and ϕ, out of the plane of the drawing).

$$T = \sin^2[\frac{\pi}{2}(\frac{V\sqrt{\cos\phi}}{V_{\frac{1}{2}}\sqrt{\cos\theta}})^2] ,$$

where T is the transmission of light through Kerr cell.

3.2 Extension of Current Analytical Theories

Because optical uniaxial crystals have many applications, several authors have developed algorithms to study the properties of light beam passing through them. These works are mainly based on the 4 x 4 matrix formula or 2 x 2 matrix formula(Gu 1993, Yeh 1982, Fritsch 1991, Barkovskii 1991, Mentel 1992, Chen 1989, Cloude 1989, Lien 1990, Lawrence 1989, Wohler 1988,Smet 1993, Yeh 1980, Chakraborty 1989, and Bell 1989). But all of them either have the difficulty that one has to transform the dielectric tensor from the principal-axes frame to the laboratory frame and solve the associated eigenvalue problem, or have no explicit formulas for light propagating through the interface formed by two uniaxial crystals. Thus it is impossible to cascade uniaxial elements by these methods.

In this section, we propose a general algorithm to calculate the wave and ray directions, polarization states, and Fresnel coefficients for light propagating through interface formed by two materials. we introduce a third polarization component k, in the addition to the conventional s and p transverse polarization components, in the incident wave because in inhomogeneous materials, these two(s and p) do not always form a complete basis for describing the reflected and refracted light. This additional state is , of course, zero in homogeneous materials. With these three polarization components, we derive a formula which

can be applied to any kind of interface(including interfaces formed by two isotropic materials, isotropic and anisotropic materials, and two anisotropic materials) directly. This allows you to use the same formula to different interfaces. Light propagating in an uniaxial crystal in general consists of an ordinary wave and an extraordinary wave. The electric field vector $\vec{E}$ (and the displacement vector $\vec{D}$) for the ordinary wave is always perpendicular to both the C axis of the crystal and the propagation vector. But, the electric field $\vec{E}$ for extraordinary wave is not in general perpendicular to the propagation vector. It lies in the plane formed by the propagation vector and the displacement vector. The electric field vectors of these wave are mutually orthogonal.

3.2.1 Wave and ray vectors of the reflected and transmitted beam

Consider a plane wave incident on the surface formed by two uniaxial crystals. The reflected waves and transmitted waves both are mixtures of ordinary waves and extraordinary waves. According to the boundary condition of the electric field, all the wave vectors lie in the plane of incidence and their tangential components along the boundary are the same. That is

$$|\vec{K}_i| \sin\vartheta_i = |\vec{K}_{or}|\sin\vartheta_{or} = |\vec{K}_{er}|\sin\vartheta_{er} = |\vec{K}_{ot}|\sin\vartheta_{ot} = |\vec{K}_{et}|\sin\vartheta_{et}. \quad (3\text{-}2\text{-}1)$$

Here $\bar{K}_i, \bar{K}_{or}, \bar{K}_{er}, \bar{K}_{ot}, \bar{K}_{et}$ are propagation vectors of the incident wave, ordinary reflected wave, extraordinary reflected wave, ordinary transmitted wave and extraordinary transmitted wave respectively, as shown in the Figure 3.2.1. From equation (3-2-1), these expressions follow,

$$n_i \sin\vartheta_i = n_{or} \sin\vartheta_{or} \tag{3-2-2}$$

$$n_i \sin\vartheta_i = n_{ot} \sin\vartheta_{ot} \tag{3-2-3}$$

for ordinary waves and

$$n_i \sin\vartheta_i = n_{er}(\vartheta_1)\sin\vartheta_{er} \tag{3-2-4}$$

$$n_i \sin\vartheta_i = n_{et}(\vartheta_2)\sin\vartheta_{et} \tag{3-2-5}$$

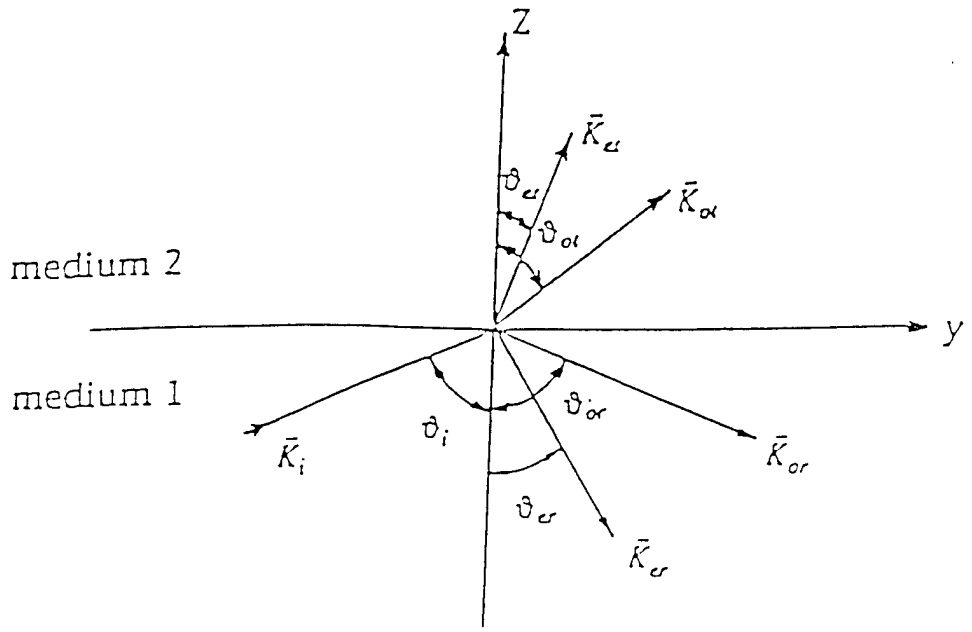

Figure 3.2.1 Wave and ray vectors of light through uniaxial media.

for extraordinary waves, where $n_i, n_{or}, n_{ot}, n_{er}(\vartheta_1)$, and $n_{et}(\vartheta_2)$ are the refractive indices for the incident beam, the ordinary reflected beam, the ordinary transmitted beam, the extraordinary reflected beam, and the extraordinary transmitted beam. The indices $n_{er}(\vartheta_1)$ and $n_{et}(\vartheta_2)$ vary with the directions of the extraordinary wave propagation. Let ϑ_1 and ϑ_2 be angles between the e-wave vectors and optic axes of the medium 1 and medium 2 respectively. The indices $n_{er}(\vartheta_1)$ and $n_{et}(\vartheta_2)$ are given(Collette 1993) by

$$n_{er}(\vartheta_1) = \frac{n_{or}\, n_{er}}{\sqrt{\left[n_{or}^2 \sin^2\vartheta_1 + n_{er}^2 \cos^2\vartheta_1\right]}} \qquad (3-2-6)$$

$$n_{et}(\vartheta_2) = \frac{n_{ot}\, n_{et}}{\sqrt{\left[n_{ot}^2 \sin^2\vartheta_2 + n_{et}^2 \cos^2\vartheta_2\right]}} \quad . \qquad (3-2-7)$$

Suppose the optic axes of the medium 1 and medium 2 are denoted by the unit vectors $\hat{c}_1 = c_{1x}\hat{x} + c_{1y}\hat{y} + c_{1z}\hat{z}$ *and* $\hat{c}_2 = c_{2x}\hat{x} + c_{2y}\hat{y} + c_{2z}\hat{z}$.

From these, it follows that

$$\cos\vartheta_1 = c_{1y}\sin\vartheta_{er} + c_{1z}(-\cos\vartheta_{er}) \qquad (3-2-8)$$

$$\cos\vartheta_2 = c_{2y}\sin\vartheta_{et} + c_{2z}\cos\vartheta_{et} \; . \qquad (3-2-9)$$

Substituting equations (3-2-8) and (3-2-9) into equations (3-2-6) and (3-2-7), we have

$$n_{er}(\vartheta_1) = \frac{n_{or}\, n_{er}}{\sqrt{\left\{ n_{or}^2\left[1-(c_{1y}\sin\vartheta_{er} - c_{1z}\cos\vartheta_{er})^2\right] + n_{er}^2\left[c_{1y}\sin\vartheta_{er} - c_{1z}\cos\vartheta_{er}\right]^2\right\}}} \qquad (3-2-10)$$

$$n_{et}(\vartheta_2) = \frac{n_{ot}\, n_{et}}{\sqrt{\left\{ n_{ot}^2\left[1-\left(c_{2y}\sin\vartheta_{et} + c_{2z}\cos\vartheta_{et}\right)^2\right] + n_{et}^2\left(c_{2y}\sin\vartheta_{et} + c_{2z}\cos\vartheta_{et}\right)^2\right\}}} \; . \qquad (3-2-11)$$

Bringing these into the equation (3-2-4) and (3-2-5) , we have the following quadratic equation in $\cot\theta_{er}$ and $\cot\theta_{et}$:

$$\left[n_{or}^2 + c_{1z}^2\left(n_{er}^2 - n_{or}^2\right)\right]\cot^2\vartheta_{er} - 2c_{1z}c_{1y}\left(n_{er}^2 - n_{or}^2\right)\cot\vartheta_{er} + n_{or}^2 + c_{1y}^2\left(n_{er}^2 - n_{or}^2\right) - \frac{n_{or}^2 n_{er}^2}{n_i^2\sin^2\vartheta_i} = 0 \qquad (3-2-12)$$

$$\left[n_{ot}^2 + c_{2z}^2\left(n_{et}^2 - n_{ot}^2\right)\right]\cot^2\vartheta_{et} + 2c_{2z}c_{2y}\left(n_{et}^2 - n_{ot}^2\right)\cot\vartheta_{et} + n_{ot}^2 + c_{2y}^2\left(n_{et}^2 - n_{ot}^2\right) - \frac{n_{et}^2 n_{ot}^2}{n_i^2\sin^2\vartheta_i} = 0 \; . \qquad (3-2-13)$$

Solving those equations, we get the angles of ϑ_{er} and ϑ_{et} as

$$\cot\vartheta_{et} = \frac{-2c_{2z}c_{2x}\left(n_{et}^2 - n_{ot}^2\right) \pm 2n_{ot}\sqrt{\left\{\frac{n_{ot}^2 n_{et}^2 + n_{et}^2 c_{2z}^2\left(n_{et}^2 - n_{ot}^2\right)}{n_i^2 \sin^2\vartheta_i} - \left[n_{ot}^2 + \left(n_{et}^2 - n_{ot}^2\right)\left(c_{2z}^2 + c_{2y}^2\right)\right]\right\}}}{2\left[n_{ot}^2 + c_{2z}^2\left(n_{et}^2 - n_{ot}^2\right)\right]} \qquad (3-2-14)$$

$$\cot\vartheta_{er} = \frac{2c_{1z}c_{1x}\left(n_{er}^2 - n_{or}^2\right) \pm 2n_{or}\sqrt{\left\{\frac{n_{or}^2 n_{er}^2 + n_{er}^2 c_{1z}^2\left(n_{er}^2 - n_{or}^2\right)}{n_i^2 \sin^2\vartheta_i} - \left[n_{or}^2 + \left(n_{er}^2 - n_{or}^2\right)\left(c_{1z}^2 + c_{1y}^2\right)\right]\right\}}}{2\left[n_{or}^2 + c_{1z}^2\left(n_{er}^2 - n_{or}^2\right)\right]} \qquad (3-2-15)$$

and the directions of $\bar{K}_{er}$ and $\bar{K}_{et}$ are

$$\hat{k}_{er} = \sin\vartheta_{er}\hat{y} + \left(-\cos\vartheta_{er}\right)\hat{z} \qquad (3-2-16)$$

$$\hat{k}_{et} = \sin\vartheta_{et}\hat{y} + \cos\vartheta_{et}\hat{z} \qquad (3-2-17)$$

The wave vectors $\bar{K}_{ot}$ and $\bar{K}_{or}$ for ordinary beams are easily found by the equations (3-2-2) and (3-2-3)

$$\hat{k}_{or} = -\sqrt{\left\{1 - \frac{n_i^2}{n_{or}^2}\sin^2\vartheta_i\right\}}\hat{z} + \frac{n_i}{n_{or}}\sin\vartheta_i\hat{y} \qquad (3-2-18)$$

$$\hat{k}_{ot} = \sqrt{\left\{1 - \frac{n_i^2}{n_{ot}^2}\sin^2\vartheta_i\right\}}\hat{z} + \frac{n_i}{n_{ot}}\sin\vartheta_i\hat{y} \; . \qquad (3-2-19)$$

So far we have all 5 unit vectors as

$$\left.\begin{aligned}
\hat{k}_i &= (0, \sin\vartheta_i, \cos\vartheta_i)^T \\
\hat{k}_{or} &= \left(0, \frac{n_i}{n_{or}}\sin\vartheta_i, -\sqrt{\left\{1 - \frac{n_i^2}{n_{or}^2}\sin^2\vartheta_i\right\}}\right)^T \\
\hat{k}_{er} &= (0, \sin\vartheta_{er}, -\cos\vartheta_{er})^T \\
\hat{k}_{ot} &= \left(0, \frac{n_i}{n_{ot}}\sin\vartheta_i, \sqrt{\left\{1 - \frac{n_i^2}{n_{ot}^2}\sin^2\vartheta_i\right\}}\right)^T \\
\hat{k}_{et} &= (0, \sin\vartheta_{et}, \cos\vartheta_{et})^T
\end{aligned}\right\} \qquad (3-2-20)$$

where ϑ_{er} and ϑ_{et} are determined by the (3-2-14) and (3-2-15).

The ray vectors for the ordinary wave are the same as wave vectors. But ray vectors for the extraordinary wave, taking the directions of the Poynting vectors, are different from wave vectors in general. Suppose the unit ray vectors for the extraordinary waves are

$$\hat{s}_r = (s_{rx}, s_{ry}, s_{rz})^T \qquad \text{for reflected beam,}$$

and $$\hat{s}_t = (s_{tx}, s_{ty}, s_{tz})^T \qquad \text{for transmitted beam.}$$

According to the reference [26], $\bar{K}_{er}, \hat{s}_r$ and $\hat{c}_1$ are coplanar; $\bar{K}_{et}, \hat{s}_t$ and $\hat{c}_2$ are coplanar also. So we have

$$\begin{vmatrix} s_{rx} & s_{ry} & s_{rz} \\ c_{1x} & c_{1y} & c_{1z} \\ 0 & \sin\vartheta_{er} & -\cos\vartheta_{et} \end{vmatrix} = 0 \qquad (3\text{-}2\text{-}21)$$

$$\begin{vmatrix} s_{tx} & s_{ty} & s_{tz} \\ c_{2x} & c_{2y} & c_{2z} \\ 0 & \sin\vartheta_{et} & \cos\vartheta_{et} \end{vmatrix} = 0 \qquad (3\text{-}2\text{-}22)$$

In other hand the dispersion angle of the extraordinary wave in the uniaxial medium is also the angle between wave vector and ray vector, and the dispersion angle α_1 in medium 1 and the dispersion angle α_2 in medium 2 satisfy following equations.

$$\tan\alpha_1 = \frac{\left(n_{er}^2 - n_{or}^2\right)\tan\vartheta_1}{n_{er}^2 + n_{or}^2\tan^2\vartheta_1} \qquad (3-2-23)$$

$$\tan\alpha_2 = \frac{\left(n_{et}^2 - n_{ot}^2\right)\tan\vartheta_2}{n_{et}^2 + n_{ot}^2\tan^2\vartheta_2} \quad . \qquad (3-2-24)$$

So we have

$$s_{ry}\sin\vartheta_{er} - s_{rz}\cos\vartheta_{er} = \cos\alpha_1 \qquad (3\text{-}2\text{-}25)$$

$$s_{ty}\sin\vartheta_{et} + s_{tz}\cos\vartheta_{et} = \cos\alpha_2 \; . \qquad (3\text{-}2\text{-}26)$$

where α_1 and α_2 are given by (3-2-23) and (3-2-24). Also we have other equations

$$s_{rx}^2 + s_{ry}^2 + s_{rz}^2 = 1 \qquad (3\text{-}2\text{-}27)$$

$$s_{tx}^2 + s_{ty}^2 + s_{tz}^2 = 1 \quad . \qquad (3\text{-}2\text{-}28)$$

Solving (3-2-21)-(3-2-28), we have the ray directions as

$$s_{rx} = \pm \frac{c_{1x} \sin \alpha_1}{\sqrt{\left\{ c_{1x}^2 + \left(\sin \vartheta_{er} c_{1z} + \cos \vartheta_{er} c_{1y} \right)^2 \right\}}} \qquad (3-2-29a)$$

$$s_{ry} = \sin \vartheta_{er} \cos \alpha_1 - \frac{\cos \vartheta_{er}}{c_{1x}} s_{rx} \qquad (3-2-30a)$$

$$s_{rz} = \frac{1}{\cos \vartheta_{er}} \left(-\cos \alpha_1 + \sin \vartheta_{er} s_{ry} \right) \qquad (3-2-31a)$$

$$s_{tx} = \pm \frac{c_{2x} \sin \alpha_2}{\sqrt{c_{2x}^2 + \left(\sin \vartheta_{et} c_{2z} - \cos \vartheta_{et} c_{2y} \right)^2}} \qquad (3-2-29b)$$

$$s_{ty} = \sin \vartheta_{et} \cos \alpha_2 + \frac{\cos \vartheta_{et}}{c_{2x}} s_{tx} \qquad (3-2-30b)$$

$$s_{tz} = \frac{1}{\cos \vartheta_{et}} \left(\cos \alpha_2 - \sin \vartheta_{et} s_{ty} \right) \qquad (3-2-31b)$$

3.2.2 Fresnel Coefficients and Polarization States

We choose the coordinate system as in Figure 3.2.2, where $\hat{s}$, $\hat{p}$ and $\hat{k}_i$ are unit vectors. The electric fields are:

$$\text{Incident:} \quad \vec{E}_i = \left(A_s\hat{s} + A_p\hat{p} + A_k\hat{k}_i\right)e^{-i(\vec{K}_i\cdot\vec{r})}e^{-i\omega t} \quad , \qquad (3-2-32)$$

$$\text{Reflected:} \quad \vec{E}_r = \left[B_o\hat{o}_r e^{-i(\vec{K}_{or}\cdot\vec{r})} + B_e\hat{e}_r e^{-i(\vec{K}_{er}\cdot\vec{r})}\right]e^{-i\omega t} \quad , \qquad (3-2-33)$$

$$\text{Transmitted:} \quad \vec{E}_t = \left[C_o\hat{o}_t e^{-i(\vec{K}_{ot}\cdot\vec{r})} + C_e\hat{e}_t e^{-i(\vec{K}_{et}\cdot\vec{r})}\right]e^{-i\omega t} \quad . \qquad (3-2-34)$$

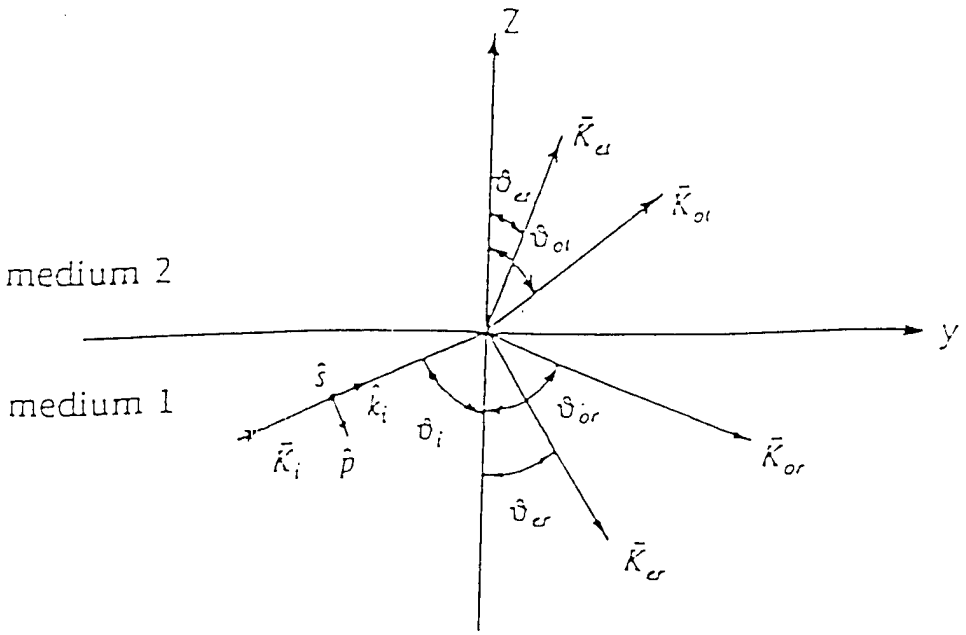

Figure 3.2.2 Reflection and refraction on surface between two uniaxial crystals.

Using the relation $\vec{H} = (\vec{K} \times \vec{E}) \div (\omega\mu)$, we have these expressions for the magnetic fields:

Incident: $$\vec{H}_i = \frac{1}{\omega\mu}\vec{K}_i \times \vec{K}_i\left(A_s\hat{s} + A_p\hat{p} + A_k\hat{k}_i\right)e^{-i(\vec{K}_i \cdot \vec{r})}e^{-i\omega t} \quad (3-2-35)$$

Reflected: $$\vec{H}_r = \frac{1}{\omega\mu}\left[\vec{K}_{or} \times B_o\hat{o}_r e^{-i(\vec{K}_{or} \cdot \vec{r})} + \vec{K}_{er} \times B_e\hat{o}_e e^{-i(\vec{K}_{er} \cdot \vec{r})}\right]e^{-i\omega t} \quad (3-2-36)$$

Transmitted: $$\vec{H}_t = \frac{1}{\omega\mu}\left[\vec{K}_{ot} \times C_o\hat{o}_t e^{-i(\vec{K}_{ot} \cdot \vec{r})} + \vec{K}_{et} \times C_e\hat{e}_t e^{-i(\vec{K}_{et} \cdot \vec{r})}\right]e^{-i\omega t}, \quad (3-2-37)$$

where $\hat{o}_r$ and $\hat{o}_t$ are unit vectors of electric fields for ordinary waves in medium 1 and medium 2 and $\hat{e}_r$ and $\hat{e}_t$ are unit vectors of electric fields for extraordinary waves in medium 1 and medium 2. They are defined as

$$\hat{o}_r = \hat{c}_1 \times \hat{k}_{or}, \quad (3-2-38)$$

$$\hat{e}_r = \hat{s}_r \times \hat{o}_r, \quad (3-2-39)$$

$$\hat{o}_t = \hat{c}_2 \times \hat{k}_{ot}, \quad (3-2-40)$$

and $$\hat{e}_t = \hat{s}_t \times \hat{o}_t . \quad (3-2-41)$$

According to the phase conditions and the boundary conditions

$$\vec{K}_i \cdot \vec{r} = \vec{K}_{or} \cdot \vec{r} = \vec{K}_{er} \cdot \vec{r} = \vec{K}_{ot} \cdot \vec{r} = \vec{K}_{et} \cdot \vec{r},$$

$$\vec{E}_{ix} + \vec{E}_{rx} = \vec{E}_{tx},$$

$$\vec{E}_{iy} + \vec{E}_{ry} = \vec{E}_{ty},$$

$$\vec{H}_{iy} + \vec{H}_{rx} = \vec{H}_{tx},$$

and $\vec{H}_{iy} + \vec{H}_{ry} = \vec{H}_{ty}$.

we have

$$
\begin{aligned}
&A_s + B_o(\hat{x}\cdot\hat{o}_r) + B_e(\hat{x}\cdot\bar{r}) = C_o(\hat{x}\cdot\hat{o}_t) + C_e(\hat{x}\cdot\hat{e}_t)\\
&A_p\cos\vartheta_i + A_k\sin\vartheta_i + B_e(\hat{y}\cdot\hat{o}_r) + B_e(\hat{y}\cdot\hat{e}_r) = C_o(\hat{y}\cdot\hat{o}_t) + C_e(\hat{y}\cdot\hat{e}_t)\\
&-K_iA_p + B_o\left[\hat{x}\cdot\left(\vec{K}_{or}\times\hat{o}_r\right)\right] + B_e\left[\hat{x}\cdot\left(\vec{K}_{er}\times\hat{e}_r\right)\right] = C_o\left[\hat{x}\cdot\left(\vec{K}_{ot}\times\hat{o}_t\right)\right] + C_e\left[\hat{x}\cdot\left(\vec{K}_{et}\times\hat{e}_t\right)\right]\\
&K_iA_s\cos\vartheta_i + B_e\left[\hat{y}\cdot\left(\vec{K}_{or}\times\hat{o}_r\right)\right] + B_e\left[\hat{y}\cdot\left(\vec{K}_{er}\times\hat{e}_r\right)\right] = C_o\left[\hat{y}\cdot\left(\vec{K}_{ot}\times\hat{o}_t\right)\right] + C_e\left[\hat{y}\cdot\left(\vec{K}_{et}\times\hat{e}_t\right)\right]
\end{aligned}
\qquad (3-2-42)
$$

Let

$$
\left.
\begin{aligned}
&a = \hat{x}\cdot\hat{o}_r, \quad b = \hat{x}\cdot\hat{e}_r, \quad c = -\hat{x}\cdot\hat{o}_t, \quad d = -\hat{x}\cdot\hat{e}_t,\\
&e = \hat{y}\cdot\hat{o}_r, \quad f = \hat{y}\cdot\hat{e}_r, \quad g = \hat{y}\cdot\hat{o}_t, \quad h = \hat{y}\cdot\hat{e}_t,\\
&l = \hat{x}\cdot\left(\vec{K}_{or}\times\hat{o}_r\right), \quad m = \hat{x}\cdot\left(\vec{K}_{er}\times\hat{e}_r\right), \quad n = -\hat{x}\cdot\left(\vec{K}_{ot}\times\hat{o}_t\right), \quad o = -\hat{x}\cdot\left(\vec{K}_{et}\times\hat{e}_t\right),\\
&p = \hat{y}\cdot\left(\vec{K}_{or}\times\hat{e}_t\right), \quad q = \hat{y}\cdot\left(\vec{K}_{er}\times\hat{e}_r\right), \quad r = -\hat{y}\cdot\left(\vec{K}_{ot}\times\hat{o}_t\right), \quad s = \hat{y}\cdot\left(\vec{K}_{et}\times\hat{e}_t\right).
\end{aligned}
\right\}
\qquad (3-2-43)
$$

The equation (3-2-42) is rewritten as

$$
\left\{
\begin{aligned}
&aB_o + bB_e + cC_o + dC_e = -A_s && (3-2-44a)\\
&eB_o + fB_e + gC_o + hC_e = -A_p\cos\vartheta_i - A_k\sin\vartheta_i && (3-2-44b)\\
&lB_o + mB_e + nC_o + oC_e = K_iA_p && (3-2-44c)\\
&pB_o + qB_e + rC_o + sC_e = -K_iA_s\cos\vartheta_i \quad . && (3-2-44d)
\end{aligned}
\right.
$$

Solving equation (3-2-44), we can get the coefficients B_O, B_e,C_O and C_e as functions of A_S, A_P and A_K.

The solutions of equation (3-2-44) are the general Fresnel coefficients. which can be used in both isotropic media and uniaxial media. We have solved this equation by the MATHEMATICA symbolically and have a general solution.

It is convenient to give expressions for the coefficients B_O, B_e, C_O and C_e in the $(\hat{s}, \hat{p}, \hat{k})$ system, as defined as Figure 3.2.3.

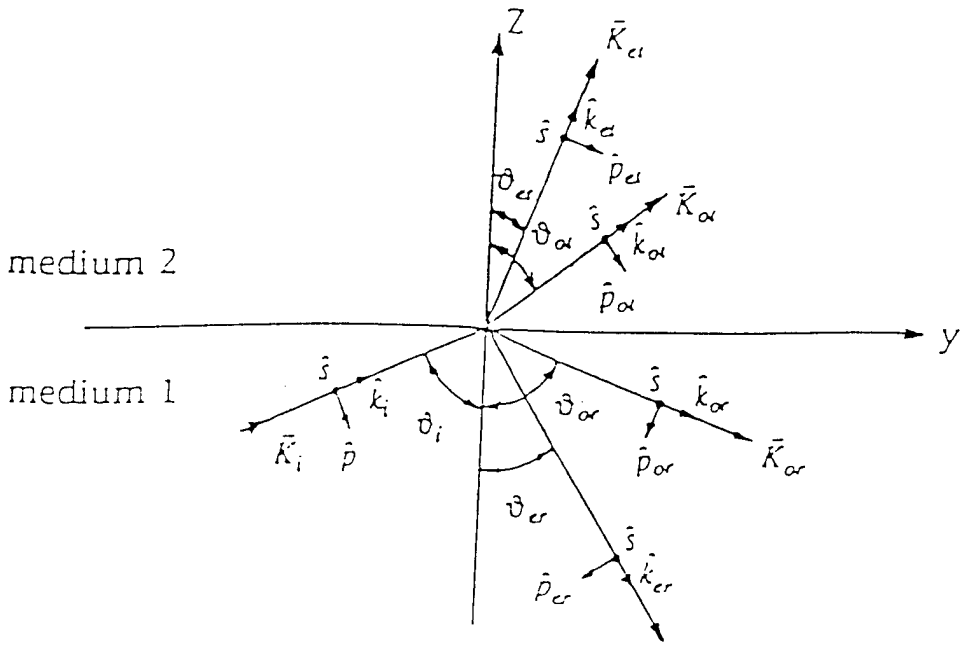

Figure 3.2.3 Reflection and refraction representation in the $(\hat{s}, \hat{p}, \hat{k})$ system.

In the $(\hat{s}, \hat{p}, \hat{k})$ system, the amplitudes of vectors $C_o\hat{o}_t, C_e\hat{e}_t, B_o\hat{o}_r$, and $B_e\hat{e}_r$ become

$$C_o = \begin{pmatrix} A^t_{os} \\ A^t_{op} \\ A^t_{ok} \end{pmatrix} = C_o \begin{pmatrix} 1 & 0 & 0 \\ 0 & \cos\vartheta_{ot} & -\sin\vartheta_{ot} \\ 0 & \sin\vartheta_{ot} & \cos\vartheta_{et} \end{pmatrix} \begin{pmatrix} o_{xt} \\ o_{yt} \\ o_{zt} \end{pmatrix} \qquad (3-2-45)$$

$$C_e = \begin{pmatrix} A^t_{es} \\ A^t_{ep} \\ A^t_{ek} \end{pmatrix} = C_e \begin{pmatrix} 1 & 0 & 0 \\ 0 & \cos\vartheta_{et} & -\sin\vartheta_{et} \\ 0 & \sin\vartheta_{et} & \cos\vartheta_{et} \end{pmatrix} \begin{pmatrix} e_{xt} \\ e_{yt} \\ e_{zt} \end{pmatrix} \qquad (3-2-46)$$

$$B_o = \begin{pmatrix} A^r_{os} \\ A^r_{op} \\ A^r_{ok} \end{pmatrix} = B_o \begin{pmatrix} 1 & 0 & 0 \\ 0 & -\cos\vartheta_{or} & -\sin\vartheta_{or} \\ 0 & \sin\vartheta_{or} & -\cos\vartheta_{or} \end{pmatrix} \begin{pmatrix} o_{xr} \\ o_{yr} \\ o_{zr} \end{pmatrix} \qquad (3-2-47)$$

$$B_e = \begin{pmatrix} A^r_{es} \\ A^r_{ep} \\ A^r_{ek} \end{pmatrix} = B_e \begin{pmatrix} 1 & 0 & 0 \\ 0 & -\cos\vartheta_{er} & -\sin\vartheta_{er} \\ 0 & \sin\vartheta_{er} & -\cos\vartheta_{er} \end{pmatrix} \begin{pmatrix} e_{xr} \\ e_{yr} \\ e_{zr} \end{pmatrix} \qquad (3-2-48)$$

Using (3-2-45), (3-2-46), (3-2-47), or (3-2-48) as a new incident field, we can use the procedure above again to calculate next surface.

3.2.3 Fresnel equation in isotropic media

In the isotropic media the equations (3-2-45)-(3-2-48) become the Fresnel equations in the isotropic media. In this case, we can choose $\hat{o}_r, \hat{o}_t, \hat{e}_r$ and $\hat{e}_t$ as shown in Figure 3.2.4, and A_K=0, $\bar{K}_{or} = \bar{K}_{er} = \bar{K}_r, \bar{K}_{ot} = \bar{K}_{et} = \bar{K}_t, K_r = K_i$. Also let

$$A_{si} = A^i_{os} + A^i_{es}, \quad A_{pi} = A^i_{op} + A^i_{ep}, \quad A_{ki} = A^i_{ok} + A^i_{ek},$$
$$A_{sr} = A^r_{os} + A^r_{es}, \quad A_{pr} = A^r_{op} + A^r_{ep}, \quad \text{and} \quad A_{kr} = A^r_{ok} + A^r_{ek}.$$

These yield the following evaluations:

$$a = 1, \quad b = 0, \quad c = -1, \quad d = 0,$$
$$e = 0, \quad f = -\cos\vartheta_i, \quad g = 0, \quad h = -\cos\vartheta_i,$$
$$l = 0, \quad m = -K_i \quad n = 0, \quad o = K_t,$$
$$p = -K_i\cos\vartheta_i, \quad q = 0, \quad r = -K_i\cos\vartheta_t, \quad s = 0.$$

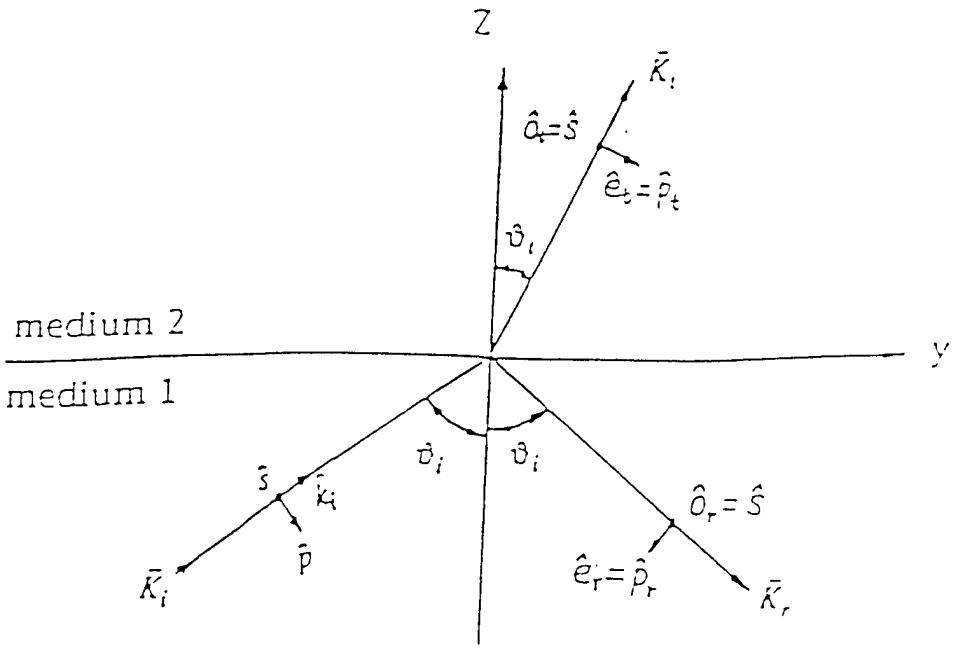

Figure 3.2.4 Reflection and refraction in isotropic media.

Equation (3-2-44) becomes

$$\begin{pmatrix} 1 & 0 & -1 & 0 \\ 0 & -\cos\vartheta_i & 0 & \cos\vartheta_t \\ 0 & -K_i & 0 & K_t \\ -K_i\cos\vartheta_i & 0 & -K_t\cos\vartheta_t & 0 \end{pmatrix} \begin{pmatrix} B_o \\ B_e \\ C_o \\ C_e \end{pmatrix} = \begin{pmatrix} -A_s \\ -A_p\cos\vartheta_i \\ K_tA_p \\ -K_iA_s\cos\vartheta_i \end{pmatrix}$$

Solving these equations, we have

$$C_o = \frac{2K_i\cos\vartheta_i}{K_i\cos\vartheta_i + K_t\cos\vartheta_t}A_s,$$

$$C_e = \frac{2K_i\cos\vartheta_i}{K_i\cos\vartheta_t + K_t\cos\vartheta_i}A_p,$$

$$B_o = \frac{K_i\cos\vartheta_i - K_t\cos\vartheta_t}{K_i\cos\vartheta_i + K_t\cos\vartheta_t}A_s,$$

$$B_e = \frac{K_t\cos\vartheta_i - K_i\cos\vartheta_t}{K_t\cos\vartheta_i + K_i\cos\vartheta_t}A_p \quad .$$

Bringing all those into equations (3-2-45)-(3-2-48), we get the Fresnel equations in isotropic media as

$$A_{st} = \frac{2K_i\cos\vartheta_i}{K_i\cos\vartheta_i + K_t\cos\vartheta_t}A_s,$$

$$A_{pt} = \frac{2K_i\cos\vartheta_i}{K_i\cos\vartheta_t + K_t\cos\vartheta_i}A_p,$$

$$A_{sr} = \frac{K_i\cos\vartheta_i - K_t\cos\vartheta_t}{K_i\cos\vartheta_i + K_t\cos\vartheta_t}A_s,$$

$$A_{pr} = \frac{K_t\cos\vartheta_i - K_i\cos\vartheta_t}{K_t\cos\vartheta_i + K_i\cos\vartheta_t}A_p \quad .$$

This is just a special case of the result we found in section 3.2.2.

The three-dimensional refraction model derived here allows us to calculate the amplitudes and directions of rays in arbitrary uniaxial and/or homogeneous dielectric systems. The algorithm here reaches the same result with McClain and Chipman's(McClain 1992) ,who took ray tracing approach. We believe this approach, due to Gu and Yeh(Gu 1993), is somewhat easier to understand or more physical than the ray tracing approach, By making them of equal generality, we create a viable choice for users.

3.3 Modified NIST Model

Suppose we have a Pockels cell shown in Figure 3.3.1, in which optical axis is at vertical direction.

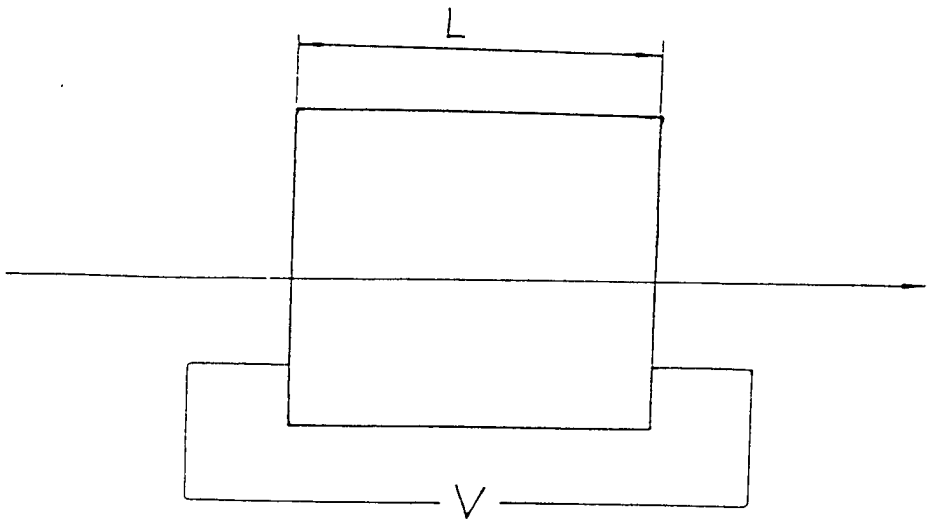

Figure 3.3.1 Pockels cell with applied voltage V.

When light is incident along axis direction, we have

$$\Delta n = n_e - n_o = \lambda \alpha E, \qquad (3\text{-}3\text{-}1)$$

$$\phi = 2\pi \alpha E L, \qquad (3\text{-}3\text{-}2)$$

$$V_{1/2} = 1/(2\alpha), \qquad (3\text{-}3\text{-}3)$$

where Δn is change of refractive index, λ is wavelength of incident light, E is electric field applied, α is Pockels coefficient, ϕ is phase shift, and $V_{1/2}$ is half-

wave voltage. The output through this Pockels cell with a pair of across polarizers is

$$T = \sin^2[\frac{\pi}{2}(\frac{V}{V_{\pi/2}})]. \qquad (3\text{-}3\text{-}4)$$

If light incident at vertical angle of θ, the change of refractive index becomes

$$\Delta n = n_e(\theta) - n_o. \qquad (3\text{-}3\text{-}5)$$

where $n_e(\theta)$ satisfies

$$\frac{1}{n_e^2(\theta)} = \frac{\cos^2\theta}{n_e^2} + \frac{\sin^2(\theta)}{n_o^2} .$$

so we have

$$\Delta n = \sqrt{\frac{n_e^2 n_o^2}{n_o^2\cos^2\theta + n_e^2\sin^2\theta}} - n_o . \qquad (3\text{-}3\text{-}6)$$

Comparing (3-3-6) with (3-3-1), we introduce a new coefficient, modified Pockels coefficient , as

$$\alpha' = \frac{\sqrt{\frac{n_e^2 n_o^2}{n_o^2\cos^2\theta + n_e^2\sin^2\theta}} - n_o}{n_e - n_o}\alpha . \qquad (3\text{-}3\text{-}7)$$

So we have following new equations:

$$\Delta n = \lambda\alpha' E, \qquad (3\text{-}3\text{-}8)$$

$$\phi = 2\pi\alpha' EL, \qquad (3\text{-}3\text{-}9)$$

$$V'_{1/2} = 1/(2\alpha'), \qquad (3\text{-}3\text{-}10)$$

$$T = \sin^2[\frac{\pi}{2}(\frac{V}{V'_{1/2}})]. \qquad (3\text{-}3\text{-}11)$$

If light incident at a horizontal angle, Δn is still the same as with light incident on axis. So the output still is

$$T = \sin^2[\frac{\pi}{2}(\frac{V}{V_{1/2}})]. \qquad (3\text{-}3\text{-}12)$$

Combining (3-3-11) and (3-3-12) for these two cases, we have an equation for a Pockels cell with a pair of crossed polarizers as

$$T = \sin^2[\frac{\pi}{2}(\frac{V}{V'_{1/2}})]. \qquad (3\text{-}3\text{-}13)$$

where

$$V'_{1/2} = \frac{1}{2\alpha}\cdot\frac{n_e - n_o}{\sqrt{\frac{n_e^2 n_o^2}{n_o^2\cos^2\theta + n_e^2\sin^2\theta}} - n_o} \qquad (3\text{-}3\text{-}14)$$

$$= V_{1/2}\cdot\frac{n_e - n_o}{\sqrt{\frac{n_e^2 n_o^2}{n_o^2\cos^2\theta + n_e^2\sin^2\theta}} - n_o}. \qquad (3\text{-}3\text{-}15)$$

Considering reflection loss at two surfaces, we add a transmission coefficient, T_c, derived from Fresnel equations[58] to the equation (3-3-13). This transmission coefficient satisfies approximately

$$T_c = \left(\frac{n_{ave}\cos(\theta_t)}{\cos(\theta_i)}\right)^2\left(\frac{2\sin(\theta_t)\cos(\theta_i)}{\sin(\theta_i + \theta_t)}\right)^4, \qquad (3\text{-}3\text{-}16)$$

where $n_{ave}=(n_e+n_o)/2$, $\theta_i= \sqrt{\theta^2 + \phi^2}$, and $\theta_t= \arcsin(1/n_{ave} \cdot \sin(\theta_i))$. Combining this with equation (3-3-13), we have a general equation for a Pockels cell with a pair of crossed polarizers as

$$T = T_c \sin^2[\frac{\pi}{2}(\frac{V}{V'_{\frac{1}{2}}})] \ . \qquad (3\text{-}3\text{-}17)$$

While this general equation integrates Fresnel reflections and birefrigent effect together, it is a more accurate model for Pockels cell than NIST model.

We applied equation (3-3-17) to two Pockels cells, as shown in Figure 3.3.2 and Figure 3.3.3. The first one, Case-a, is a model of converging beams through a Pockels cell. The second, Case-b, is a model of converging beams through a reflected Pockels cell. Both Pockels cells use KDP materials, whose n_e is 1.467 and n_o is 1.507. Incident converging beams for the first model have angular ranges of θ = -45° ~ +45° and ϕ = -45°~+45°. But incident converging beams for the reflected Pockels cell have angular ranges of θ = 0~45° and ϕ = -45°~+45°.

Following tables are computer simulation results of Pockels cells. Table 2 contains intensity values of 11x11 incident beams with incident angles of θ = -45° ~ +45° and ϕ = -45°~+45° for Case-a. Table 8 contains intensity values of 11x11 incident beams with incident angles of θ = 0° ~ +45° and ϕ = -45°~+45° for Case-b. Table 3 ~ Table 7 are output results for Case-a, each of which

contains relative intensity values(modulation) of 11x11 output beams with output angles of θ = -45° ~ +45° and ϕ = -45°~+45° for different applied voltage V. In the same way, Table 9 ~ Table 13 are the results for Case-b. These results

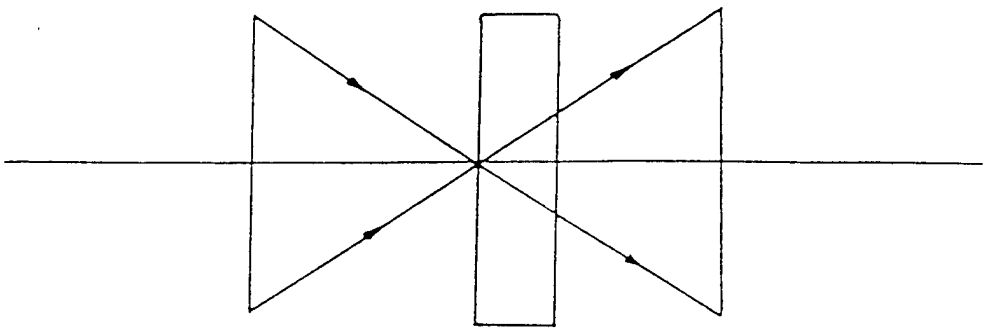

Figure 3.3.2 Case-a: converging beams through a Pockels cell

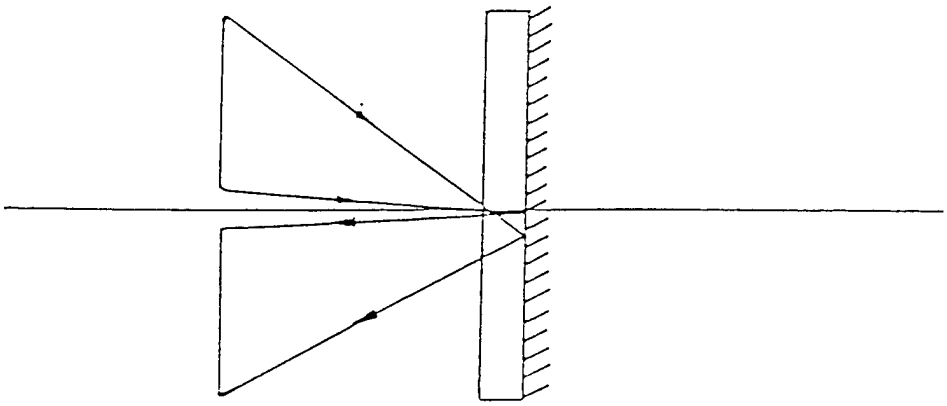

Figure 3.3.3 Case-b: converging beams through a reflected Pockels cell

apparently show that the combination of Fresnel reflections and angular birefringent effects reduces the modulation and limits the field of view of a Pockels cell. Reflected Pockels cell (CAse-b) only need half of applied voltage to reach its best modulation. Last two tables, Table 14 and Table 15, are output results without Fresnel reflection losses for Case-a and Case-b. These results are achieved through equation (3-3-13). Comparing these two tables with Table 7 and Table 11, we can conclude that Fresnel reflections have significant contribution to limit field of view.

Figure 3.3.4 and Figure 3.3.5 are 3-D visuallized charts for data of Table 7 and Table 11. These figures clearly show that modulation is reduced as angular fields are increased.

Table 2 Incident beams with angles of $\theta = -45° \sim +45°$ and $\varphi = -45° \sim +45°$

1.00	1.00	1.00	1.00	1.00	1.00	1.00	1.00	1.00	1.00	1.00
1.00	1.00	1.00	1.00	1.00	1.00	1.00	1.00	1.00	1.00	1.00
1.00	1.00	1.00	1.00	1.00	1.00	1.00	1.00	1.00	1.00	1.00
1.00	1.00	1.00	1.00	1.00	1.00	1.00	1.00	1.00	1.00	1.00
1.00	1.00	1.00	1.00	1.00	1.00	1.00	1.00	1.00	1.00	1.00
1.00	1.00	1.00	1.00	1.00	1.00	1.00	1.00	1.00	1.00	1.00
1.00	1.00	1.00	1.00	1.00	1.00	1.00	1.00	1.00	1.00	1.00
1.00	1.00	1.00	1.00	1.00	1.00	1.00	1.00	1.00	1.00	1.00
1.00	1.00	1.00	1.00	1.00	1.00	1.00	1.00	1.00	1.00	1.00
1.00	1.00	1.00	1.00	1.00	1.00	1.00	1.00	1.00	1.00	1.00
1.00	1.00	1.00	1.00	1.00	1.00	1.00	1.00	1.00	1.00	1.00

Table 3 Output beams with applied voltage V=0 for Case-a

0.00	0.00	0.00	0.00	0.00	0.00	0.00	0.00	0.00	0.00	0.00
0.00	0.00	0.00	0.00	0.00	0.00	0.00	0.00	0.00	0.00	0.00
0.00	0.00	0.00	0.00	0.00	0.00	0.00	0.00	0.00	0.00	0.00
0.00	0.00	0.00	0.00	0.00	0.00	0.00	0.00	0.00	0.00	0.00
0.00	0.00	0.00	0.00	0.00	0.00	0.00	0.00	0.00	0.00	0.00
0.00	0.00	0.00	0.00	0.00	0.00	0.00	0.00	0.00	0.00	0.00
0.00	0.00	0.00	0.00	0.00	0.00	0.00	0.00	0.00	0.00	0.00
0.00	0.00	0.00	0.00	0.00	0.00	0.00	0.00	0.00	0.00	0.00
0.00	0.00	0.00	0.00	0.00	0.00	0.00	0.00	0.00	0.00	0.00
0.00	0.00	0.00	0.00	0.00	0.00	0.00	0.00	0.00	0.00	0.00
0.00	0.00	0.00	0.00	0.00	0.00	0.00	0.00	0.00	0.00	0.00

Table 4 Output beams with applied voltage V=1/4 $V_{1/2}$ for Case-a

0.02	0.03	0.03	0.03	0.03	0.03	0.03	0.03	0.03	0.03	0.02
0.05	0.05	0.06	0.06	0.06	0.06	0.06	0.06	0.06	0.05	0.05
0.07	0.08	0.08	0.08	0.09	0.09	0.09	0.08	0.08	0.08	0.07
0.10	0.10	0.11	0.11	0.11	0.11	0.11	0.11	0.11	0.10	0.10
0.12	0.12	0.13	0.13	0.13	0.13	0.13	0.13	0.13	0.12	0.12
0.12	0.13	0.13	0.13	0.13	0.13	0.13	0.13	0.13	0.13	0.12
0.12	0.12	0.13	0.13	0.13	0.13	0.13	0.13	0.13	0.12	0.12
0.10	0.10	0.11	0.11	0.11	0.11	0.11	0.11	0.11	0.10	0.10
0.07	0.08	0.08	0.08	0.09	0.09	0.09	0.08	0.08	0.08	0.07
0.05	0.05	0.06	0.06	0.06	0.06	0.06	0.06	0.06	0.05	0.05
0.02	0.03	0.03	0.03	0.03	0.03	0.03	0.03	0.03	0.03	0.02

Table 5 Output beams with applied voltage V=1/2 $V_{1/2}$ for Case-a

0.10	0.11	0.12	0.12	0.13	0.13	0.13	0.12	0.12	0.11	0.10
0.18	0.20	0.21	0.21	0.22	0.22	0.22	0.21	0.21	0.20	0.18
0.27	0.29	0.30	0.31	0.31	0.31	0.31	0.31	0.30	0.29	0.27
0.35	0.37	0.38	0.39	0.39	0.39	0.39	0.39	0.38	0.37	0.35
0.40	0.42	0.43	0.44	0.44	0.44	0.44	0.44	0.43	0.42	0.40
0.41	0.44	0.45	0.46	0.46	0.46	0.46	0.46	0.45	0.44	0.41
0.40	0.42	0.43	0.44	0.44	0.44	0.44	0.44	0.43	0.42	0.40
0.35	0.37	0.38	0.39	0.39	0.39	0.39	0.39	0.38	0.37	0.35
0.27	0.29	0.30	0.31	0.31	0.31	0.31	0.31	0.30	0.29	0.27
0.18	0.20	0.21	0.21	0.22	0.22	0.22	0.21	0.21	0.20	0.18
0.10	0.11	0.12	0.12	0.13	0.13	0.13	0.12	0.12	0.11	0.10

Table 6 Output beams with applied voltage V=3/4 $V_{1/2}$ for Case-a

0.20	0.23	0.25	0.26	0.26	0.27	0.26	0.26	0.25	0.23	0.20
0.36	0.39	0.41	0.42	0.43	0.43	0.43	0.42	0.41	0.39	0.36
0.51	0.54	0.57	0.58	0.59	0.59	0.59	0.58	0.57	0.54	0.51
0.62	0.66	0.68	0.69	0.70	0.70	0.70	0.69	0.68	0.66	0.62
0.69	0.72	0.75	0.76	0.77	0.77	0.77	0.76	0.75	0.72	0.69
0.71	0.74	0.77	0.78	0.79	0.78	0.79	0.78	0.77	0.74	0.71
0.69	0.72	0.75	0.76	0.77	0.77	0.77	0.76	0.75	0.72	0.69
0.62	0.66	0.68	0.69	0.70	0.70	0.70	0.69	0.68	0.66	0.62
0.51	0.54	0.57	0.58	0.59	0.59	0.59	0.58	0.57	0.54	0.51
0.36	0.39	0.41	0.42	0.43	0.43	0.43	0.42	0.41	0.39	0.36
0.20	0.23	0.25	0.26	0.26	0.27	0.26	0.26	0.25	0.23	0.20

Table 7 Output beams with applied voltage V=$V_{1/2}$ for Case-a

0.32	0.37	0.40	0.42	0.43	0.43	0.43	0.42	0.40	0.37	0.32
0.54	0.59	0.62	0.64	0.65	0.65	0.65	0.64	0.62	0.59	0.54
0.70	0.75	0.78	0.80	0.81	0.81	0.81	0.80	0.78	0.75	0.70
0.79	0.84	0.87	0.88	0.89	0.90	0.89	0.88	0.87	0.84	0.79
0.82	0.87	0.89	0.91	0.92	0.92	0.92	0.91	0.89	0.87	0.82
0.83	0.87	0.90	0.91	0.92	0.91	0.92	0.91	0.90	0.87	0.83
0.82	0.87	0.89	0.91	0.92	0.92	0.92	0.91	0.89	0.87	0.82
0.79	0.84	0.87	0.88	0.89	0.90	0.89	0.88	0.87	0.84	0.79
0.70	0.75	0.78	0.80	0.81	0.81	0.81	0.80	0.78	0.75	0.70
0.54	0.59	0.62	0.64	0.65	0.65	0.65	0.64	0.62	0.59	0.54
0.32	0.37	0.40	0.42	0.43	0.43	0.43	0.42	0.40	0.37	0.32

Table 8 Incident beams with angles of $\theta = 0° \sim +45°$ and $\phi = -45° \sim +45°$

1.00	1.00	1.00	1.00	1.00	1.00	1.00	1.00	1.00	1.00	1.00
1.00	1.00	1.00	1.00	1.00	1.00	1.00	1.00	1.00	1.00	1.00
1.00	1.00	1.00	1.00	1.00	1.00	1.00	1.00	1.00	1.00	1.00
1.00	1.00	1.00	1.00	1.00	1.00	1.00	1.00	1.00	1.00	1.00
1.00	1.00	1.00	1.00	1.00	1.00	1.00	1.00	1.00	1.00	1.00
1.00	1.00	1.00	1.00	1.00	1.00	1.00	1.00	1.00	1.00	1.00
1.00	1.00	1.00	1.00	1.00	1.00	1.00	1.00	1.00	1.00	1.00
1.00	1.00	1.00	1.00	1.00	1.00	1.00	1.00	1.00	1.00	1.00
1.00	1.00	1.00	1.00	1.00	1.00	1.00	1.00	1.00	1.00	1.00
1.00	1.00	1.00	1.00	1.00	1.00	1.00	1.00	1.00	1.00	1.00
1.00	1.00	1.00	1.00	1.00	1.00	1.00	1.00	1.00	1.00	1.00

Table 9 Output beams with applied voltage V=0 for Case-b

0.00	0.00	0.00	0.00	0.00	0.00	0.00	0.00	0.00	0.00	0.00
0.00	0.00	0.00	0.00	0.00	0.00	0.00	0.00	0.00	0.00	0.00
0.00	0.00	0.00	0.00	0.00	0.00	0.00	0.00	0.00	0.00	0.00
0.00	0.00	0.00	0.00	0.00	0.00	0.00	0.00	0.00	0.00	0.00
0.00	0.00	0.00	0.00	0.00	0.00	0.00	0.00	0.00	0.00	0.00
0.00	0.00	0.00	0.00	0.00	0.00	0.00	0.00	0.00	0.00	0.00
0.00	0.00	0.00	0.00	0.00	0.00	0.00	0.00	0.00	0.00	0.00
0.00	0.00	0.00	0.00	0.00	0.00	0.00	0.00	0.00	0.00	0.00
0.00	0.00	0.00	0.00	0.00	0.00	0.00	0.00	0.00	0.00	0.00
0.00	0.00	0.00	0.00	0.00	0.00	0.00	0.00	0.00	0.00	0.00
0.00	0.00	0.00	0.00	0.00	0.00	0.00	0.00	0.00	0.00	0.00

Table 10 Output beams with applied voltage V=1/4 $V_{1/2}$ for Case-b

0.41	0.44	0.45	0.46	0.46	0.46	0.46	0.46	0.45	0.44	0.41
0.41	0.43	0.44	0.45	0.46	0.46	0.46	0.45	0.44	0.43	0.41
0.40	0.42	0.43	0.44	0.44	0.44	0.44	0.44	0.43	0.42	0.40
0.37	0.40	0.41	0.42	0.42	0.42	0.42	0.42	0.41	0.40	0.37
0.35	0.37	0.38	0.39	0.39	0.39	0.39	0.39	0.38	0.37	0.35
0.31	0.33	0.34	0.35	0.35	0.35	0.35	0.35	0.34	0.33	0.31
0.27	0.29	0.30	0.31	0.31	0.31	0.31	0.31	0.30	0.29	0.27
0.22	0.24	0.25	0.26	0.26	0.26	0.26	0.26	0.25	0.24	0.22
0.18	0.20	0.21	0.21	0.22	0.22	0.22	0.21	0.21	0.20	0.18
0.13	0.15	0.16	0.17	0.17	0.17	0.17	0.17	0.16	0.15	0.13
0.10	0.11	0.12	0.12	0.13	0.13	0.13	0.12	0.12	0.11	0.10

Table 11 Output beams with applied voltage V=1/2 $V_{1/2}$ for Case-b

0.83	0.87	0.90	0.91	0.92	0.91	0.92	0.91	0.90	0.87	0.83
0.83	0.87	0.90	0.91	0.92	0.92	0.92	0.91	0.90	0.87	0.83
0.82	0.87	0.89	0.91	0.92	0.92	0.92	0.91	0.89	0.87	0.82
0.81	0.86	0.89	0.90	0.91	0.91	0.91	0.90	0.89	0.86	0.81
0.79	0.84	0.87	0.88	0.89	0.90	0.89	0.88	0.87	0.84	0.79
0.75	0.80	0.83	0.85	0.86	0.86	0.86	0.85	0.83	0.80	0.75
0.70	0.75	0.78	0.80	0.81	0.81	0.81	0.80	0.78	0.75	0.70
0.63	0.68	0.71	0.73	0.74	0.74	0.74	0.73	0.71	0.68	0.63
0.54	0.59	0.62	0.64	0.65	0.65	0.65	0.64	0.62	0.59	0.54
0.43	0.48	0.51	0.53	0.54	0.54	0.54	0.53	0.51	0.48	0.43
0.32	0.37	0.40	0.42	0.43	0.43	0.43	0.42	0.40	0.37	0.32

Table 12 Output beams with applied voltage V=3/4 $V_{1/2}$ for Case-b

0.42	0.44	0.45	0.46	0.46	0.46	0.46	0.46	0.45	0.44	0.42
0.43	0.45	0.46	0.47	0.47	0.48	0.47	0.47	0.46	0.45	0.43
0.46	0.48	0.50	0.51	0.51	0.51	0.51	0.51	0.50	0.48	0.46
0.51	0.54	0.56	0.57	0.57	0.57	0.57	0.57	0.56	0.54	0.51
0.57	0.61	0.63	0.64	0.65	0.65	0.65	0.64	0.63	0.61	0.57
0.64	0.68	0.71	0.72	0.73	0.74	0.73	0.72	0.71	0.68	0.64
0.70	0.75	0.78	0.80	0.81	0.81	0.81	0.80	0.78	0.75	0.70
0.73	0.79	0.83	0.85	0.86	0.87	0.86	0.85	0.83	0.79	0.73
0.72	0.79	0.83	0.86	0.87	0.87	0.87	0.86	0.83	0.79	0.72
0.66	0.73	0.78	0.81	0.82	0.83	0.82	0.81	0.78	0.73	0.66
0.55	0.62	0.67	0.70	0.72	0.72	0.72	0.70	0.67	0.62	0.55

Table 13 Output beams with applied voltage V=$V_{1/2}$ for Case-b

0.00	0.00	0.00	0.00	0.00	0.00	0.00	0.00	0.00	0.00	0.00
0.00	0.00	0.00	0.00	0.00	0.00	0.00	0.00	0.00	0.00	0.00
0.00	0.00	0.01	0.01	0.01	0.01	0.01	0.01	0.01	0.00	0.00
0.02	0.02	0.02	0.02	0.03	0.03	0.03	0.02	0.02	0.02	0.02
0.07	0.07	0.07	0.07	0.07	0.07	0.07	0.07	0.07	0.07	0.07
0.15	0.16	0.16	0.17	0.17	0.17	0.17	0.17	0.16	0.16	0.15
0.27	0.29	0.30	0.31	0.31	0.31	0.31	0.31	0.30	0.29	0.27
0.41	0.44	0.47	0.48	0.48	0.49	0.48	0.48	0.47	0.44	0.41
0.54	0.60	0.63	0.65	0.66	0.66	0.66	0.65	0.63	0.60	0.54
0.63	0.70	0.75	0.77	0.79	0.79	0.79	0.77	0.75	0.70	0.63
0.63	0.72	0.77	0.81	0.82	0.83	0.82	0.81	0.77	0.72	0.63

Table 14 Output beams without Fresnel reflections at $V=V_{1/2}$ for Case-a

0.52	0.52	0.52	0.52	0.52	0.52	0.52	0.52	0.52	0.52	0.52
0.75	0.75	0.75	0.75	0.75	0.75	0.75	0.75	0.75	0.75	0.75
0.90	0.90	0.90	0.90	0.90	0.90	0.90	0.90	0.90	0.90	0.90
0.98	0.98	0.98	0.98	0.98	0.98	0.98	0.98	0.98	0.98	0.98
1.00	1.00	1.00	1.00	1.00	1.00	1.00	1.00	1.00	1.00	1.00
1.00	1.00	1.00	1.00	1.00	1.00	1.00	1.00	1.00	1.00	1.00
1.00	1.00	1.00	1.00	1.00	1.00	1.00	1.00	1.00	1.00	1.00
0.98	0.98	0.98	0.98	0.98	0.98	0.98	0.98	0.98	0.98	0.98
0.90	0.90	0.90	0.90	0.90	0.90	0.90	0.90	0.90	0.90	0.90
0.75	0.75	0.75	0.75	0.75	0.75	0.75	0.75	0.75	0.75	0.75
0.52	0.52	0.52	0.52	0.52	0.52	0.52	0.52	0.52	0.52	0.52

Table 15 Output beams without Fresnel reflections at $V=1/2\ V_{1/2}$ for Case-b

1.00	1.00	1.00	1.00	1.00	1.00	1.00	1.00	1.00	1.00	1.00
1.00	1.00	1.00	1.00	1.00	1.00	1.00	1.00	1.00	1.00	1.00
1.00	1.00	1.00	1.00	1.00	1.00	1.00	1.00	1.00	1.00	1.00
0.99	0.99	0.99	0.99	0.99	0.99	0.99	0.99	0.99	0.99	0.99
0.98	0.98	0.98	0.98	0.98	0.98	0.98	0.98	0.98	0.98	0.98
0.95	0.95	0.95	0.95	0.95	0.95	0.95	0.95	0.95	0.95	0.95
0.90	0.90	0.90	0.90	0.90	0.90	0.90	0.90	0.90	0.90	0.90
0.84	0.84	0.84	0.84	0.84	0.84	0.84	0.84	0.84	0.84	0.84
0.75	0.75	0.75	0.75	0.75	0.75	0.75	0.75	0.75	0.75	0.75
0.64	0.64	0.64	0.64	0.64	0.64	0.64	0.64	0.64	0.64	0.64
0.52	0.52	0.52	0.52	0.52	0.52	0.52	0.52	0.52	0.52	0.52

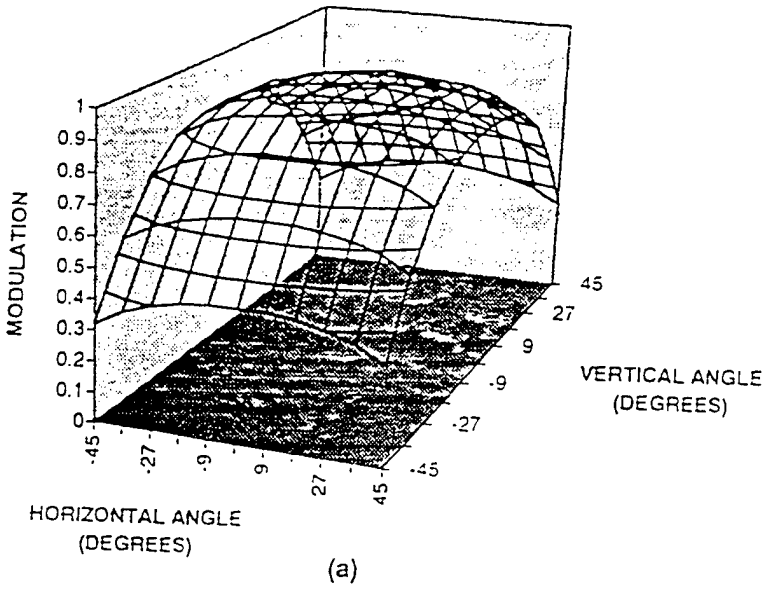

(a)

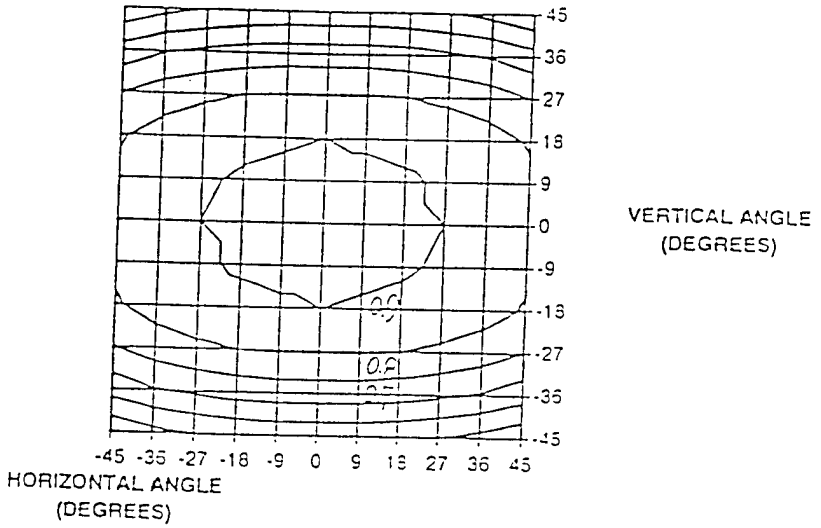

(b)

Figure 3.3.4 Output beams through a Pockels cell at applied voltage $V = V_{1/2}$. Both show transmission vs angle.

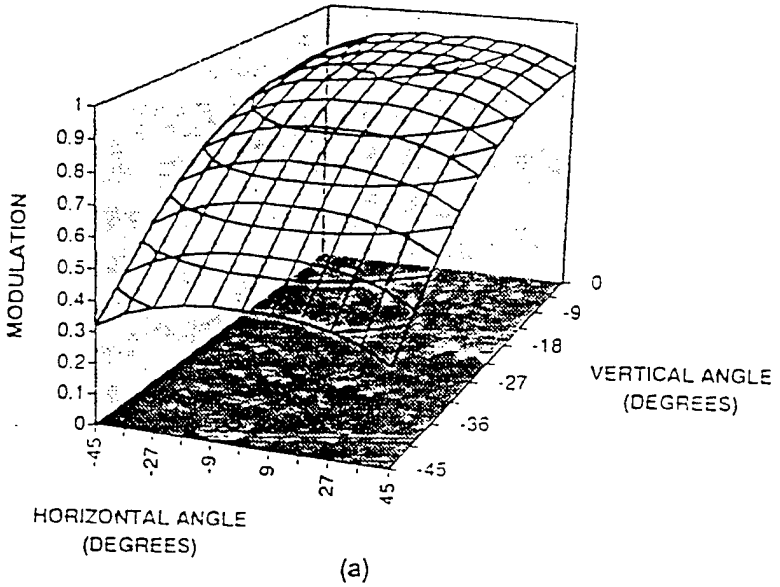

(a)

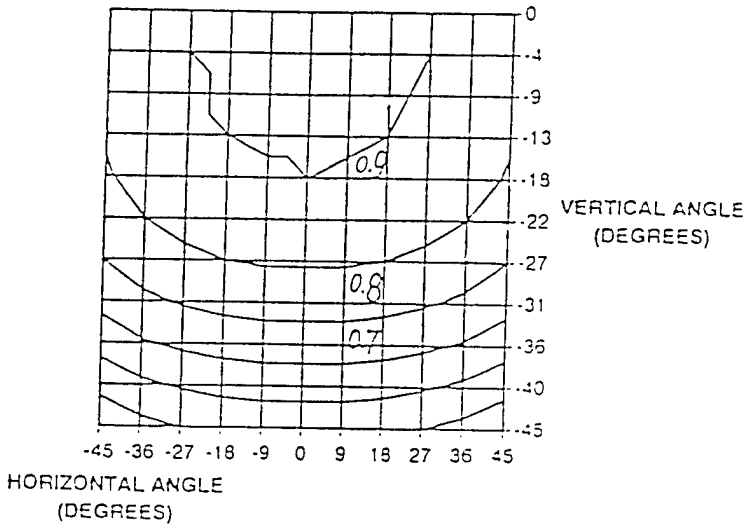

(b)

Figure 3.3.5 Output beams through a reflective Pockels cell at applied voltage V= 1/2 $V_{1/2}$. Both show transmission vs angle.

CHAPTER IV

FIELD OF VIEW

4.1 Definition of FOV and Current State of FOV in EO modulator

Manufacturers list it. Scientists talk about it. But few of them really define the FOV (field of view) of a modulator. Here we offer some serviceable concepts. FOV can be given in solid angle or linear angle as we may prefer.

Suppose we plot the transmission vs. linear angle for a modulator. From such a curve, we can pick some definition such as the full width at half maximum. We call this the transmission angular FOV, $\Delta\theta_t$.

We can also plot the depth of modulation vs. angle. In a similar way, we can define a modulation FOV, $\Delta\theta_m$.

As both are important, we can define an effective angular FOV,

$$\Delta\theta_E = min\,(\Delta\theta_t,\ \Delta\theta_m).$$

This, of course, is the fuzzy AND operation. We must have both good $\Delta\theta_t$ AND good $\Delta\theta_m$ out to $\Delta\theta_E$.

4.2 Thickness Effect

Suppose we choose the crystal axis perpendicular to the plane of incidence. In this case, the index of refraction for the extraordinary wave always is a constant (n_e) in any incident angle(Collette 1993). As shown in Figure 4.2.1, the optical path difference between ordinary wave and extraordinary wave at incident angle θ is

$$(OPD)_\theta = n_e l_e - n_0 l_0 - x, \qquad (4\text{-}2\text{-}1)$$

where n_e, l_e, n_o, l_o, and x are shown in Figure 4.2.1.

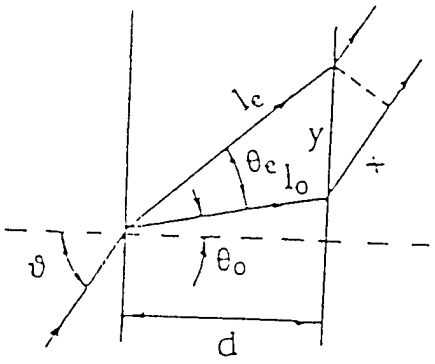

Figure 4.2.1 Light incident an uniaxial crystal at an angle θ.

According to Figure 4.2.1, x is given as

$$x = y\sin\theta = \sqrt{l_e^2 + l_0^2 - 2l_e l_0\cos(\theta_e - \theta_0)}\sin\theta. \qquad (4\text{-}2\text{-}2)$$

Suppose θ_e, θ_0, and θ are small. We have

$$\theta_e \cong \theta/n_e,$$

$$\theta_0 \cong \theta/n_o,$$

$$x \cong (l_e - l_o)\,\theta.$$

So equations (4-2-2) and (4-2-1) become:

$$\begin{aligned} x &= \left[\frac{d}{\cos(\theta/n_e)} - \frac{d}{\cos(\theta/n_0)}\right]\theta \\ &= \left[d\left(1 + \frac{\theta^2}{2n_e^2}\right) - d\left(1 + \frac{\theta^2}{2n_0^2}\right)\right]\theta \\ &= \frac{\theta^3 d}{2n_e^2 n_0^2}\left(n_0^2 - n_e^2\right), \end{aligned} \qquad (4\text{-}2\text{-}3)$$

$$(OPD)_\theta = \left[\frac{n_e d}{\cos(\theta/n_e)} - \frac{n_0 d}{\cos(\theta/n_0)}\right] - \frac{\theta^3 d}{2n_e^2 n_0^2}(n_0^2 - n_e^2)$$

$$= \left[n_e d\left(1 + \frac{\theta^2}{2n_e^2}\right) - n_0 d\left(1 + \frac{\theta^2}{2n_0^2}\right)\right] - \frac{\theta^3 d}{2n_e^2 n_0^2}(n_0^2 - n_e^2)$$

$$= (n_e - n_0)d + \frac{\theta^2 d}{2n_e n_0}(n_0 - n_e) - \frac{\theta^3 d}{2n_e^2 n_0^2}(n_0^2 - n_e^2). \qquad (4-2-4)$$

The difference between $(OPD)_\theta$ for off-axis and $(OPD)_N$ for normal or on-axis is

$$(OPD)_\theta - (OPD)_N = \frac{\theta^2 d}{2n_e n_0}(n_0 - n_e) - \frac{\theta^3 d}{2n_0^2 n_e^2}(n_0^2 - n_e^2) \qquad (4-2-5)$$

For the crystal axis parallel the incident plane, we have similar result as

$$(OPD)_\theta - (OPD)_N = \frac{\theta^2 d}{2n_\theta n_0}(n_\theta - n_0) - \frac{\theta^3 d}{2n_0^2 n_\theta^2}(n_0^2 - n_\theta^2). \qquad (4-2-6)$$

But the index of refractive n_θ varies with incident angle here. We can simplify the equations (4-2-5) and (4-2-6) further to obtain

$$(OPD)_\theta - (OPD)_N = C\,d\,, \qquad (4-2-7)$$

where C is a constant which is equal to either

$$\frac{\theta^2}{2n_e n_0}(n_0 - n_e) - \frac{\theta^3}{2n_0^2 n_e^2}(n_0^2 - n_e^2)$$

for the crystal axis perpendicular to the incident plane or

$$\frac{\theta^2}{2 n_\theta n_0}\left(n_0 - n_0\right) - \frac{\theta^3}{2 n_0^2 n_\theta^2}\left(n_0^2 - n_0^2\right)$$

for the crystal axis parallel the incident plane. Note that C only depends on the material's properties. Equation (4-2-7) explicitly shows that the difference between $(OPD)_\theta$ for off-axis and $(OPD)_N$ for on-axis is linearly dependent on the material thickness d. Based on this, we can reduce the off-axis effects of electro-optic materials (like Pockels cells) by reducing the thickness of the material. So the thinner the electro-optic modulators the better their FOVs. This is what happens with Pockels cells. The limit occurs when the crystal becomes so thin that the half-wave voltage applied across the crystal reaches the breakdown field.

4.3 Extended FOV

We may want a linear angular field of view of $m\Delta\theta_E$, where m>1 and $\Delta\theta_E$ is what our material allows us to achieve in a conventional modulator. We may also want an aperture A for this modulator. In a diffraction-limited optical system, the product

$$T = m\Delta\theta_E A$$

is conserved. This is variously called throughput conservation(Gabor 1961), etendue conservation, or the Rayleigh invariant. Thus if we place a modulator of aperture mA in the m magnified image of the input to our modulator box, that modulator only needs a field of view $\Delta\theta_E$.

From the points of view of input and output to the box, see Figure 4.3.1, the modulator has aperture A and FOV $m\Delta\theta_E$. Yet from the point of view of the Pockels material, it has aperture mA and FOV $\Delta\theta_E$. By hypothesis, the material can do this. The two field flattening lenses play a critical role in this system. Each field flattening lens is placed at the image plane of the input plane (A) or output plane. They bend the off-axis rays back to on-axis or close to on-axis. Thus all beams fill the $\Delta\theta_E$ of FOV. This also allows any polarizer, analyzer, and Pockels cell sitting between these two field flattening lenses to operate approximately on-axis. Polarizers do not work well off-axis[56]. This system should give better contrast for off-axis beams than would any conceivable Pockels cell of area A. Thus, for a given

field of view, this new configuration also improves contrast. Of course, this method requires that the polarizer be placed next to the first field lens and the analyzer be placed before the second lens to minimize the range of angles they encounter and thus achieve high contrast.

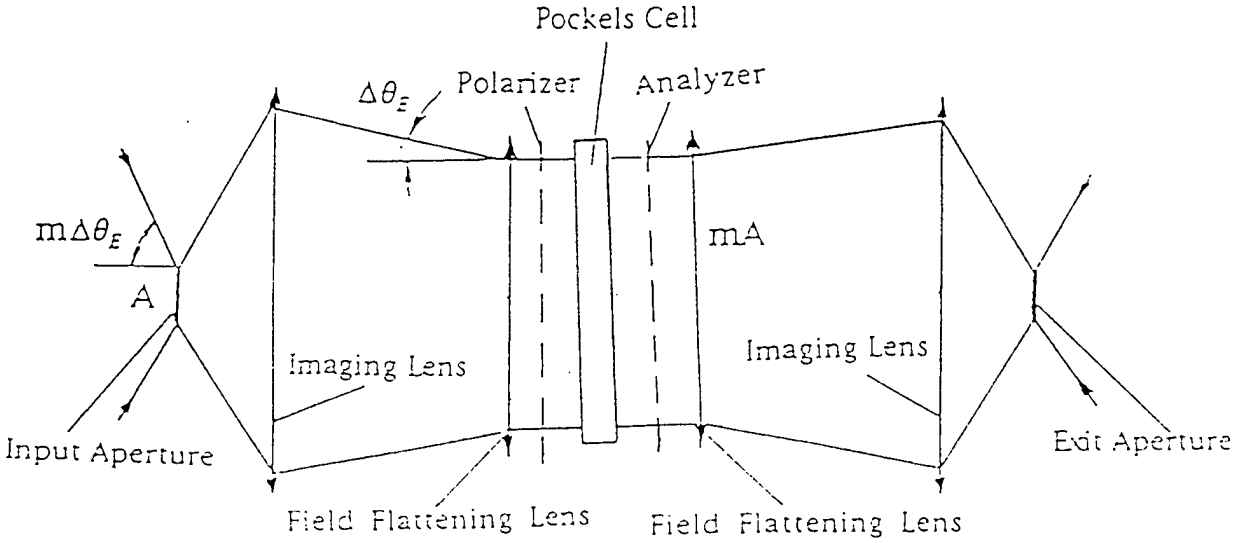

(a)

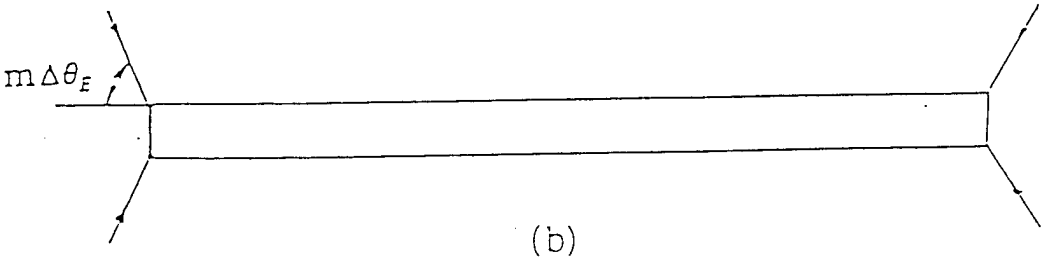

(b)

Figure 4.3.1. The actual "box" (a) contains a magnified image of the input aperture where the Pockels cell is placed. The equivalent "box" (b) has the aperture and field of view we seek.

4.4 Fundamental Constraints on SLM

Spatial light modulators are optimized to operate with light of one polarization entering the device at normal incidence. most optical processors, however, require light to enter at other angles, some far from normal incidence and with varying (angle-dependent) polarization. We discuss the implications of the limited filed of view of spatial light modulators for optical processing and propose a solution to this problem.

To take advantage of the parallelism of optics, many optical processors, such as correlators and matrix processors, use a large amount of fanin and fanout[57]. When array elements or SLM(spatial light modulator) pixels are used to operate on a large fanin of beams, accuracy problems are inevitable. That is because each beam differs from the rest in angle of incidence and polarization, the modulation of each beam is different. The best we can do is to restrict the allowable angles of incidence enough to keep the errors within whatever we determine to be acceptable bounds. This create a problem-dependent effective solid angular field of view, Ω_e, for each pixel.

The problem we address here are twofold. First, what fundamental statements can we make about pixels fanin beams? Second, practically, how can we construct optical systems that utilize Ω_e optimally for given F? In other words, how can we approach in an actual system the fundamental limits imposed by Ω_e for any F?

First we want to list a few problems that will cause SLM pixels to have a very small Ω_e regardless how tolerant of error we may be. A conservative and natural limit on error tolerance is to make the maximum modulation error in a single due to fanin equal to the maximum between_pixel variation. Here are some of the angle dependent causes of modulation variation(2):

- The Fresnel equations (governing transmission and reflection) depend on angle and polarization(Neff 1990).
- Obliquity is entirely an angular factor.
- The physical path of rays through the crystal varies with angle and polarization.
- The index of refraction encountered change (in most SLMs) with angle as well as polarization.
- Polarizers and analyzers are polarization dependent by definition, but they are also strongly angularly dependent.

These and similar effects severely limit Ω_e given any criterion for error tolerance.

To make our discussion concrete, let us consider the standard f correlator system shown in Figure 4.4.1. SLM! has a fanin of 1 (F = 1), so fanin is not a problem. Each pixel of SLM2 (which serves as a Fourier plane filter) receives light from every pixel of SLM1, so F >> 1. As shown in Figure 4.4.2, each pixel of SLM2 receives light over a rather large range of angles. It is inconceivable that all beams reaching a given pixel would be modulated

equally to with even 25% with any SLM known to us. If we want 5% error, we will probably want to reduce the field of view to a cone of half angle of a few degrees or even less.

How large can F be, for a given SLM pixel? What are the theoretical limits? We are not the first to ask those questions. In fact, those questions are simply rephrasings of the question Dennis Gabor asked and answered(Gabor 1961). "What is the optical information handling capability of a surface?" He noted the bigger areas allowed both more spatial information, if we partition the information that way, and/or better angular definition/separation through the diffraction limits. Neglecting near_unity factors, he noted that the number of independent information channels or "logons" in an area A illuminated over a solid angle Ω at a wavelength λ is (see Figure 4.4.2),

$$L = A\,\Omega/\,\lambda^2. \qquad (4\text{-}4\text{-}1)$$

A most important property of logons is that logons are conserved in a diffraction limited optical system. Logons are related to the space_bandwidth product of the optical system. Any optical system can only decrease, but never increase the logon count of a system. A diffraction limited system, a single mode or spatially coherent beam have logon counts of 1. Gaussian beams, if they are nearly collimated, also have a small logon number.

For optical processor , however, matters are quite different. The advantage of optical interconnections is the ease of fanin and fanout. Thus,

typical optical processors have very large fanin, and correspondingly large logon numbers if they are to calculate meaningful results.

For example, take a field of view of 5°, a value greater than most SLMs support, but smaller than that required by most optical processor. Further assume a square pixel with 100 μm on each side and a wavelength of 500nm. Thus,

$$\Omega = 2\pi(1-\cos 5°) = \pi(5^{\circ})^2 = 0.024 \text{ sterad.}$$

Now we have L = 960 for one pixel, and 245760 logons for a 16 x 16 pixel SLM. The number of fanin/fanout must be smaller than the logon number. For this system the maximal useable fanin/fanout is 31 x 31.

Obviously, each pixel must satisfy

$$L \geq F, \qquad (4\text{-}4\text{-}2)$$

where F is the fanin. In fact, as we usually want beams more-than-Rayleigh separated, we will in practice use L significantly greater than F. Nevertheless, L = F, is the theoretical bound.

The problem then becomes that matching an input fanin of area A_i and solid angle Ω_i to a pixel of area A_p and the maximal tolerable solid angle Ω_e. A_i is determined by the physical size of the SLM pixel, wholeΩ_i is a function of how much error the optical processor can tolerate. "Matching" means

$$A_p\Omega_e \geq A_i\Omega_i \qquad (4\text{-}4\text{-}3)$$

and transforming the input fanin to a new area A_i and new solid angle Ω_i such

$$A_i' \Omega_i' = A_i \Omega_i \qquad (4\text{-}4\text{-}4)$$

(no loss information) so that both

$$A_i' \leq A_p \qquad (4\text{-}4\text{-}5a)$$

and

$$\Omega_i' \leq \Omega_e \qquad (4\text{-}4\text{-}5b)$$

can such a transformation be done? Again the optical literature has the answer. The term

$$T = A\Omega \qquad (4\text{-}4\text{-}6)$$

is called the throughput. The amount of light collected by an optical system of throughput T looking at an infinitely large, diffuse object is proportional to T. Essentially equivalent terms are the etendue and the Rayleigh invariant, used by some authors. We will use throughput , because it relates to logons so well:

$$L = T / \lambda^2 \qquad (4\text{-}4\text{-}7)$$

The critical things to note about T are

- no optics can increase the T of an input beam (or fan of beams) and
- T is conserved in all transformations by diffraction-limited optics.

Associating T and L makes this obvious. Increasing T would increase information. This would amount to decreasing entropy. As L is governed by diffraction limits, diffraction-limited optics can only conserve L, not decrease it.

We must satisfy expression(2) . To find the fundamental limit, we take the equality, i.e.

$$F = L = A\Omega_e \quad / \lambda^2 \tag{4-4-8}$$

Given F, Ω_e, and λ we can find the minimum pixel size

$$A_i = F\lambda^2/\Omega_e. \tag{4-4-9}$$

It is more common to speak of the pixel's side, s, than of its area. So we set

$$s = (F\lambda^2/\Omega_e)^{1/2}. \tag{4-4-10}$$

If the SLM also has F pixels, its size must at least

$$S = F^{1/2}s = \lambda F\sqrt{\Omega_e}\,. \tag{4-4-11}$$

Assuming $\lambda = 0.5 \times 10^{-14}$ cm (green) and several reasonable Ω_e values, we have plotted s and S as functions of F in Figure 4.4.3 and Figure 4.4.4.

The important thing to note is, that for large F values that make optical computing attractive, both s and S are uncomfortably large.

Furthermore, these are minimum theoretical sizes. To go beyond diffraction-limited bean separation, we must increase the effective F. In addition, not all diffraction-limited transforms utilize the full throughput at each pixel!

Suppose the Fourier transform in Figure 4.4.1 requires a fanin F and results in a just resolvable spot of size δs in the Fourier transform plane. To accommodate F, however, the SLM pixel must have a size

$$s >> \delta s \tag{4-4-12}$$

Clearly, we must magnify the Fourier transform by a factor

$$s/\delta s. \tag{4-4-13}$$

This can be accomplished with a longer focal length lens, or a system such as shown in Figure 4.4.5. A long focal length lens results in impractically long optical system. In both cases the areas now match (the equality of condition (5a)). Unfortunately the solid angles do not match (the equality of condition(5b)). The cone of light traveling toward the bottom pixel is incident at one angle while light traveling toward a pixel at the center of the SLM is incident at another. Both beams must be accommodated by the pixel's field of view, so we require

$$\Omega_e > \Omega_i' \tag{4-4-14}$$

To solve this problem we must place a field lens adjacent to the SLM as shown in Figure 4.4.6. This bends all beams back on axis allowing

$$\Omega_e = \Omega_i'. \tag{4-4-15}$$

Since we also have

$$A_p = A_i', \tag{4-4-16}$$

this constitutes a perfect usage of the pixel's throughput.

Real SLMs do not work like "paper" SLMs. The result is that high accuracy optical computers operated at high fanin require very large pixel size for the fanin operations and also very large assemblies of pixels (SLMs). This is a fundamental, theoretical limitation.

Practical optical computers are unlikely to reach limits, so even larger pixels and SLMs will be necessary. Nevertheless, optical transformations described here allow us to make optimum use of the fanin modulation capability of a given SLM.

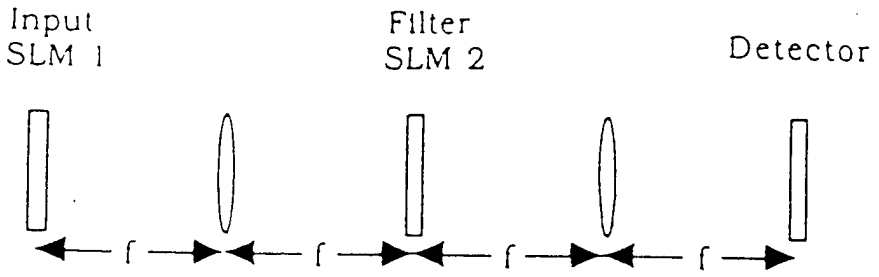

Figure 4.4.1 A conventional 4f spatial filtering system.

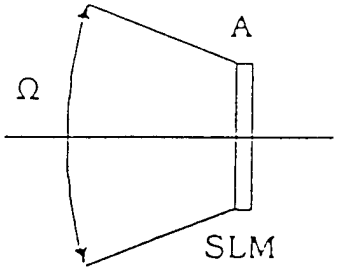

Figure 4.4.2 The geometry that determines the Logon number.

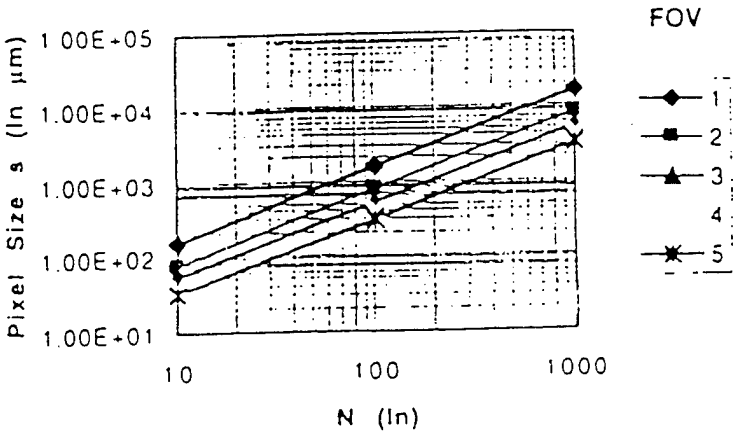

Figure 4.4.3 Pixel size (length of edge of square pixel) versus N, and field of view (FOV) in degree.

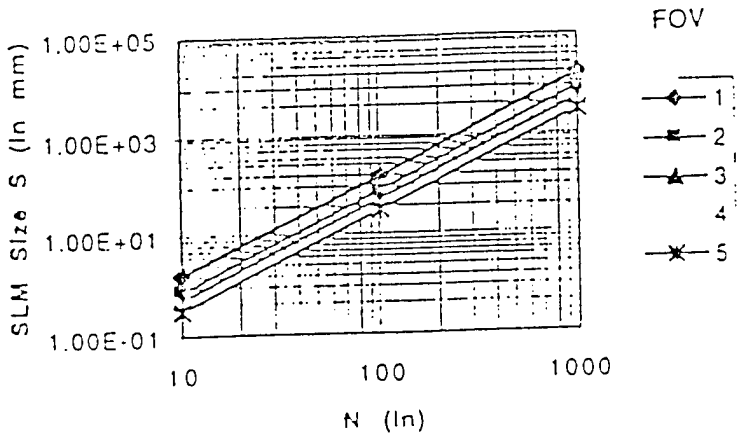

Figure 4.4.4 SLM size (length of side) versus N, and field of view (FOV) In degree.

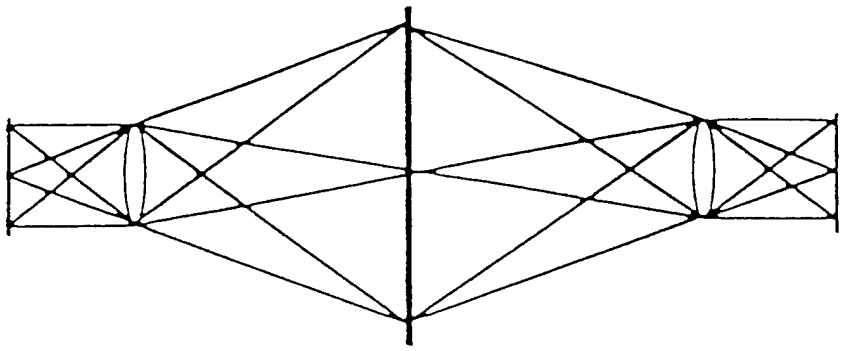

Figure 4.4.5 A Fourier transform system using magification. It does not use the available field of view of the SLM, but effectively uses the area of each pixel.

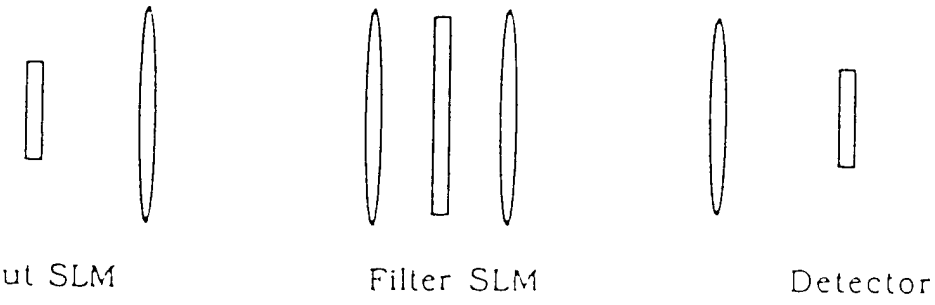

Figure 4.4.6 The modified optical correlator system

4.5 Large FOV with Real Thin Material

Considering the phase shift equation (3-3-9) in modified NIST model, we can write the phase shift $\Delta\Phi_{NIST}$ in the modified NIST model as

$$\Delta\Phi_{NIST} \approx \beta\, d\,, \tag{4-5-1}$$

Where β is a coefficient constant and d is the thickness of a Pockels cell. But considering the phase shift equation (4-2-7) of thickness effect, we can also have the thickness effect phase shift $\Delta\Phi_T$ as

$$\Delta\Phi_T \approx \gamma\, d\, \theta^2\,, \tag{4-5-2}$$

where γ is a coefficient constant, d is the thickness of a Pockels cell and θ is the incident angle of light. The over all phase shift should be determined by the combination of these two effects. So we have total phase shift $\Delta\Phi_{Total}$ as

$$\Delta\Phi_{Total} = \sqrt{\Delta\Phi_{NIST}^2 + \Delta\Phi_T^2} \tag{4-5-3}$$

$$= \sqrt{\beta^2 d^2 + \gamma^2 d^2 \theta^4}\,. \tag{4-5-4}$$

This clearly show that the total phase shift is contributed by two parts: the first part only depends on the thickness, but the second part is the product of thickness and incident angle. So only the second part has contribution on angular effect of a Pockels cell and limits the FOV of a Pockels cell. In order to achieve a large FOV, we have to reduce the thickness d of a Pockels cell to very small number so that we can ignore the angular effect.

CHAPTER V

SPEED OF EO MODULATOR

5.1 RC Limited

We assume that before switch S of Figure 5.1.1 is closed, the capacitor C is uncharged, and shall mark time from the instant the switch is closed. For t<0, no current flows in the circuit, and the voltage across the resistor is therefore zero; since the capacitor is initially uncharged, the potential across it is zero for t<0. Consequently, for t<o, the entire emf of the battery appears across the terminals A and B of the switch.

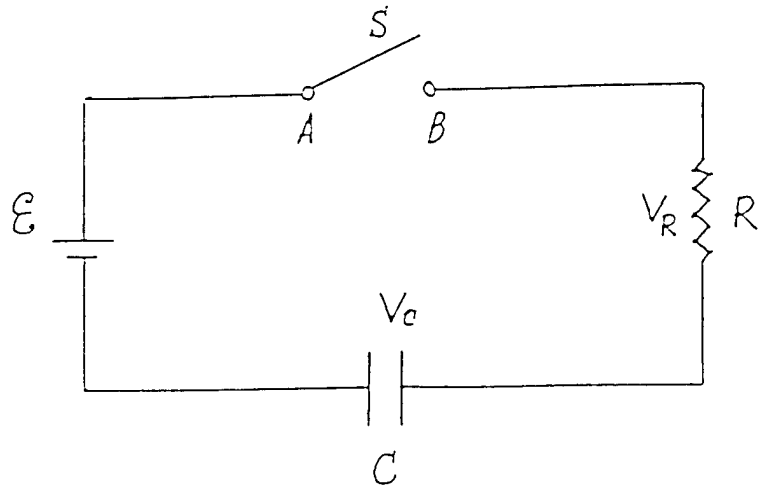

Fig 5.1.1 A Simple RC Circuit

As soon as the switch is closed, $V_{AB} = 0$, and to satisfy Kirchhoffs Rule 2, V_R+V_C must equal ε. Thus,

$$V_R+V_C=iR + q/C = \varepsilon \qquad (5\text{-}1\text{-}1)$$

must hold at all times.

The problem posed in attempting to solve this equation is as follows. Since charge cannot pass across the insulating material separating the capacitor plates, a current through the resistor must result in the deposition of charge on the capacitor plates. Thus the two terms on the left-hand side of equation (5-1-1) are not independent but intimately related. Still, we can see, at least qualitatively, the expected course of events for this circuit, Just after S is closed, there is no charge on C and hence $V_C=0$ at t=0. All the emf ε of the battery must therefore appear as iR drop across the resistor, and so the magnitude of the resistance determines the value of the initial current; i.e.,

$$i_o=\varepsilon/R \qquad (5\text{-}1\text{-}2)$$

As charge continues to flow, equal but opposite charges accumulate on the two capacitor plates, and V_C increases. So that equation (5-1-1) will be satisfied, the gradual increase in V_C must be offset by an equal decrease of V_R. Hence the current I gradually diminishes with time as more and more change appears on C. In the limit as $t \rightarrow \infty$, we find $V_C \rightarrow \varepsilon$ and $I \rightarrow 0$.

Using elementary calculus and the definition of the instantaneous current, $I=\lim_{\Delta t\to 0}(\Delta q/\Delta t)$, one can show that the asymptotic approach of V_C to its limiting value ε is exponential. The mathematical relations that express the time dependences of V_C, V_R, and I in this particular case are

$$V_C = \varepsilon(1-e^{-t/\tau}) \qquad (5\text{-}1\text{-}3)$$

$$V_R = \varepsilon e^{-t/\tau} \qquad (5\text{-}1\text{-}4)$$

$$I = V_R/R = (\varepsilon/R)\, e^{-t/\tau} \qquad (5\text{-}1\text{-}5)$$

where τ, a parameter with the dimension of time, is called the time constant.

The time constant τ characterizes the rate at which the various observables, such as voltages and currents, approach their steady-state values. For a circuit consisting of a capacitance C and resistence R in series, the time constant is given by

$$\tau = RC\,. \qquad (5\text{-}1\text{-}6)$$

It is reasonable that the values of resistance and capacitance should determine the rate at which the capacitor approaches its asymptotic voltage, and that this process should be slower-have a long time constant-the greater R or C. If R is increased in the circuit of Fig 5.1.1, the for any value of v_R, the corresponding current I is reduced proportionally, and so is the rate at which charge is deposited on the capacitor plates. Consequently, an increase in R must increase the time required to charge the capacitor. If C is increased, this increase the amount of charge that must be placed on the capacitor

plates to bring the capacitor to within a given fraction of its asympotic potential. If, by holding R fixed, we do not allow an increase in current, the only way this greater charge can be transported is if the current flow for a longer time.

If a charged capacitor is discharged through a resistor R, the charge does not vanish from the plates instantaneously but decays to zero exponetially with the time constant RC.

5.2 RC Limited - Ω Tradeoff

For a Pockels cell, equation (5-1-6) becomes

$$\tau = RC = R\ \varepsilon\frac{A}{d}\ , \qquad (5\text{-}1\text{-}7)$$

where ε is permittivity of this material, A is area, and d is thickness of Pockels cell. This equation explicitly show that increasing of thickness d will reduce time constant and increase speed of this cell. But increasing of thickness d results decreasing of FOV-Ω, which was shown in CHAPTER IV. So there are only optimal results, which can best balance between FOV and speed.

CHAPTER VI

SUMMARY AND CONCLUSIONS

Based on fully understanding polarization and electrooptic modulators, new analytical models for electrooptic modulators were invented and overall performance of electrooptic modulators was improved significantly. These improvements are summarized below.

1. Most of ray tracing and matrix algorithms today are very complex. The three-dimensional refraction model derived in this dissertation allows us to calculate the amplitudes and directions of rays in arbitrary uniaxial and/or homogeneous dielectric systems. The algorithm here reaches the same result with McClain and Chipman's, who took ray tracing approach. We believe this approach, due to Gu and Yeh, is somewhat easier to understand or more physical than the ray tracing approach. By making them of equal generality, we create a viable choice for users.

2. An optimal usage of a electro-optic modulator in terms of field of view has been proposed here. To maximize field inherent of view $\Delta\theta_E$, we make the cell as thin as possible. To achieve field effective field of view greater than $\Delta\theta_E$, we must use lenses to trade off area and field of view optimally. In

the process, we also increase contrast at any off-axis angle by using the polarizer and analyzer closer to on-axis.

3. NIST model for electro-optic modulator is very effective, but it does not consider angular effects and only works on-axis. The modified NIST model presented here makes the simulation of electro-optic modulators both more effective and more accurate. This extended model not only considers angular birefringent effects but also includes Fresnel reflections on the surfaces of a Pockels cell. Computer simulations prove that the combination of angular birefringent effects and Fresnel reflections limits the field of view of Pockels cells and reflective Pockels cell only need half driving voltage to reach its best modulation.

4. Real SLMs do not work like "paper" SLMs. There is a fundamental, theoretical limitation. We show the theoretical limits and how to achieve them.

5. The new algorithm and modified NIST's model can be extended and applied to computer simulate and optimize LCD operations.

APPENDICE A

STOKES VECTORS AND JONES'S VECTORS

Table 16 Stokes vectors and Jones vectors(Shurcliff 1966)

Polarization form					Normalized Stokes vector				Jones vector
	α	b/a	A_y/A_x	γ	{I,	M,	C,	S}	Normalized
linear	0	0	0	--	{1,	1,	0,	0}	$\begin{bmatrix}1\\0\end{bmatrix}$
linear	90°	0	∞	--	{1,	-1,	0,	0}	$\begin{bmatrix}0\\1\end{bmatrix}$
linear	45°	0	1	0	{1,	0,	1,	0}	$\frac{\sqrt{2}}{2}\begin{bmatrix}1\\1\end{bmatrix}$
linear	-45°	0	1	±180°	{1,	0,	-1,	0}	$\frac{\sqrt{2}}{2}\begin{bmatrix}1\\-1\end{bmatrix}$
General linear		0	--	--	{1,	cos2 α,	sin2α,	0}	$\begin{bmatrix}\cos R\\ \pm\sin R\end{bmatrix}$
Right circular		1	1	90°	{1,	0,	0,	1}	$\frac{\sqrt{2}}{2}\begin{bmatrix}-i\\1\end{bmatrix}$
Left circular		1	1	-90°	{1,	0,	0,	-1}	$\frac{\sqrt{2}}{2}\begin{bmatrix}i\\1\end{bmatrix}$
Elliptical	0	1/2	1/2	90°	{1,	0.6,	0,	0.8}	$\frac{2\sqrt{5}}{5}\begin{bmatrix}-i\\1/2\end{bmatrix}$

Elliptical	90°	1/2	2	90°	{1, -0.6, 0, 0.8}	$\frac{2\sqrt{5}}{5}\begin{bmatrix} -i/2 \\ 1 \end{bmatrix}$
General elliptical					$\begin{bmatrix} 1 \\ \cos 2\omega \cos 2\lambda \\ \cos 2\omega \sin 2\lambda \\ \sin 2\omega \end{bmatrix}$	$\begin{bmatrix} (\cos R)e^{-i\frac{\gamma}{2}} \\ (\sin R)e^{i\frac{\gamma}{2}} \end{bmatrix}$
Unpolarized					{1, 0, 0, 0}	None

APPENDICE B

MUELLER'S AND JONES MATRIXES

Optical device	Mueller matrix	Jones matrix
Miscellaneous devices		
Ideal plate of isotropic glass	$\begin{bmatrix} 1 & 0 & 0 & 0 \\ 0 & 1 & 0 & 0 \\ 0 & 0 & 1 & 0 \\ 0 & 0 & 0 & 1 \end{bmatrix}$	$\begin{bmatrix} 1 & 0 \\ 0 & 1 \end{bmatrix}$
Absorbing glass(transmittance:k or p^2)	$\begin{bmatrix} k & 0 & 0 & 0 \\ 0 & k & 0 & 0 \\ 0 & 0 & k & 0 \\ 0 & 0 & 0 & k \end{bmatrix}$	$\begin{bmatrix} p & 0 \\ 0 & p \end{bmatrix}$
Totally absorbing glass	$\begin{bmatrix} 0 & 0 & 0 & 0 \\ 0 & 0 & 0 & 0 \\ 0 & 0 & 0 & 0 \\ 0 & 0 & 0 & 0 \end{bmatrix}$	$\begin{bmatrix} 0 & 0 \\ 0 & 0 \end{bmatrix}$
Ideal depolarizer	$\begin{bmatrix} 1 & 0 & 0 & 0 \\ 0 & 0 & 0 & 0 \\ 0 & 0 & 0 & 0 \\ 0 & 0 & 0 & 0 \end{bmatrix}$	None
Ideal homogeneous linear polarizer		
Azimuth θ of transmission axis		

0°

$$\frac{1}{2}\begin{bmatrix}1 & 1 & 0 & 0\\ 1 & 1 & 0 & 0\\ 0 & 0 & 0 & 0\\ 0 & 0 & 0 & 0\end{bmatrix} \qquad \begin{bmatrix}1 & 0\\ 0 & 0\end{bmatrix}$$

90°

$$\frac{1}{2}\begin{bmatrix}1 & -1 & 0 & 0\\ -1 & 1 & 0 & 0\\ 0 & 0 & 0 & 0\\ 0 & 0 & 0 & 0\end{bmatrix} \qquad \begin{bmatrix}0 & 0\\ 0 & 1\end{bmatrix}$$

45°

$$\frac{1}{2}\begin{bmatrix}1 & 0 & 1 & 0\\ 0 & 0 & 0 & 0\\ 1 & 0 & 1 & 0\\ 0 & 0 & 0 & 0\end{bmatrix} \qquad \frac{1}{2}\begin{bmatrix}1 & 1\\ 1 & 1\end{bmatrix}$$

-45°

$$\frac{1}{2}\begin{bmatrix}1 & 0 & -1 & 0\\ 0 & 0 & 0 & 0\\ -1 & 0 & 1 & 0\\ 0 & 0 & 0 & 0\end{bmatrix} \qquad \frac{1}{2}\begin{bmatrix}1 & -1\\ -1 & 1\end{bmatrix}$$

Ideal homogeneous nonlinear polarizer

Right circular

$$\frac{1}{2}\begin{bmatrix}1 & 0 & 0 & 1\\ 0 & 0 & 0 & 0\\ 0 & 0 & 0 & 0\\ 1 & 0 & 0 & 1\end{bmatrix} \qquad \frac{1}{2}\begin{bmatrix}1 & -i\\ -i & 1\end{bmatrix}$$

Left circular

$$\frac{1}{2}\begin{bmatrix}1 & 0 & 0 & -1\\ 0 & 0 & 0 & 0\\ 0 & 0 & 0 & 0\\ -1 & 0 & 0 & 1\end{bmatrix} \qquad \frac{1}{2}\begin{bmatrix}1 & i\\ -i & 1\end{bmatrix}$$

Right elliptical($\theta=0°$, b/a=0.5)

$$\frac{1}{2}\begin{bmatrix} 1 & 0.6 & 0 & 0.8 \\ 0.6 & 0.36 & 0 & 0.48 \\ 0 & 0 & 0 & 0 \\ 0.8 & 0.48 & 0 & 0.64 \end{bmatrix} \qquad \frac{2}{5}\begin{bmatrix} 2 & -i \\ i & 0.5 \end{bmatrix}$$

Right elliptical(($\theta=22.5°$, b/a=0.318)

$$\frac{1}{2}\begin{bmatrix} 1 & \sqrt{\frac{1}{3}} & \sqrt{\frac{1}{3}} & \sqrt{\frac{1}{3}} \\ \sqrt{\frac{1}{3}} & \frac{1}{3} & \frac{1}{3} & \frac{1}{3} \\ \sqrt{\frac{1}{3}} & \frac{1}{3} & \frac{1}{3} & \frac{1}{3} \\ \sqrt{\frac{1}{3}} & \frac{1}{3} & \frac{1}{3} & \frac{1}{3} \end{bmatrix} \qquad 0.288\begin{bmatrix} 2.73 & 1-i \\ 1+i & 0.733 \end{bmatrix}$$

Ideal homogeneous linear retarder with retardance $\delta=90°$

Azimuth ρ of fast axis

0°

$$\begin{bmatrix} 1 & 0 & 0 & 0 \\ 0 & 1 & 0 & 0 \\ 0 & 0 & 0 & 1 \\ 0 & 0 & -1 & 0 \end{bmatrix} \qquad \begin{bmatrix} e^{i\pi/4} & 0 \\ 0 & e^{-i\pi/4} \end{bmatrix}$$

90°

$$\begin{bmatrix} 1 & 0 & 0 & 0 \\ 0 & 1 & 0 & 0 \\ 0 & 0 & 0 & -1 \\ 0 & 0 & 1 & 0 \end{bmatrix} \qquad \begin{bmatrix} e^{-i\pi/4} & 0 \\ 0 & e^{i\pi/4} \end{bmatrix}$$

45°

$$\begin{bmatrix} 1 & 0 & 0 & 0 \\ 0 & 0 & 0 & -1 \\ 0 & 0 & 1 & 0 \\ 0 & 1 & 0 & 0 \end{bmatrix} \qquad \frac{1}{\sqrt{2}}\begin{bmatrix} 1 & i \\ i & 1 \end{bmatrix}$$

-45°

$$\begin{bmatrix} 1 & 0 & 0 & 0 \\ 0 & 0 & 0 & 1 \\ 0 & 0 & 1 & 0 \\ 0 & -1 & 0 & 0 \end{bmatrix} \qquad \frac{1}{\sqrt{2}}\begin{bmatrix} 1 & -i \\ -i & 1 \end{bmatrix}$$

Ideal homogeneous linear retarder with retardance $\delta=180°$

Azimuth ρ of fast axis

0° or 90°

$$\begin{bmatrix} 1 & 0 & 0 & 0 \\ 0 & 1 & 0 & 0 \\ 0 & 0 & -1 & 0 \\ 0 & 0 & 0 & -1 \end{bmatrix} \qquad \begin{bmatrix} 1 & 0 \\ 0 & -1 \end{bmatrix}$$

±45°

$$\begin{bmatrix} 1 & 0 & 0 & 0 \\ 0 & -1 & 0 & 0 \\ 0 & 0 & 1 & 0 \\ 0 & 0 & 0 & -1 \end{bmatrix} \qquad \begin{bmatrix} 0 & 1 \\ 1 & 0 \end{bmatrix}$$

Ideal homogeneous nonlinear retarders

Right circular($\delta=45°$)

$$\begin{bmatrix} 1 & 0 & 0 & 0 \\ 0 & 0 & 1 & 0 \\ 0 & -1 & 0 & 0 \\ 0 & 0 & 0 & 1 \end{bmatrix} \qquad \frac{1}{\sqrt{2}}\begin{bmatrix} 1 & 1 \\ -1 & 1 \end{bmatrix}$$

Left circular($\delta=90°$)

$$\begin{bmatrix} 1 & 0 & 0 & 0 \\ 0 & 0 & -1 & 0 \\ 0 & 1 & 0 & 0 \\ 0 & 0 & 0 & 1 \end{bmatrix} \qquad \frac{1}{\sqrt{2}}\begin{bmatrix} 1 & -1 \\ 1 & 1 \end{bmatrix}$$

Right or Left circular(δ=180°)

$$\begin{bmatrix} 1 & 0 & 0 & 0 \\ 0 & -1 & 0 & 0 \\ 0 & 0 & -1 & 0 \\ 0 & 0 & 0 & 1 \end{bmatrix} \qquad \begin{bmatrix} 0 & -1 \\ -1 & 0 \end{bmatrix}$$

Right circular (any δ)

$$\begin{bmatrix} 1 & 0 & 0 & 0 \\ 0 & \cos\delta & \sin\delta & 0 \\ 0 & -\sin\delta & \cos\delta & 0 \\ 0 & 0 & 0 & 1 \end{bmatrix} \qquad \begin{bmatrix} \cos\frac{1}{2}\delta & \sin\frac{1}{2}\delta \\ -\sin\frac{1}{2}\delta & \cos\frac{1}{2}\delta \end{bmatrix}$$

Left circular (any δ)

$$\begin{bmatrix} 1 & 0 & 0 & 0 \\ 0 & \cos\delta & -\sin\delta & 0 \\ 0 & \sin\delta & \cos\delta & 0 \\ 0 & 0 & 0 & 1 \end{bmatrix} \qquad \begin{bmatrix} \cos\frac{1}{2}\delta & -\sin\frac{1}{2}\delta \\ \sin\frac{1}{2}\delta & \cos\frac{1}{2}\delta \end{bmatrix}$$

BIBLIOGRAPHY

Barkovskii L. M. and Fedorov F. I. 1991. Stokers tensor relations on the anisotropic media Boundary. J. Mod. Opt.. Vol. 40. No.6. 1015-1022.

Bell B. W. 1989. Muller matrix: an experimental and analytical tool for magneto-optics. Optical Engineering. Vol.28. No.2. February. 235-246.

Bennett H., Fenimore C., Field B. F., and Kelly E. F. 1995. Making Displays Deliver a Full Measure. Information Display. 1. 181-190.

Bennett J. M. and Bennett H. E. 1978. Polarization. Handbook of Optics. Edited by Walter G. Driscall. Mcgraw-Hill. 24-35.

Blaker J. W. 1975. Optics. pergamon. 280-315.

Bossi D. E. and Ade R. W. 1992. Integrated-optic modulators benefit high-speed fiber links. Laser Focus World. Setember. 135-142.

Burton F.A. and Cassidy S.A. 1991. Simple model and measurement technique for single-mode waveguide polarizers". J. Opt. Soc. Am. A/Vol.8. No.7. 1070-1073.

Caulfield H. J. 1992. Multidimensional systems and signal processing. Vol.2. 373-395.

Chakraborty A. K., Das S., Basu D. K. and Ghosf A. 1989. Imaging characteristics of a birefringent lens. SPIE. Vol.1166. polarization considerationsfor Optical Systems II. 130-134.

Chen J. and Minemoto T. 1989. Numerical analysis of the modulation transfer function of a Pockels readout optical modulator device. J. Opt. Soc. Am. A Vol.6. No.9. September. 1281-1291.

Chorey C. M., Ferendici A. and Bhasin K. 1988. A high frequency GaAlAs travelling wave electro-optic modulator at 0.82μm. IEEE MTT-S Digest. 735-738.

Chung H., Chang W. S. C.. and Adler E. L. 1991. Modeling and optimization of traveling-wave $LiNbO_3$ interferometric modulators. IEEE Journal of Quantum Electronics. Vol.27. No.3. 608617.

Cloude S. R. 1989. Conditions for the physical realisability of matrix operators in polarimetry. SPIE. Vol.1166 Polarization Considerations for Optical Systems II. 177-219.

Collett E. 1993. Polarized Light: Fundamentals and Applications. Marcel Dekker. 434-467.

Dolfi D. W., Nazarathy M., and Jungerman R. L. 1988. 40 Ghz electro-optic modulator with 7.5 V drive voltage. Electronics letters. Vol. 24. No.9. 499-500.

Fainman Y. and Shamir J.1984. Polarization of nonplanar wave fronts. Appl. Opt.. Vol.23. 3188-3194.

Fritsch H. W., Haas M. G. and Mlynski D. A. 1991. Chriacteristic matrix method for stratified anisotropic media: optical properties of special configurations. J. Opt. Soc. Am. A. Vol.8. No.3. March. 536-540.

Gabor D. 1961. Light and Information. Prog. in Optics. 1. 109-153.

Giguere S. R., Friedman L., Soref R. A. and Lorenzo J. P. Simulation. 1990 Studies of silicon E-O waveguide devices. J. Appl. Phys.. Vol.68. No.10. 4964-4970.

Gomatam B. N. 1992. The distributed feedback waveguide modulator. IEEE Photonics Technology Letters. Vol.4. No.11. 1227-1230.

Gu C. and Yeh P. 1993. Extended Jones Matrix method II. J. Opt. Soc. Am. a. Vol.10. No.5. May. 966-973.

Hecht E. and Zajac A. 1979. Optics. Addison-Wesley. 219-266.

Heriter J. M. 1990. EO devices make good amplitude and phase modulation. Laser Focus World. April. 113-120.

Higgins T. V. 1994. Optical modulation controls the properties of light. Laser Focus World. January. 83-87.

Huang T. C.,Chung Y. C., and Dagli N. 1993. Field-induced waveguides and their application to modulators. IEEE Journal of Quantum Electronics. Vol.29. No.4. 1131-1143.

Ishikawa T. 1992. Plarization-independent $LiNbo_3$ waveguide optical modulator for bidirectional transmission. Electronics Letters. Vol.28. No.6. 566-567.

Jiang P., Zhou F., Laybourn P.j.R.. and Buried R.M. 1992. optical waveguide polarizer by Titanium indiffusion and proto-exchange in $LiNbO_3$. IEEE Photonice Technilogy Letters. Vol.4. No.8. 881-883.

Jungerman R. L., Johnsen C., McQuate D. J., alomaa K. Zurakowski M. P. Bray R. C., Conrad G., Cropper D. and Hernday P. 1990. High-speed optical modulator for application in instrumentation. Journal of Lightwave Technology. Vol.8. No.9. 1363-1370.

Kurokawa T. and Fukushima S. 1992. Spatial light modulators using ferroelectric liquid crystal. Optical and Quantum Electronics. Vol.24. 1151-1163.

Lawrence G. N. 1989. Polarization modeling in physical optics analysis. SPIE. Vol.1166. Polarization Considerations for Optical Systems II. 60-68.

Liang Q. T. 1990. Simple ray tracing fomulas for uniaxial optical crystals. Appl. Opt.. Vol.29. No.7. 1008-1010.

Lien A. 1990. Extened Jones matrix representation for the twisted nematic liquid-crystal display at oblique incidence. Appl. Phys. lett. 57(26). 24 december. 2767-2769.

McClain S. C. and Chipman R. A. 1992. Polarization ray tracing in anisotropic optically active media. SPIE. Vol. 1746. 107-118.

McClain S. C., Chipman R. A. and Hilliman L. W. 1992. Aberrations of a horizontal-vertical depolarizer. Appl. Opt.. Vol.31. No.13. 107-118.

Mentel J. Schmidt E. and Mavrudis T. 1992. Birefringent filter with arbitrary orientation of the optic axics: an analysis of improved accuracy. Appl. Opt.. Vol.31. No.24. 20 August. 5022-5029.

Neff J. A., Athale R. A., and Lee S. H. 1990. Two-dimensional spatial light modulators; a tutorial. Proc. IEEE. Vol.78. No.5. 826-855.

Neyer A. 1990. Integrated-optic devices in Lithum Niobate: technology and applications. SPIE. Vol.1274. 2-17.

Railton C.J. and McGeehan J. P. 1989. A rigorous and computationally efficient analysis of microstrip for use as an electr-optic modulator. IEEE Transactions on Miscrowave and Techniques. Vol.37. No.7. 1099-1104.

Robb P. and Pawlowski B. 1990. Computer ray tracing speeds. Appl. Opt.. Vol.29. No.13. 1933-1934.

Robert O. JR F. and Chen X. 1990. Electrooptic Modulation in an arbitrary cross section waveguide. IEEE Journal of Quantum Electronices. Vol.26. No.3. March. 532-540

Shurcliff W. A. 1966. Polarized Light. Harvard University. 166-171.

Simon J. M. and Simon M. C. 1978. Wollaston prism as a beam splitter in convergent light. Appl. Opt.. Vol.17. No.21. 3352-3353.

Simon M. C. 1983. Ray tracing formulas for monoaxial optical componenets. Appl. Opt.. Vol.22. No.2. 354-360.

Simon M. C. and Echarri R. M. 1986. Ray tracing formulas for monoaxial optical components:vectorial formulation. Appl. Opt.. Vol.25. No.12. 1935-1939.

Simon M. C. 1987. Ray tracing in monoaxial crystals: are the exact formulas nessary?. Appl. Opt.. Vol.26. No.16. 3187-3189.

Simon M. C. 1988. Image formation through monoaxial plane-parallel plates. Appl. Opt.. Vol.27. No.20. 4176-4182.

Smet D. J. 1993. 4 X 4 matrix formalism applied to internal conical refraction. J. Opt. Soc. Am. A. Vol.10. No.1. January. 186-190.

Solgaard O., Gidil A. A., Hemenway B. R. and Bloom D. M. 1991. All-Silicon integrated optical modulator. IEEE Jpurnal on Selected Areas in Communications. Vol.9. No.5. 704-710.

Swindell W. 1975. Extraordinary-ray and -wave tracing in uniaxial crystals. Appl. Opt.. Vol.14. No.13. 2298-2301.

Tan M.R.T., Kim I., Chang J. and Wang S.Y. 1990. Velocity matching of III-V travelling-wave electro-optic modulators structures. Electronics Letters. Vol.26. No.1. 32-33.

Trollinger J. D. Jr., Chipman R. A., and Wilson D. K. 1991. Polarization ray tracing in birefringent media. Optical Engineering.Vol.30. No.4. 461-466.

Walker R. G. 1991. High-speed III-V semiconductor intensity modulators. IEEE Journal of Quantum Electronics. Vol.27. No.3. 654-667.

Waluschka E. 1988. Polarization ray tracing. SPIE. Vol.891. 104-111.

Wohler H., Haas G., Fritsch M., and mlynski D. A. 1988. Faster 4X4 matrix method for uniaxial inhomogeneous media. J. Opt. Soc. Am. A. Vol.5. No.9. september. 1554-1556.

Yeh P. 1980. Optics anisotropic layered media: anew 4 x 4 matrix algebra. Surface Science 96. 41-53

Yeh P. 1982. Extended Jones Matrix method. J. Opt. Soc. Am.. Vol.72. No.4. April. 507-513.

Zhang W. Q. 1992. General ray-tracing formulas for crystal. Appl. Opt.. Vol.31. No.34. 7328-7331.